Local Motion of Polymer Chains Studied by the Fluorescence Depolarization Method(Dissertation_全文)

AUTHOR(S):

Horinaka, Jun-ichi

Local Motion of Polymer Chains Studied by the Fluorescence Depolarization Method

Jun-ichi HORINAKA

1998

Local Motion of Polymer Chains Studied by the Fluorescence Depolarization Method

Jun-ichi HORINAKA

1998

Contents

Chapter 1. General Introduction

1-1. Background of the Local Chain Dynamics....1
1-2. Fluorescence Depolarization Method....3
1-2-1. Concept of the Fluorescence Depolarization Method....3
1-2-2. Apparatus for the Fluorescence Depolarization Method....7
1-2-3. Previous Fluorescence Depolarization Study on the Local Polymer Chain Motion....9
1-3. MD Simulation....9
1-4. Motivation of This Thesis....11
1-5. Outline of This Thesis....12
References....17

Chapter 2. Local Chain Dynamics of Poly(oxyethylene) Studied by the Fluorescence Depolarization Method

2-1. Introduction....21
2-2. Experimental Section....23
2-2-1. Sample Preparation....23
2-2-2. Data Analysis....24
2-3. Results and Discussion....26
2-3-1. Molecular Weight Effect of POE....26
2-3-2. Comparison with Other Polymers....27
2-3-3. Activation Energy....30
2-4. Conclusion....33
References....35

Chapter 3. Molecular Weight Effect on Local Motion of Polystyrene Studied by the Fluorescence Depolarization Method

3-1. Introduction....37
3-2. Experimental Section....38
3-2-1. Sample Preparation....38
3-2-2. Data Analysis....40
3-3. Results and Discussion....40
3-3-1. Relaxation Time....40
3-3-2. Activation Energy....46
3-3-3. Chain Length of Cooperative Motion....46
3-4. Conclusion....49
References....50

Chapter 4. Local Motion of Oligo- and Polystyrene Chain End Studied by the Fluorescence Depolarization Method

4-1. Introduction....52
4-2. Experimental Section....54
4-2-1. Sample Preparation....54
4-2-2. Data Analysis....56
4-3. Results and Discussion....56
4-3-1. Relaxation Time....56
4-3-2. Activation Energy....61
4-3-3. Comparison with Chain Center....63
4-4. Conclusion....65
References....67

Chapter 5. ***Molecular Dynamics Simulation of Local Motion of Polystyrene Chain End; Comparison with the Fluorescence Depolarization Study***

5-1. Introduction....69
5-2. Simulation Methodology....71
5-3. Results and Discussion....75
5-3-1. Molecular Weight Effect on the Local Motion of PS Chain End....75
5-3-2. Effect of Restraints on the Chain Mobility....79
5-3-3. Chain Mobility at the Different Positions along the Main Chain....81
5-4. Conclusion....81
References....83

Chapter 6. ***Influence of a Fluorescent Probe on the Local Relaxation Times for a Polystyrene Chain in the Fluorescence Depolarization Method***

6-1. Introduction....85
6-2. Experimental Section....88
6-2-1. Fluorescence Depolarization Study....88
6-2-1-1. Sample Preparation....88
6-2-1-2. Data Analysis....89
6-2-2. MD Simulation Methodology....89
6-3. Results and Discussion....91
6-3-1. Fluorescence Depolarization Study....91
6-3-1-1. Relaxation Time....91
6-3-1-2. Activation Energy....93
6-3-2. MD Simulation....95
6-4. Conclusion....99
References....100

Chapter 7. Microscopic Observation of Thermally-Induced Phase Separation of Poly(ethoxyethyl Vinyl Ether) by the Fluorescence Method

7-1. Introduction....102
7-2. Experimental Section....104
7-2-1. Sample Preparation....104
7-2-2. Fluorescence Measurements....105
7-2-3. Light Scattering Measurement....105
7-3. Results and Discussion....106
7-3-1. Scattering Intensity....106
7-3-2. Fluorescence Intensity and Lifetime....106
7-3-3. Chain Mobility....109
7-3-4. Dynamic Quenching....111
7-3-5. Systems without Phase Separation....112
7-3-6. Effect of Surfactant....112
7-4. Conclusion....115
References....117

Chapter 8. Local Chain Dynamics of Several Polymers in Θ Solvents Studied by the Fluorescence Depolarization Method

8-1. Introduction....119
8-2. Experimental Section....120
8-3. Results and Discussion....121
8-3-1. Relaxation Time and Activation Energy....121
8-3-2. Relation of Glass Transition Temperature to the Reduced Relaxation Time....123
8-4. Conclusion....123
References....124

Summary.....125

List of Publications.....129

Acknowledgments.....131

Chapter 1

General Introduction

1-1. Background of the Local Polymer Chain Dynamics

Almost all useful and interesting features characteristic of polymer materials originate in an abundance of the internal degrees of freedom of polymer chains constituting the materials.[1-7] Above all, the abundant internal degrees of freedom let a polymer chain have many conformations and the transfer among them is the elemental process of the polymer chain motion. The subjects concerning the polymer dynamics, which widely spread in time and/or space, are essentially governed by this elemental process. For example, the viscoelasticity,[3-6,8] which is one of the distinctive properties of the polymer bulk, originates in the restoring stress of each polymer chain against the deformation. Polymers have been widely used as industrial materials, so the comprehension of their macroscopic characteristics, such as the mechanical properties, is undoubtedly valuable. However, as mentioned above, the polymer properties are fundamentally controlled by the chain dynamics and therefore the information of the polymer chain dynamics is indispensable for the further detailed material design. Moreover, the polymer chain dynamics is also interesting as an academic subject and has been extensively studied both theoretically and experimentally.

Rouse was the first who dealt with the polymer chain dynamics concerning the viscoelasticity in dilute solution theoretically on the basis of the bead-spring model,[9,10] which is widely known as Rouse or Rouse-Zimm model and represents experimental results well. In concentrated polymer solutions and in polymer melt, the intermolecular entanglement is responsible for the viscoelasticity of the system. In the field of the polymeric viscoelasticity with considerable entanglement, the Rouse model

laid the groundwork for the tube model, which was proposed by Doi and Edwards.[5,6] The tube model represents the anisotropy of the chain dynamics caused by the entanglement of polymer chains with the deformed tube and the concept of reptation dynamics is adopted. Although the bead-spring model and the tube model succeeded in the field of the viscoelasticity, which is rather a macroscopic property, the bead-spring chain is too simple compared with the chemical structure of a real polymer chain. Therefore, more realistic models are required for the discussion of the polymer chain dynamics, e.g., the relationship between the chemical structure of a polymer and its chain mobility. The individual chemical structure is especially important for the local properties of the chain dynamics, which is the subject of this thesis. So far, many models taking account of structure of real polymers have been proposed,[11-17] but none of them are universally applicable to the local chain dynamics of various polymers. This fact is probably due to the variety of the chemical structure and the complexity of the motional modes of the real polymer chain. At the present moment, the local motion is considered to consist of the coupled libration, which is the coupled small amplitude motion within the potential well, as well as the conformational transition.[18-21]

With regard to the experimental approach for the local chain dynamics, many techniques are available and they have each specific feature for measurement both in time and space.[22-68] Among them, the fluorescence depolarization method is powerful for the local chain motion in a dilute solution having the relaxation time of nano- to subnanoseconds[22-47] and the result is nearly comparable with those by other techniques such as the dielectric relaxation,[51-56] NMR,[61-63] and ESR.[64,65] In the fluorescence depolarization method, the orientational autocorrelation function is obtained without any assumptions of models as shown below. However, the polymer sample used in the fluorescence depolarization method needs a fluorescent probe labeled in the polymer chain, so the synthesis of highly structure controlled samples is often not easy.[69,70]

As another approach to the polymer chain dynamics, the computer simulation has recently become one of the major techniques along the improvement in the calculation capacity.[71-83] Many polymer dynamics simulations have been carried out and the results have been compared with the corresponding theories[71-74] or experimental results.[75-83] The advantage of the computer simulation is the capability in obtaining the

coordinates of every atom at each time step, which makes it possible to estimate various dynamic properties from the atomic level to the macroscopic level. However, at the present stage, the size of the system and the number of treated atoms are not still sufficient to reproduce the real polymer system faithfully.

In this thesis, the local chain motion of polymers in dilute solutions is examined by the fluorescence depolarization method. Moreover, molecular dynamics (MD) simulation of the local motion is carried out and the result is compared with that of the fluorescence depolarization study. In the following section, the backgrounds of the fluorescence depolarization and MD simulation studies are introduced. The motivation of this thesis is stated on the basis of the previous fluorescence depolarization studies.

1-2. Fluorescence Depolarization Method

1-2-1. Concept of the Fluorescence Depolarization Method

The fluorescent probe, such as anthryl group, has the intrinsic direction of the transition moment. When the fluorescent probes isotropically distributed in the system are irradiated by a plane-polarized light, the probes that have their transition moments nearly in the direction of the polarization of the excitation light are selectively excited. Then, the generated anisotropy of the excited probe relaxes with time due to the rotational relaxation of the probe. Here, it is noteworthy that the rate of the rotational relaxation reflects the microscopic environment around the probe as well as the shape and the volume of the probe. Therefore, if the fluorescent probe is labeled in the polymer chain, the rate of the rotational relaxation will reflect the chain mobility especially in the vicinity of the probe. Then, if the probe is labeled at a required position along the polymer chain, the chain mobility of the designated position is obtained. In this sense, not only the high microscopic sensitivity but also the selectivity about the position along the chain is the advantage of the fluorescence depolarization method in the study of the local chain dynamics. It is also important

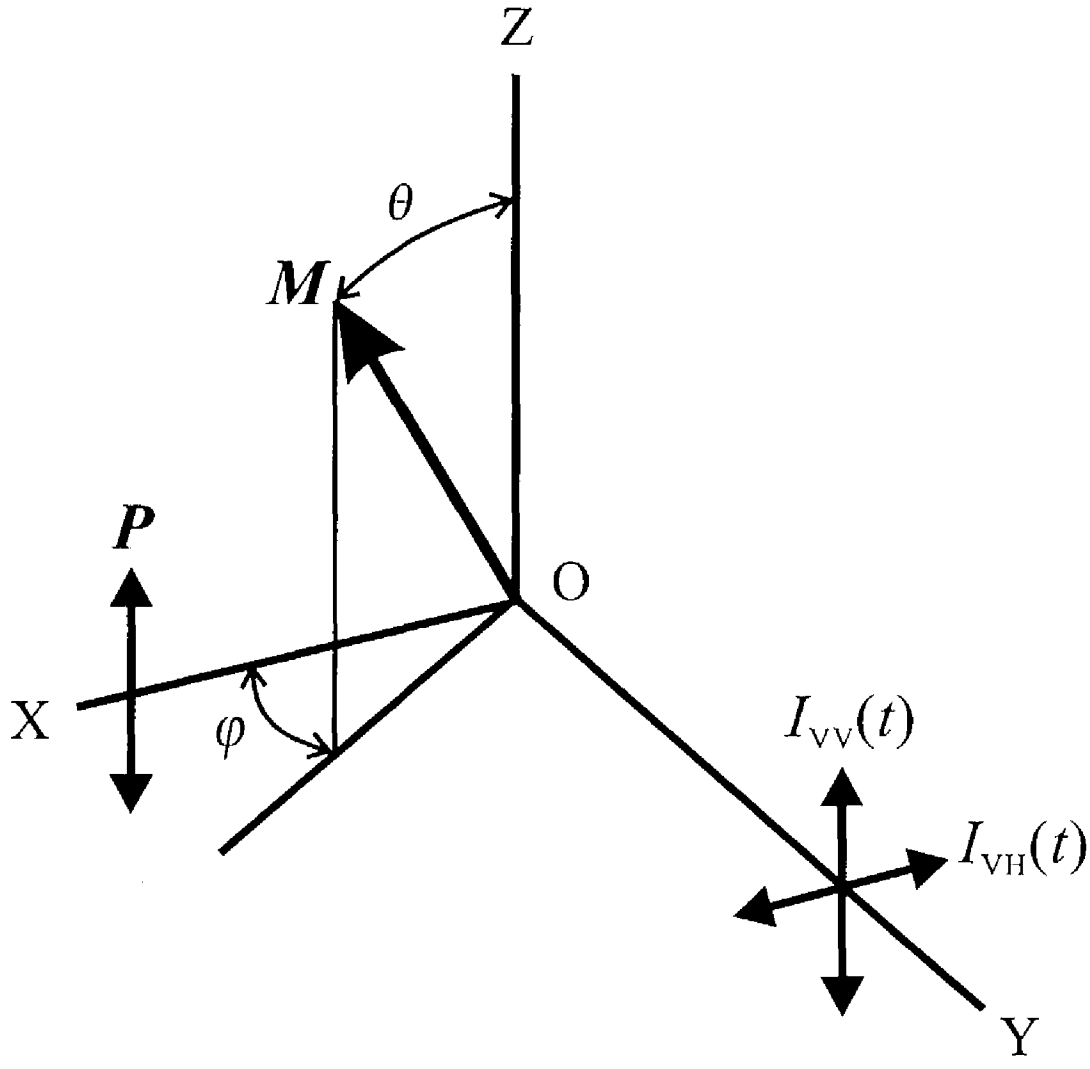

Figure 1-1. Experimental geometry of the fluorescence depolarization method. X, Y, and Z are laboratory fixed axes.

that the time-scale appropriate for the observation by the fluorescence depolarization method is determined by the fluorescence lifetime of the probe. That is, the rotational relaxation that has a correlation time in the order of the lifetime of the excited state can be measured most efficiently. The local motion which leads to the rotational relaxation of the attached fluorescent probe generally has the relaxation time (correlation time) of around nanoseconds and the fluorescence lifetime of the anthryl group is close to it. This is another advantage of the fluorescence depolarization method for the measurement of the local chain motion with respect to time scale.

Now, for simplification, suppose that the transition moments, $\boldsymbol{M}$, of both excitation and emission lie in the same direction, which is the case for L_a of anthryl group. The excitation light, $\boldsymbol{P}$, is linearly polarized in the direction of Z-axis as shown in Figure 1-1. When $\boldsymbol{P}$ is incident on the fluorescent probe at time $t = 0$, the probe is excited with the excitation probability of $\cos^2\theta$. The fluorescence intensity is observed for two components, $I_{VV}(t)$ and $I_{VH}(t)$; $I_{VV}(t)$ is the fluorescence intensity for the vertical direction (Z-axis) and $I_{VH}(t)$ is the fluorescence intensity for the horizontal direction (perpendicular to $I_{VV}(t)$).

The fluorescence anisotropy ratio, $r(t)$, which indicates the anisotropy of the distribution of the excited probe, is defined as the difference between the two components.

$$r(t) = \frac{I_{VV}(t) - GI_{VH}(t)}{I_{VV}(t) + 2GI_{VH}(t)} \tag{1-1}$$

where G is the compensating factor and $I_{VV}(t) + 2GI_{VH}(t)$ is proportional to the total fluorescence intensity.

The fluorescence intensity from the excited probe, $\boldsymbol{M}$, in Figure 1-1 observed for each component is given as

$$i_{VV} \propto \cos^2\theta \tag{1-2}$$

$$i_{VH} \propto \sin^2\theta\cos^2\varphi \tag{1-3}$$

The ground-state probes are distributed isotropically in the system, so the experimentally observed fluorescence intensity for each component at $t = 0$ is given as

$$I_{VV}(0) = \frac{\int_0^{\frac{\pi}{2}} \cos^2\theta \cdot \sin\theta \cos^2\theta \, d\theta}{\int_0^{\frac{\pi}{2}} \sin\theta \cos^2\theta \, d\theta} = \frac{3}{5} \tag{1-4}$$

$$I_{VH}(0) = \frac{\int_0^{2\pi} \int_0^{\frac{\pi}{2}} \sin^2\theta \cos^2\varphi \cdot \sin\theta \cos^2\theta \, d\theta \, d\varphi}{\int_0^{2\pi} \int_0^{\frac{\pi}{2}} \sin\theta \cos^2\theta \, d\theta \, d\varphi} = \frac{1}{5} \tag{1-5}$$

Then, the initial anisotropy ratio $r(0) = 0.4$ is obtained for $G = 1$.

Since the ensemble average of $\cos^2 \varphi$ is 1/2 and time-independent, the time decay of $r(t)$ (the randomization of the excited probes) is given with θ as

$$r(t) = \frac{3 < \cos^2\theta > -1}{2} \tag{1-6}$$

With ϕ, which is the rotating angle during the lifetime of the excited state, instead of θ and $r(0)$, $r(t)$ is also represented as

$$r(t) = r(0) \frac{3 < \cos^2\phi > -1}{2} \tag{1-7}$$

The orientational autocorrelation function, $C_2(t)$, is defined as

$$C_2(t) = < P_2(0) P_2(t) > = \frac{3 < \cos^2\phi > -1}{2} \tag{1-8}$$

where $P_2(t)$ is the Legendre polynomial of the second order. It is noteworthy that the time decay of $r(t)$ directly corresponds to the orientational autocorrelation function $C_2(t)$. The rate of the rotational relaxation, that is, the chain mobility, is estimated from the correlation time (the relaxation time), T_m, of the autocorrelation function. T_m is defined as the time integral of the autocorrelation function, namely

$$T_m = \int_0^\infty C_2(t) dt = r(0)^{-1} \int_0^\infty r(t) dt \tag{1-9}$$

Next, by using the continuous excitation light, the steady-state measurement is carried out as follows.[22,23] The observed anisotropy ratio, $\bar{r}$, is given as

$$\bar{r} = \frac{\int_0^\infty I(t) r(t) dt}{\int_0^\infty I(t) dt} \tag{1-10}$$

where $I(t)$ is the fluorescence intensity. Suppose that either $I(t)$ and $r(t)$ can be

represented with one time constant, τ and τ_R, respectively,

$$I(t) = I_0 \exp(-t/\tau) \tag{1-11}$$

$$r(t) = r_0 \exp(-t/\tau_R), \tag{1-12}$$

then, the following equation holds.

$$\frac{1}{\bar{r}} = \frac{1}{r_0}\left(1 + \frac{\tau}{\tau_R}\right) \tag{1-13}$$

On the assumption that the hard sphere approximation holds for the rotational relaxation of the probe, the following equation is obtained.

$$\frac{1}{\bar{r}} = \frac{1}{r_0}\left(1 + \frac{k_B}{v}\frac{T}{\eta}\cdot\tau\right) \tag{1-14}$$

where k_B is the Boltzmann constant, v is the volume of the equivalent hard sphere, T is absolute temperature, η is the solvent viscosity. r_0 is obtained from the $1/\bar{r}$ vs. T/η plot according to eq 1-14 and τ_R is evaluated from eq 1-13.

1-2-2. Apparatus for the Fluorescence Depolarization Method

The measurement of time-resolved anisotropy decay was carried out by the single photon counting system. Figure 1-2 shows the schematic diagram of the apparatus. The second harmonic of Ti:sapphire laser (Spectra-Physics Tsunami) was used at a wavelength of 393 nm for poly(oxyethylene) (POE) or 397 nm for PS as a light source according to the absorption peak of the labeled fluorescent probe, anthryl group, and 4 MHz pulse was picked up by a pulse selector (Spectra-Physics Model 3980). The excitation light was vertically polarized through a π-phase plate and a polarizer (Glan-Thompson prism). The parallel and perpendicular fluorescence components to the plane of the excitation light, $I_{VV}(t)$ and $I_{VH}(t)$, were measured by a microchannel plate-photomultiplier tube (MCP-PMT) (Hamamatsu Photonics R3809) through an analyzer (Polaroid HNPB) and cutoff filters, B370 and SC42 for POE, Y-44 and V-42 (HOYA) for PS. $I_{VV}(t)$ and $I_{VH}(t)$ were measured alternately to avoid data distortions due to time drift. The signal of MCP-PMT was inputted to a time-to-amplitude converter (Ortec Model 457) as a start signal through a constant fraction discriminator (Ortec Model 583). The stop signal was the split fundamental laser

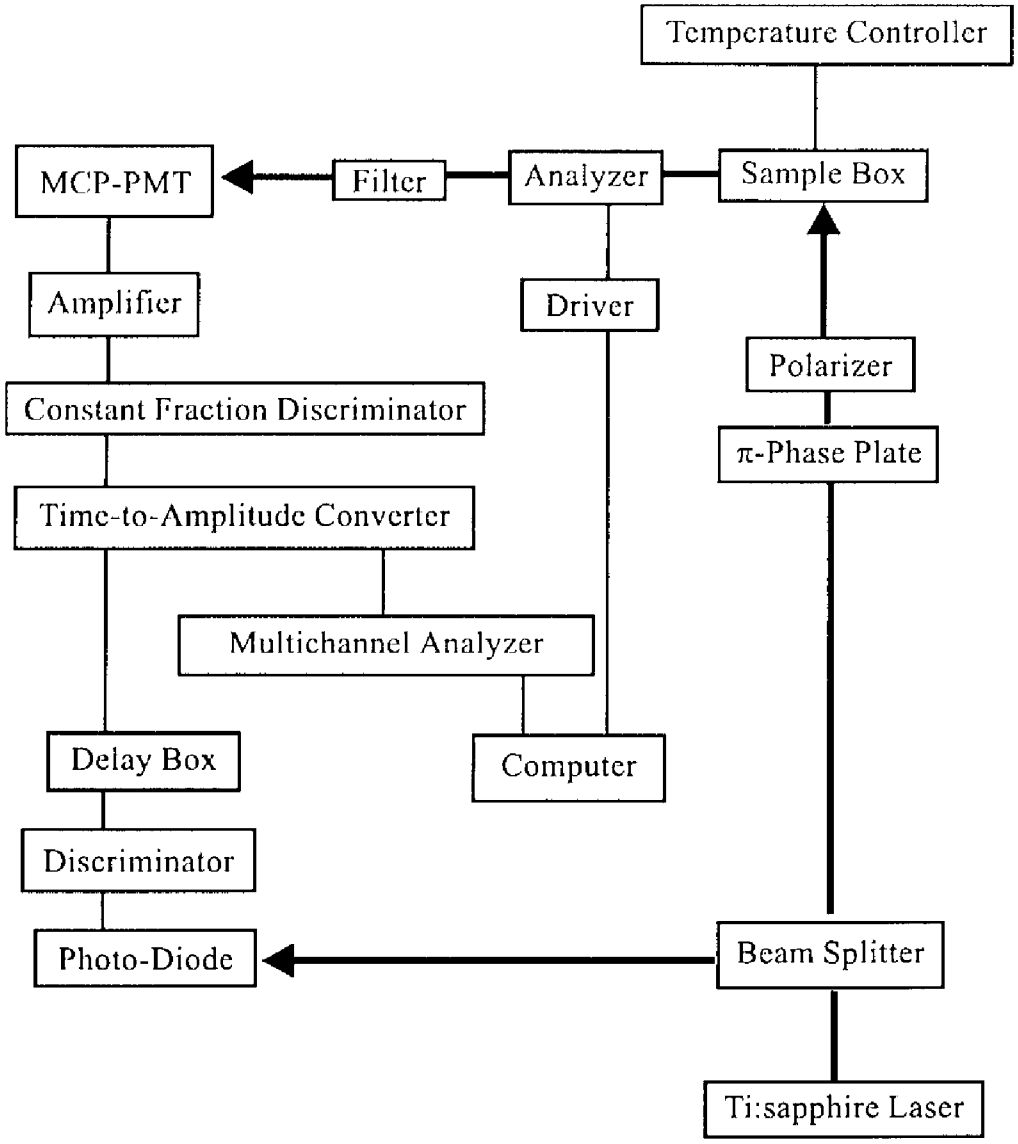

Figure 1-2. Block diagram of the single photon counting system used for the fluorescence depolarization method.

beam detected by a photo-diode (Antel Optronics AR-S2). The time-resolved fluorescence intensity was analyzed by a multichannel analyzer (Norland Ino-Tech 5300). The FWHM of the total instrumental function was measured by using Ludox as a scatterer and evaluated to be *ca.* 60 ps. The temperature of the sample box was controlled within ± 0.1 °C by the circulating water with a temperature controller (TOHO TM-104).

For the steady-state measurement, a spectrofluorophotometer (Hitachi 850) was used. The vertically-polarized continuous light from a Xe lamp at 400 nm was irradiated through a polarizer and the fluorescence intensity at 435 nm was continuously collected and the accumulated intensity of every 20 seconds was recorded for both the vertical and the horizontal components alternately through an analyzer.

1-2-3. Previous Fluorescence Depolarization Study on the Local Polymer Chain Motion

The local motion of the polymer chain has been extensively studied by the fluorescence depolarization method.[22-47] Monnerie et al. and Ediger et al. studied polystyrene (PS), polybutadiene, and polyisoprene: they were labeled with anthryl group as the fluorescent probe in the middle of the main chain. In our laboratory, Sasaki studied the local chain dynamics of poly(alkyl methacrylate)s and Ono examined that of polystyrene derivatives, polyisoprene, and poly(methyl methacrylate) mostly in dilute solutions. Many factors that influence the chain mobility were examined, e.g., the chemical structure,[26,43,45] stereoregularity,[46] molecular weight,[32,37,47] position along the chain,[27] solvent condition,[43,44,47] and solvent viscosity.[32,33,42] Nowadays, time-resolved measurement becomes popular with the development of the electronics including laser. The time-resolved decay function of the autocorrelation function is considered to include detailed information about the relaxation mode. The comparison of the decay data with models was also examined.[37]

1-3. MD Simulation

The computer simulation of the polymer chain dynamics has been extensively

utilized[71-82] and the results have been compared with theories[71-73] and experimental results.[74-82] Weber et al. carried out a Brownian dynamics (BD) simulation of polyethylene chain and analyzed the result with the Hall-Helfand model.[71-73] In this simulation, an ethylene unit was represented by a united mass center and only the interactions between the neighboring carbon atoms were considered. In the BD simulation, the effect of the medium (solvent or other polymer molecules) surrounding the carbon center is replaced by the Gaussianly distributed random forces. With the growth of the calculation capacity, more realistic systems have become available and various interactions between nonbonded atoms can be taken into consideration. Ediger et al. performed molecular dynamics (MD) simulations on polyisoprene, which is isolated,[80] in melt,[78] and in solution,[79] and poly(ethylene oxide) in toluene.[81,82] In these simulations, all the atoms were described explicitly and nonbonded interactions were modeled by a Lennard-Jones-like 6-9 potential and Coulombic partial charge terms. The results showed that the coupled libration as well as the conformational transition is important in the local polymer dynamics.[80-82] Moreover, the estimated reorientational correlation times for the local chain axis agree well with the trends obtained from NMR measurements. In this way, MD simulation is a promising technique in comparison with experimental results because of its atomic level information and the possibility in the precise representation of the system, but there remain future works to be solved. To compare with the experimental results, the size of the system, the duration time and the force field often needs further improvement.[83-85] In other words, one has to remember to check the validity of the result of the MD simulation by comparing with the experimental result. In this thesis, the MD simulation is carried out for the local motion of PS chain end and the result is compared with the result of the fluorescence depolarization study. MD simulation is also utilized to estimate the effect of the fluorescent probe and the molecular structure around the probe. Moreover, the effect of the direction of the transition moment of the fluorescent probe in the fluorescence depolarization study is estimated. The unique information from MD simulation helps the understanding of the local motion observed in the fluorescence depolarization method.

1-4. Motivation of This Thesis

Thanks to the accumulation of the previous data, the local chain dynamics has been understood deeper, but some problems still remain to be clarified. First, what is the length scale of the local motion? In this thesis, the issue is discussed with the molecular weight effect on the relaxation time of the local motion mainly in the low molecular weight region. The author previously studied the molecular weight effect on the local motion of *syndiotactic*-poly(methyl methacrylate) with two samples with MW = 2×10^4 and 1.5×10^5.[47] The relaxation time did not change with the increase of molecular weight in a good solvent, while the relaxation time increased with molecular weight in a poor solvent. It was concluded that the result was explained by the concept of the segment density in the vicinity of the fluorescent probe labeled in the middle of the main chain, that is, the segment density in a good solvent is kept constant due to the excluded volume effect. Previous to the study, Waldow et al. examined the molecular weight effect on the local chain dynamics of polyisoprene above molecular weight of 10^4.[32] They explained their result by the segment density and showed the molecular weight dependence of the segment density by simple calculations for both good and poor solvent conditions. However, it is considered that the relaxation time even in a good solvent will depend on the molecular weight in lower molecular weight region, and in a poor solvent, the relaxation time of the local motion will become constant at a certain higher molecular weight. In this thesis, these subjects are reexamined with oligo- and polystyrene. And second, how far is the local motion perturbed by the introduction of the fluorescent probe? The perturbation by the probe for the local motion is unavoidable in the fluorescence depolarization method. However, as for this subject, few works have been reported.[37,88] Pant et al. proposed the complex damped orientational diffusion model of local polymer chain motion including the effects of attached probes on the dynamics.[88] The relaxation time in the fluorescence depolarization study is also considered to be influenced by the molecular structure around the probe, that is, by the way how the probe is introduced in the polymer chain. In this thesis, the chain mobility of two kinds of polystyrene are compared and the effect of the molecular structure around the probe is discussed. Two kinds of polystyrene

have different chemical structure in the vicinity of the fluorescence probe in the middle of the main chain. In addition to the above subjects, the difference of the chain mobility by the position along the main chain is examined with chain center- and chain end-labeled PS samples. Monnerie et al. compared the relaxation time between two PS samples, one of which was labeled with anthryl group in the middle of the main chain and the other has the probe in the side chain.[27] The relaxation time of the side chain-type PS was shorter than that of the main chain-type PS. They compared the PS samples with respect to the direction of the transition moment to the polymer main chain. In this thesis, the chain mobility of the main chain center is compared with that of the main chain end with the main chain-type samples. Moreover, the subject concerning the direction of the transition moment is examined by MD simulation.

1-5. Outline of This Thesis

This thesis mainly aims to solve some problems remaining in the previous fluorescence depolarization studies. In Chapter 1, the backgrounds of the polymer chain dynamics, the fluorescence depolarization study, and MD simulation are described and the aim of this thesis is explained. In Chapter 2, 3, and 4, the local motion of poly(oxyethylene) (POE) and polystyrene (PS) in dilute solutions is examined by the fluorescence depolarization method. Figure 1-3 shows the molecular structure of the polymer samples used in these chapters, which is covalently labeled with anthryl group as a fluorescent probe in the main chain. In Chapter 5 and 6, MD simulations are utilized to elucidate the local motion of polystyrene chains in comparison with the fluorescence depolarization study. In Chapter 7, the fluorescence methods are applied to examine a phase separation system. In Chapter 8, the relationship between the molecular structure and the chain mobility is collected.

(a) POE

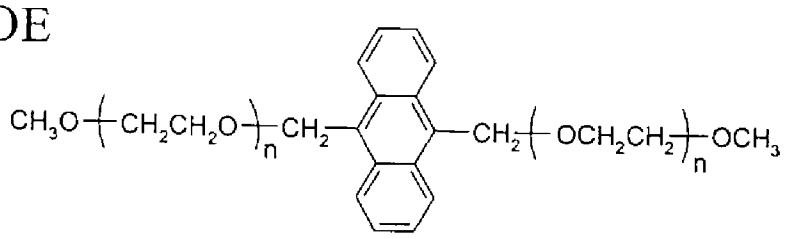

(b) a-PS

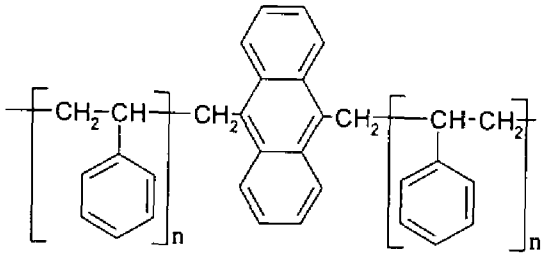

(c) r-PS

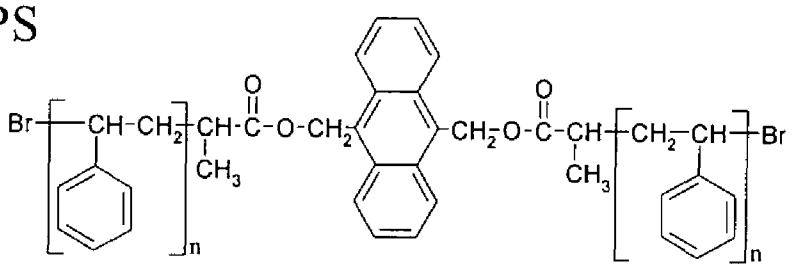

(d) e-PS

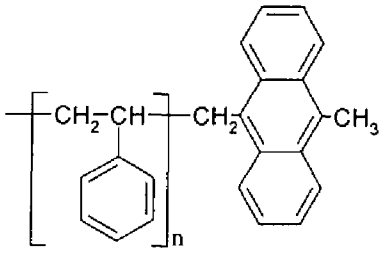

Figure 1-3. Molecular structures of the anthryl group-labeled samples used in the fluorescence depolarization study: (a) poly(oxyethylene); (b), (c) chain center-labeled polystyrene with different molecular structure around the probe; (d) chain end-labeled polystyrene.

In Chapter 2, the local motion of the chain center of POE chain in dilute solutions is examined by the fluorescence depolarization method. POE has no substituents attached to the main chain except hydrogen and the chain mobility is higher than that of other polymers which have larger substituents. The molecular weight effect is also examined and the length scale of the local motion is estimated to be 70 bonds.

In Chapter 3, the molecular weight effect on the local motion of PS is examined in dilute solutions by the fluorescence depolarization method. Four PS samples used in this chapter are labeled with anthryl group in the middle of the main chain (a-PS). The molecular weights of samples vary from ca. 6.4×10^3 to 9.2×10^4. The relaxation time for PS ($\cong$ 2 ns) is longer than that of POE ($\cong$ 0.3 ns) by about one order. The length scale of the local motion for PS (200 bonds) is accordingly longer than that for POE.

In Chapter 4, the local motion of the oligo- and polystyrene chain end (e-PS) in dilute solution is examined by the fluorescence depolarization method and the relaxation time and its molecular weight dependence are compared with those of the polystyrene chain center. The molecular weights of the sample vary from 5.1×10^2 to 2.5×10^4. The relaxation time of the chain end ($\cong$ 0.3 ns) is shorter than that of the chain center and the result shows that the chain mobility is considerably different with the position along the main chain. The length scale of the local motion of polystyrene chain end is estimated to be 40 bonds.

In Chapter 5, MD simulation of PS chain with anthryl group at the chain end surrounded by benzene molecules is performed and the results are compared with the experimental result on the local motion of PS chain end studied by the fluorescence depolarization method, which is described in Chapter 4. The molecular weight dependence of the relaxation time is estimated for the end-to-end vector as well as the probe vector. The result shows that the entire rotation of the polymer coil becomes more and more irresponsible for the relaxation of the probe vector with the increase of molecular weight. Furthermore, some sets of artificial restraints are put on some bond rotations and bond bending motions and the effect on the relaxation of the probe are estimated to obtain information about the effective motional modes for the local motion.

The cooperativity of the local motion for styrene chain is obtained. Finally, the difference of the chain mobility with the position along the PS main chain is examined.

In Chapter 6, perturbation of the fluorescent probe on the fluorescence depolarization study is examined by using MD simulation together with the fluorescence depolarization measurement. The relaxation times of the local motion for two series of PS (a-PS and r-PS), which have different molecular structure in the vicinity of the fluorescent probe, anthryl group, are compared. The relaxation time of a-PS is larger than that of r-PS by a factor of 2. In comparison with the fluorescence depolarization study, MD simulation of anthryl group-labeled PS chain is run for the cases of various numbers of methylene group between the probe and styrene unit. The results show that the molecular structure around the probe is important in the fluorescence depolarization method. The local motion of the probe-free PS is also simulated. Moreover, the effect of the direction of the transition moment in the fluorescent probe for the relaxation time is examined and it is concluded that the samples used in this thesis are appropriate for the measurement of the reorientation of the main chain bond.

In Chapter 7, the phase separation behavior of poly(ethoxyethyl vinyl ether) (PEVE) in aqueous solution is examined both below and above the phase separation temperature, T_{sp} (20 °C), with the fluorescence techniques including the fluorescence depolarization method. Figure 1-4 shows the molecular structure of the PEVE sample used in the fluorescence studies. The fluorescence intensity and lifetime decrease just below T_{sp}. On the other hand, the relaxation time for the local motion of PEVE estimated from the fluorescence depolarization measurement increases above T_{sp}. The dynamic fluorescence quenching disappeared by addition of a surfactant and the fluorescence lifetime increases up to the estimated value assuming no phase separation. Moreover, in both the hexane solution of PEVE and the PEVE bulk, no phase separation occurs and the fluorescence lifetime decreases monotonically and gradually with the increase of temperature. It is concluded that preceding the phase separation, the dynamic fluorescence quenching occurs by the collision between the fluorescent probe and the PEVE segments due to the thermal fluctuation of segment density. Then, at 20 °C, intra- and intermolecular aggregation due to the phase separation suppresses the

chain mobility and the dynamic quenching disappears.

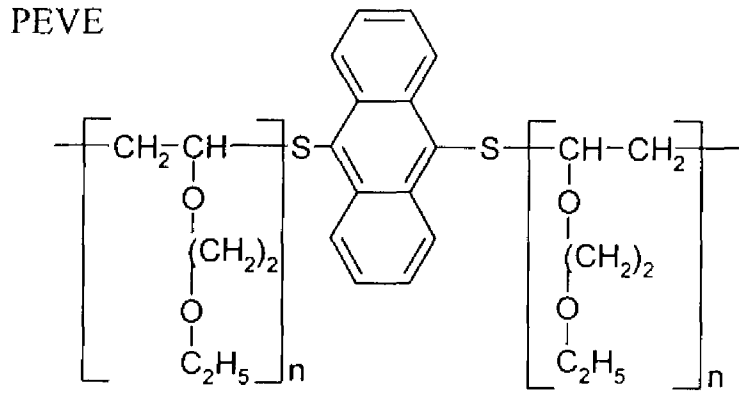

Figure 1-4. Molecular structure of poly(ethoxyethyl vinyl ether) (PEVE) with anthryl group labeled in the middle of the main chain.

In Chapter 8, the relaxation times of local motion for five kinds of polymers: *cis*-polyisoprene, PS, poly(α-methylstyrene), *syndiotactic*-poly(methyl methacrylate), and poly(*N*-vinylcarbazole) are measured in the Θ solvents by the fluorescence depolarization technique. The viscosity-reduced relaxation times are compared between these various polymers and the result shows that the larger substituents of a polymer the lower the chain mobility. The relationship between the relaxation time of the local motion and the glass transition temperature, T_g, of the bulk polymer is also proposed.

References

(1) Flory, P. J. *Statistical Mechanics of Chain Molecules*, Interscience: New York, 1969.

(2) Yamakawa, H. *Modern Theory of Polymer Solutions*, Harper & Row: New York, 1971.

(3) de Gennes, P. -G. *Scaling Concepts in Polymer Physics*, Cornell Univ. Press: Ithaca, N.Y., 1979.

(4) Ferry, J. D. *Viscoelastic Properties of Polymers 3rd Ed.*, John Wiley and Sons: New York, 1980.

(5) Doi, M.; Edwards, S. F. *The Theory of Polymer Dynamics*, Clarendon Press: Oxford, 1986.

(6) Matsuoka, S. *Relaxation Phenomena in Polymers*, Carl Hanser Verlag: New York, 1992.

(7) Yamakawa, H. *Helical Wormlike Chains in Polymer Solutions*, Springer-Verlag: Berlin, 1997.

(8) Doi, M.; Edwards, S. F. *J. Chem. Soc., Faraday Trans. II* **1978**, *74*, 1789; 1802; 1818.

(9) Rouse, P. E., Jr. *J. Chem. Phys.* **1953**, *21*, 1272.

(10) Zimm, B. H., *J. Chem. Phys.* **1956**, *24*, 269.

(11) Helfand, E. *J. Chem. Phys.* **1971**, *54*, 4651.

(12) Yamakawa, H.; Yoshizaki, T. *J. Chem. Phys.* **1981**, *75*, 1016.

(13) Hall, C. K.; Helfand, E. *J. Chem. Phys.* **1982**, *77*, 3275.

(14) Verdier, P. H.; Stockmayer, W. H. *J. Chem. Phys.* **1962**, *36*, 227.

(15) Iwata, K. *J. Chem. Phys.* **1973**, *58*, 4184.

(16) Valeuer, B.; Jarry, J. -P.; Geny, F.; Monnerie, L. *J. Polym. Sci., Polym. Phys. Ed.* **1975**, *13*, 667.

(17) Fixman, M. *J. Chem. Phys.* **1978**, *69*, 1527.

(18) Perico, A. *Acc. Chem. Res.* **1989**, *22*, 336.

(19) Moro, G. *J. Chem. Phys.* **1992**, *97*, 5749.

(20) Liao, T. -P.; Morawetz, H. *Macromolecules* **1980**, *13*, 1228.

(21) Mansfield, M. J. *J. Chem. Phys.* **1980**, *72*, 3923.

(22) Perrin, F. *Compt. Rend.* **1925**, *180*, 581; *181*, 514.

(23) Weber, G. *Biochem.* **1952**, *51*, 145.

(24) North, A. M.; Soutar, I. *J. Chem. Soc., Faraday Trans. I* **1972**, *68*, 1101.

(25) Soutar, I.; Swanson, L.; Christensen, R. L.; Drake, R. C.; Phillips, D. *Macromolecules* **1996**, *29*, 4931.

(26) Anufrieva, E. V.; Gotlib, Y. Y. *Adv. Polym. Sci.* **1981**, *40*, 1.

(27) Valeuer, B.; Monnerie, L. *J. Polym. Sci., Polym. Phys. Ed.* **1976**, *14*, 11.

(28) Viovy, J. L.; Curtis, W. F.; Monnerie, L.; Brochon, J. C. *Macromolecules* **1983**, *16*, 1845.

(29) Kasparyan, N. -T.; Valeuer, B.; Monnerie, L.; Mita, I. *Polymer* **1983**, *24*, 205.

(30) Valeuer, B.; Viovy, J. L.; Monnerie, L. *Polymer* **1989**, *30*, 1262.

(31) Viovy, J. -L.; Curtis, W. F.; Monnerie, L. *Macromolecules* **1985**, *18*, 2606.

(32) Waldow, D. A.; Johnson, B. S.; Hyde, P. D.; Ediger, M. D.; Kitano, T.; Ito, K. *Macromolecules* **1989**, *22*, 1345.

(33) Waldow, D. A.; Ediger, M. D.; Yamaguchi, Y.; Matsushita, Y.; Noda, I. *Macromolecules* **1991**, *24*, 3147.

(34) Adolf, D. B.; Ediger, M. D.; Kitano, T.; Ito, K. *Macromolecules* **1992**, *25*, 867.

(35) Nishijima, Y.; Teramoto, A.; Yamamoto, M.; Hiratsuka, S. *J. Polym. Sci., A-2* **1967**, *5*, 23.

(36) Teramoto, A.; Hiratsuka, S.; Nishijima, Y *J. Polym. Sci., A-2* **1967**, *5*, 37.

(37) Sasaki, T.; Yamamoto, M.; Nishijima, Y. *Macromolecules* **1988**, *21*, 610.

(38) Sasaki, T.; Yamamoto, M. *Macromolecules* **1989**, *22*, 4009.

(39) Yokotsuka, S.; Okada, Y.; Tojo, Y.; Sasaki, T.; Yamamoto, M. *Polym. J.* **1991**, *23*, 95.

(40) Sasaki, T.; Arisawa, H.; Yamamoto, M. *Polym. J.* **1991**, *23*, 95.

(41) Sasaki, T.; Nawa, K.; Yamamoto, M.; Nishijima, Y. *Eur. Polym. J.* **1989**, *25*, 79.

(42) Ono, K.; Okada, Y.; Yokotsuka, S.; Ito, S.; Yamamoto, M. *Polym. J.* **1994**, *26*, 199.

(43) Ono, K.; Okada, Y.; Yokotsuka, S.; Sasaki, T.; Ito, S.; Yamamoto, M. *Macromolecules* **1994**, *27*, 6482.

(44) Ono, K.; Ueda, K.; Yamamoto, M. *Polym. J.* **1994**, *26*, 1345.

(45) Ono, K.; Ueda, K.; Sasaki, T.; Murase, S.; Yamamoto, M. *Macromolecules* **1996**, *29*, 1584.

(46) Ono, K.; Sasaki, T.; Yamamoto, M.; Yamasaki, Y.; Ute, K.; Hatada, K. *Macromolecules* **1995**, *28*, 5012.

(47) Horinaka, J.; Ono, K.; Yamamoto, M. *Polym. J.* **1995**, *27*, 429.

(48) Yoshizaki, T.; Yamakawa, H. *J. Chem. Phys.* **1993**, *99*, 9145.

(49) Takaeda, Y.; Yoshizaki, T.; Yamakawa, H. *Macromolecules* **1994**, *27*, 4248.

(50) Takaeda, Y.; Yoshizaki, T.; Yamakawa, H. *Macromolecules* **1995**, *28*, 682.

(51) Stockmayer, W. H. *Pure Appl. Chem. Suppl. Macromol. Chem.* **1973**, *8*, 379.

(52) Mashimo, S.; Yagihara, S.; Chiba, A. *Macromolecules* **1984**, *17*, 630.

(53) Mashimo, S.; Winsor IV, P.; Cole, R. H.; Matsuo, K.; Stockmayer, W. H. *Macromolecules* **1983**, *16*, 965.

(54) Adachi, K.; Kotaka, T. *Macromolecules* **1984**, *17*, 120.

(55) Adachi, K.; Kotaka, T. *Macromolecules* **1985**, *18*, 466.

(56) Adachi, K. *Macromolecules* **1990**, *23*, 1816.

(57) Tsunashima, Y.; Nemoto, N.; Kurata, M. *Macromolecules* **1983**, *16*, 1184.

(58) Han, C. C.; Akcasu, A. Z.; *Macromolecules* **1981**, *14*, 1080.

(59) Kanaya, T.; Kawaguchi, T.; Kaji, K. *J. Chem. Phys.* **1993**, *98*, 8262.

(60) Gordon, R. G. *Adv. Mag. Res.* **1968**, *3*, 1.

(61) Lauprêtre, F.; Noël, C.; Monnerie, L. *J. Polym. Sci., Polym. Phys. Ed.* **1977**, *15*, 2127.

(62) Dejean de la Batie, R.; Lauprêtre, F.; Monnerie, L. *Macromolecules* **1988**, *21*, 2052.

(63) Glowinkowski, S.; Gisser, D. J.; Ediger, M. D. *Macromolecules* **1990**, *23*, 3520.

(64) Bullock, A. T.; Cameron, G. G.; Smith, P. M. *J. Phys. Chem.* **1973**, *77*, 1635.

(65) Shiotani, M.; Sohma, J.; Freed, J. H. *Macromolecules* **1983**, *16*, 1495.

(66) Winnik, M. A.; Redpath, A. E. C.; Richards, D. H. *Macromolecules* **1980**, *13*, 328.

(67) Winnik, M. A.; Redpath, A. E. C.; Paton, K.; Danhelka, J. *Polymer* **1984**, *25*, 91.

(68) Winnik, F. M. *Polymer* **1990**, *31*, 2125.

(69) Sasaki, T.; Yamamoto, M.; Nishijima, Y. *Makromol. Chem., Rapid Commun.* **1986**, *7*, 345.

(70) Ohno, K.; Fujimoto, K.; Tsujii, Y.; Fukuda, T. *Polymer* **1999**, *40*, 759.

(71) Helfand, E. *J. Chem. Phys.* **1978**, *69*, 1010.

(72) Helfand, E.; Wasserman, Z. R.; Weber, T. A. *Macromolecules* **1980**, *13*, 526.

(73) Weber, T. A.; Helfand, E. *J. Phys. Chem.* **1983**, *87*, 2881.

(74) Bahar, I.; Erman, B.; Monnerie, L. *Macromolecules* **1990**, *23*, 1174.

(75) Bahar, I.; Erman, B.; Monnerie, L. *Adv. Polym. Sci.* **1994**, *116*, 147.

(76) Gény, F.; Monnerie, L. *J. Polym. Sci., Polym. Phys. Ed.* **1979**, *17*, 131; 147.

(77) Ediger, M. D.; Adolf, D. B. *Adv. Polym. Sci.* **1994**, *116*, 73.

(78) Moe, N.; Ediger, M. D. *Polymer* **1996**, *37*, 1787.

(79) Moe, N.; Ediger, M. D. *Macromolecules* **1995**, *28*, 2329.

(80) Moe, N.; Ediger, M. D. *Macromolecules* **1996**, *29*, 5484.

(81) Fuson, M. M.; Ediger, M. D. *Macromolecules* **1997**, *30*, 5704.

(82) Fuson, M. M.; Hanser, K. H.; Ediger, M. D. *Macromolecules* **1997**, *30*, 5714.

(83) Jaffe, R. L.; Smith, G. D.; Yoon, D. Y. *J. Phys. Chem.* **1993**, *97*, 12745.

(84) Smith, G. D.; Jaffe, R. L.; Yoon, D. Y. *J. Phys. Chem.* **1993**, *97*, 12752.

(85) Paul, W.; Smith, G. D.; Yoon, D. Y. *Macromolecules* **1997**, *30*, 7772.

(86) Abe, A.; Furuya, H.; Mitra, M. K.; Hiejima, T. *Comp. Theor. Polym. Sci.* **1998**, *8*, 253.

(87) Allegra, G.; Ganazzoli, F.; Bontempelli, S. *Comp. Theor. Polym. Sci.* **1998**, *8*, 209.

(88) Pant, B. B.; Skolnick, J.; Yaris, R. *Macromolecules* **1985**, *18*, 253.

Chapter 2

Local Chain Dynamics of Poly(oxyethylene) Studied by the Fluorescence Depolarization Method

2-1. Introduction

The microscopic dynamics of the polymer chain essentially governs the macroscopic properties of polymers. Therefore, comprehension of the local polymer chain dynamics is an important fundamental subject in the polymer science. The chain motion, which results from the local conformational transitions, has relaxation times in the order of nano- to subnanoseconds.[1,2] Many experimental methods are available for investigation of such local chain motions, e.g., NMR,[3,4] ESR,[5,6] dielectric relaxation,[7-9] dynamic light scattering,[10,11] and fluorescence depolarization.[12-18,34] The fluorescence depolarization method applies to examine the relaxation behavior of a polymer chain directly through a fluorescent probe that is covalently bonded to the polymer chain. By using this method, the local chain dynamics of the polymers in dilute solutions has been examined,[12-17] e.g., styrene polymers,[13] methacrylate polymers,[12,17] and poly(*cis*-1,4-isoprene) (*cis*-PIP),[16] which is labeled with an anthryl group in the middle of the main chain. The influences of molecular structure,[13,15] stereoregularity,[14] and quality of solvent[13,15-17] on the chain mobility were discussed.

As for the relationship between the molecular structure and the local chain mobility, the series of styrene polymers,[13] polystyrene (PS), poly(α-methylstyrene) (PαMS), and poly(*p*-methylstyrene) (P*p*MS) were studied. In the Θ solvents, the relaxation time and the activation energy were compared among these polymers. The chain mobility was in the order of PS > P*p*MS > PαMS. The hydrodynamic volume of

the methyl group substituted at the α- or para-position increases the steric hindrance for the chain rotation, thereby suppressing the local chain mobility. Moreover the methyl group at the α position makes the energy hindrance for the chain rotation higher than that at the para position. The local chain dynamics for four kinds of polymers, *cis*-PIP, PS, PαMS, and *syndiotactic*-poly(methyl methacrylate) (*s*-PMMA) in each Θ solvent was also compared.[15] The local chain mobility estimated from the relaxation time and the activation energy were in the order of *cis*-PIP > PS > PαMS > *s*-PMMA. The size of the substituents attached to the main chain was concluded to be the predominant factor in the local chain mobility. From the standpoint of molecular structure, poly(oxyethylene) (POE) is an attractive polymer, i.e., it does not have a large substituent attached to the main chain (only hydrogen) and has an ether bond in the main chain. The main chain motion is little influenced by the substituents. Therefore, study of the local chain dynamics of POE by the fluorescence depolarization method should provide fruitful information.

On the other hand, POE is a unique industrial material because of its solubility both in water and in organic solvents and has been used in biomedical applications.[19] Regarding the interest in hydrophilicity of POE, the structural properties have been extensively examined in water.[20-29] Some experimental results suggested that the conformation of POE in an aqueous solution is a helix,[24,26,27] but others supported a random coil.[28,29] The conformational change of POE with the solvent has also been clarified by spectroscopic[26] and NMR[24] measurements.

Recently molecular dynamics (MD) simulations of POE have provided insight into the local conformation as well as the hydration of POE at the atomic level.[25,30] The solvent effects on the conformation and the dynamics have also been discussed from MD simulations. MD simulations were in good agreement with the experimental results. POE maintained a helical conformation in an aqueous solution, while in a benzene solution, the conformation quickly changed to a random coil.[30] Concerning dynamics, the bond vector reorientation, which had relaxation time in the picosecond order, was examined in water and in benzene.[30] Although MD simulation is useful for examining the conformational and dynamic properties at the atomic level, there are some problems, i.e., the molecular size, the potential energy function, and the duration

time available for simulation are limited by the calculation capacity. Therefore the local chain dynamics of POE, which is in the order of nanoseconds, has not yet been clarified and more detailed experimental studies are needed.

In this chapter, the local chain dynamics of POEs with various molecular weights in dilute solutions was examined. The relaxation time of local motion was evaluated and the molecular weight dependence was shown. The chain mobility of POE was also compared with those of other polymers mentioned above and the characteristics of the POE chain were discussed concerning the relationship between the local chain mobility and the molecular structure.

2-2. Experimental Section

2-2-1. Sample Preparation

Anthryl group-labeled POE samples used in this study were synthesized as follows. Poly(ethylene glycol) methyl ethers (m-PEGs) with a molecular weight of *ca.* 350, 550, 750, 2000, and 5000 were used as starting materials. m-PEGs of molecular weight of 350, 550, and 750 were purchased from Aldrich, and of 2000 and 5000 were given by NOF Co., Oleo Chem. Res. Lab. Each m-PEG was allowed to react with sodium hydride in benzene at 30 °C under reflux. The resulting sodium poly(ethylene glycoxide) was coupled with 9,10-bis(bromomethyl)anthracene in dimethylformamide (DMF) at 40 °C under stirring for several days. Both benzene and DMF were distilled

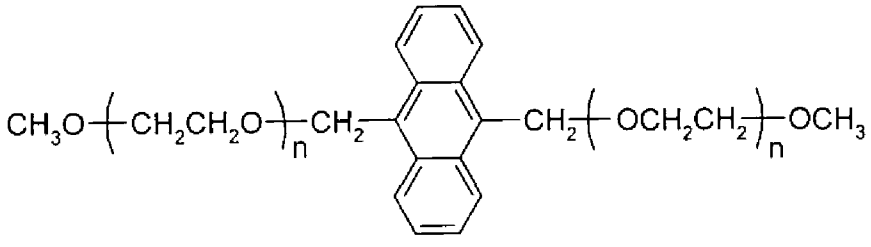

Figure 2-1. Molecular structure of POE sample labeled with anthryl group in the middle of the main chain.

by each conventional method before use. The higher molecular weight polymers obtained from m-PEG 2000 and 5000 were purified by reprecipitation from benzene in hexane. The others were used without purification for the measurement. The POE sample labeled in the middle of the main chain was fractionated from an incompletely labeled product by GPC. The molecular structure and the characterization of POE samples used in this study are shown in Figure 2-1 and Table 2-1, respectively. Standard POE (Scientific Polymer Products) was used to determine the molecular weight. The molecular weight ranges from *ca.* 800 to 10000.

Table 2-1. Characterization of Synthesized POE Used in This Study

	$M_w \times 10^{-3}$	$M_n \times 10^{-3}$	M_w/M_n
POE700	0.779	0.769	1.01
POE1000	1.18	1.03	1.14
POE2000	2.02	1.66	1.21
POE5000	5.30	5.01	1.06
POE10000	9.84	8.30	1.19

Solvents used in measurement were DMF (Dojin, spectrophotometric grade) and cyclohexanone (Wako, guaranteed grade). DMF was used without further purification and cyclohexanone was distilled before use. In preparing the sample solution, each polymer concentration was kept less than 10^{-5} M, so that the value of absorbance of sample solution at the wavelength of excitation was less than 0.1. The solution was put into a quartz cell and degassed.

2-2-2. Data Analysis

The fluorescence anisotropy ratio, $r(t)$, is defined as

$$r(t) = (I_{VV}(t) - GI_{VH}(t))/(I_{VV}(t) + 2GI_{VH}(t)) \quad (2\text{-}1)$$

where G is the compensating factor and was estimated to be unity in this study. For discussion about the chain mobility, the mean relaxation time, T_m, which is defined as eq 2-2, was used.

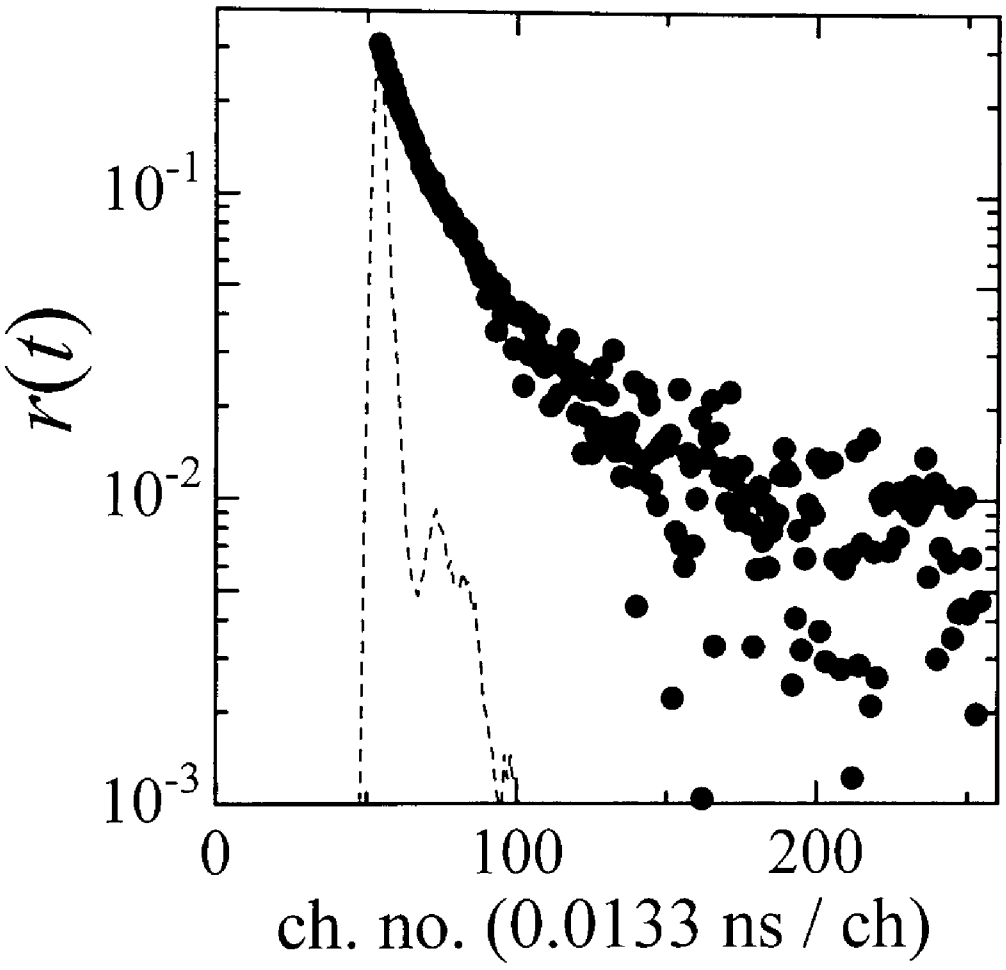

Figure 2-2. Example of measurement data for POE5000 in DMF at 13 °C; anisotropy ratio (filled circle) and the instrumental function (broken line).

$$T_m = r_0^{-1} \int_0^\infty r(t)dt \qquad (2\text{-}2)$$

2-3. Results and Discussion

2-3-1. Molecular Weight Effect of POE

Figure 2-2 shows an example of measurement data for POE5000 in DMF. The instrumental function, the broken line, has a shape narrow enough to measure the anisotropy decay of the relaxation time in the order of sub-nanoseconds. The solid line is the fitting function for the measured anisotropy ratio represented by the closed circle.

Figure 2-3 shows the molecular weight dependence of the relaxation time of POE in DMF at 13 °C. The open circle in Figure 2-3 indicates the rotational relaxation time of the model compound, 9,10-dimethyl anthracene (DMA), in DMF estimated by the steady-state measurement on the assumption that the hard sphere approximation holds. The rotational relaxation time of DMA can be treated as the limiting value of low molecular weight POE. Figure 2-3 shows that every POE used in this study has the relaxation time in the order of sub-nanoseconds. T_m increases with the molecular weight in the low molecular weight region and reaches an asymptotic value, T_m = 0.3 ns, at MW of about 1000.

Figure 2-3 indicates that the local motion of POE of MW < 1000 measured by the fluorescence depolarization method reflects the entire chain motion as well. The longer chain has a larger relaxation time for the entire rotation. On the other hand, the local motion in MW > 1000 is independent of the effect of the entire motion. In other words, this molecular weight, MW = 1000, corresponds to the longest length scale of the local motion of POE in DMF measured by the fluorescence depolarization method.

Bahar et al.[32,33] calculated the effects of chain connectivity on the local orientational motions in the flexible polyethylene chain according to the dynamic rotational isomeric state (DRIS) scheme. When the central bond of 20 bonds undergoes an isomeric transition, this rotation propagates along both sides of the mobile chain, leading to a displacement of 2 Å for each end. They concluded that such a

displacement is sufficiently small to be easily accommodated by compensating motions. In other words, the cooperative length scale of one-bond orientational motion is less than 20 bonds for the flexible chain.

The segment density around the fluorescent probe also affects the local chain dynamics.[13,15-17] The molecular weight effect on the local chain dynamics of *s*-PMMA of MW > 2×10^4 was examined in good solvents and showed that the local motion is not influenced by the change of molecular weight.[17] It was concluded that in a good solvent, the segment density about the chain center is kept constant because of the intramolecular excluded-volume effect. A similar tendency was also observed in a self-avoiding random walk calculation for PIP chain by Waldow et al.[18] DMF is a good solvent for POE, so that the segment density around the chain center of POE is kept constant in a high molecular weight region because of the intramolecular excluded-volume effect.[17,18] Therefore, the local chain dynamics of POE in DMF is independent of the molecular weight in a high MW region and T_m = 0.3 ns can be regarded as an asymptotic value.

Hence, POE5000 can be considered to have a large molecular weight enough to examine the local chain dynamics of the chain center. So, in the next section, the result for POE5000 was discussed as a representative one in the comparison with other polymers.

2-3-2. Comparison with Other Polymers

The relaxation time for POE5000 was compared with those for PS, PαMS, P*p*MS, *s*-PMMA, and poly(ethyl methacrylate) (PEMA) in cyclohexanone,[15] which is a good solvent for these polymers. Characterization of the polymers used for comparison is shown in Table 2-2. Each polymer has a molecular weight of ca. 10^5 or above. The difference in the molecular weight between POE and the others is not serious, because every polymer had a sufficiently high molecular weight for the study of the respective local motion.[12,17]

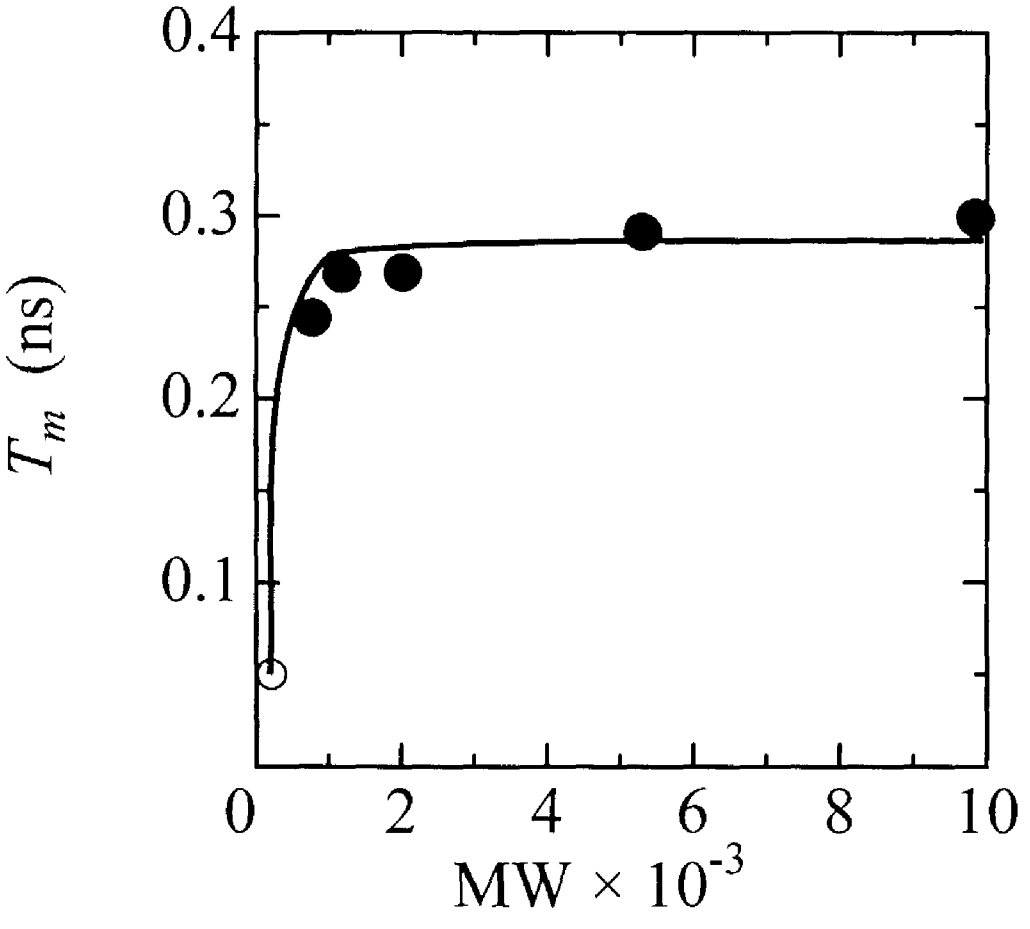

Figure 2-3. Molecular weight dependence of the relaxation time for POE (filled circle) and DMA (unfilled circle) measured in DMF at 13 °C. The rotational relaxation time of DMA was estimated by the steady-state measurement.

Table 2-2. Characterization of Polymers Used in This Study

Polymer	$M_w \times 10^{-4}$	$M_n \times 10^{-4}$	M_w/M_n	Ref.
POE	0.530	0.501	1.06	
PS	9.7	9.2	1.05	13
PαMS	21.5	20.5	1.05	13
P*p*MS	28.5	27.5	1.03	13
PEMA	17.7	15.7	1.12	15
PMMA	15.0	12.8	1.18	15
cis-PIP	14.5	13.1	1.10	16

Table 2-3 shows the relaxation time for each polymer in cyclohexanone at 13 °C. The value of T_m for POE is about of one order of magnitude smaller than those for other polymers, i.e., POE has a much higher local chain mobility than other polymers. This noticeable difference arises from the characteristic molecular structure of POE. POE does not have a large substituent attached to the main chain carbon (only hydrogen) compared with other polymers. Therefore, the local motion of POE is not suppressed by the steric hindrance between substituents and POE main chain shows high chain mobility. The tendency existed that the larger the substituent the more suppressed the chain mobility in the series of styrene polymers.[13] Moreover in the case of POE, the ether bond in the main chain contributes to the flexibility.[36]

Table 2-3. Mean Relaxation Time of POE in Comparison with Other Polymers

Polymer	T_m / ns
POE	0.55
PS	8.5
PαMS	10
P*p*MS	13
PEMA	13
PMMA	17

Measured in cyclohexanone, 13 °C.

Now let us mention the perturbation of the fluorescent probe to the chain dynamics. Since anthryl group in the middle of the main chain is larger than ethoxy unit, the fluorescent probe may perturb the local motion toward decreasing the chain mobility, comparing with unlabeled chain, but every sample has the same structure in the vicinity of the fluorescent probe. Hence, it can be said that the difference of the relaxation time comes from the molecular structure of polymer itself. Consequently the fluorescent probe does not perturb our conclusion that POE has high chain mobility because of its molecular structure. Further discussion about the perturbation of the probe is given in Chapter 6.

2-3-3. Activation Energy

Next, the activation energy for local motion was evaluated by the theory of Kramers' diffusion limit from the temperature dependence of relaxation time.[1] According to the theory, the velocity coefficient, k, of a particle with a frictional coefficient, ζ, passing over an energy barrier of the height E is represented as

$$k \propto \zeta^{-1} \exp(-E/RT), \tag{2-3}$$

where R is the gas constant and T is absolute temperature. The fact that T_m is proportional to the reciprocal of k and the solvent viscosity, η, is proportional to ζ, according to the Stokes' law, leads to

$$T_m/\eta = A\exp(E^*/RT). \tag{2-4}$$

Figure 2-4 shows T_m/η vs. $1/T$ plot for POE5000 in DMF. The viscosity at each temperature was estimated from the reported value in the literature.[31] The activation energy, E^*, was evaluated to be 1.1 kcal/mol from the slope of the plot. This value was compared with those for PS, *s*-PMMA, and *cis*-PIP in good solvents.[15,16] The characterization of *cis*-PIP is shown in Table 2-2.

Table 2-4 shows the value of the activation energy for each polymer. The value of E^* for POE is smaller than half of that for *s*-PMMA and slightly smaller than that for *cis*-PIP. This indicates that the local motion of POE has a lower energy barrier than other polymers. POE does not have a large side group, and the steric hindrance for local motion is not serious. That is, the high chain mobility was also supported by the comparison of the activation energy from the standpoint of the relationship between

the local chain mobility and the molecular structure.

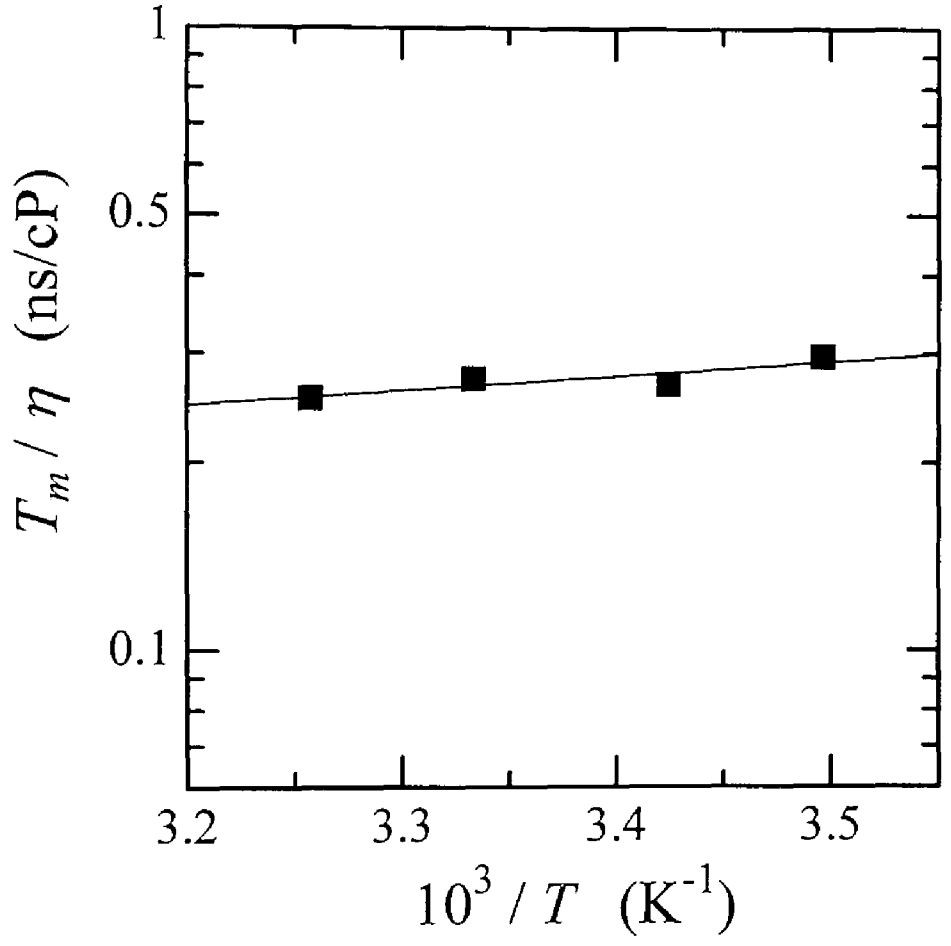

Figure 2-4. T_m/η vs. $1/T$ plot according to the theory of Kramers' diffusion limit. T_m was measured in DMF. The viscosity at each temperature was estimated from the reported value.

Table 2-4. Activation Energy of POE Local Motion in Comparison with Other Polymers

Polymer	E_a kcal / mol
POE	1.1
cis-PIP	1.2 - 1.3
PS	1.3 - 1.7
PMMA	2.4 - 2.7

Measured in good solvents.

Concerning the evaluation of the activation energy for local motion, some other approaches have been proposed.[16,37-43] In Kramers' theory the correlation time of the motion of the solvent particles is thought to be much shorter than that of the solute (polymer chain) so that the assumption of white noise holds and the local chain dynamics linearly depends on the zero frequency shear viscosity of the solvent. Grote and Hynes[44] removed the assumption of white noise and considered that the transition rate of solute depends on the friction of solvent at a frequency comparable to that of solute at the barrier. When the frequency at the barrier is quite high, effective friction is much smaller than the zero frequency shear viscosity of the solvent. That is, in such a case the effect of solvent viscosity is overestimated by Kramers' theory and the activation energy is underestimated. Fleming et al.[42,43] found that their photochemical isomerization rate data shows a power law dependence on the solvent viscosity with a power of less than unity. Bagchi and Oxtoby[45] calculated the multiplicative factor x, which is the ratio of the observed rate constant to the transition state rate constant, starting with generalized Langevin equation proposed by Grote and Hynes assuming time dependent friction and showed that a plot of x against zero shear viscosity can be fitted very well to the power law form proposed by Fleming et al. Ediger et al. showed that in the study of the local chain dynamics of PIP in a dilute solution the power law form also holds, i.e., $\tau_c \propto \eta^{0.75}$ at constant temperature in the fluorescence depolarization study,[38] while in NMR study[39] $\tau_c \propto \eta^{0.41 \pm 0.02}$. Accordingly, the activation energy was re-evaluated assuming that the power law dependence holds for the POE data, namely

$$T_m \propto \eta^{\alpha} \exp(E^* / RT) . \qquad (2\text{-}5)$$

α was estimated to be 0.69 at 13 °C from the gradient of the logarithm plot of T_m vs. η. Although only two solvents were used in this study, the value of α for POE is appropriate comparing with that for PIP by Ediger et al. Then the activation energy was re-evaluated to be 1.9 kcal/mol with α = 0.69. On the other hand, the power law dependence of the local dynamics on solvent viscosity results from the breakdown of the white noise assumption, and the value of α should change with the chain mobility and solvent viscosity. That is, α becomes small as the chain mobility and/or the solvent viscosity becomes high. DMA and cyclohexanone have viscosities of 1.0 cP and 2.6 cP at 13 °C, respectively. Hence α for POE in DMF should be larger than 0.69 and so the activation energy should be less than 1.9 kcal/mol. Ono et al.[16] examined whether Kramers' theory is valid for local motion of PIP in low viscosity (< 2 cP) solvents studied by the fluorescence depolarization method and obtained a power of unity instead of 0.75 by Ediger et al. Consequently as long as the chain mobility was compared in low viscosity solvents below 1 cP, the evaluation of activation energy with Kramers' theory is appropriate.

2-4. Conclusion

Anthryl group-labeled POE in the middle of the main chain was synthesized by coupling of sodium poly(ethylene glycoxide) with 9,10-bis(bromomethyl)anthracene. Five POE samples, which vary in molecular weight, were obtained and the local chain dynamics in dilute solutions was examined by the fluorescence depolarization method. The molecular weight effect on the relaxation time was observed below MW = 1000 and reached an asymptotic value at MW of about 1000. This molecular weight corresponds to the largest scale of the local motion measured by the fluorescence depolarization method. Next, the relaxation time for POE5000 was compared with those for PS, PαMS, P*p*MS, *s*-PMMA, and PEMA in cyclohexanone. POE has a sub-nanosecond relaxation time, which is shorter than one-tenth of those for other polymers. This high local chain mobility results from the molecular structure of the POE chain. The activation energy for local motion of POE was also compared with those for other

polymers including *cis*-PIP. POE has the lowest activation energy among the polymers compared. It was concluded that POE has high chain mobility because of the characteristic molecular structure. That is, POE does not have a large substituent attached to the main chain and has an ether bond in the main chain.

References

(1) Helfand, E. *J. Chem. Phys.* **1971**, *54*, 4651.

(2) Yamakawa, H. *Macromolecules* **1977**, *10*, 692.

(3) Glowinkowski, S.; Gisser, D. J.; Ediger, M. D. *Macromolecules* **1990**, *23*, 3520.

(4) Lauprêtre, F.; Noël, C.; Monnerie, L. *J. Polym. Sci., Polym. Phys. Ed.* **1977**, *15*, 2127.

(5) Bailey, R. T.; North, A. M.; Pethrick, R. A. *Molecular Motion in High Polymers*; Clarendon Press: Oxford, 1981.

(6) Bullock, A. T.; Cameron, G. G.; Smith, P. M. *J. Phys. Chem.* **1973**, *77*, 1635.

(7) Mashimo, S. *Macromolecules* **1976**, *9*, 91.

(8) Mashimo, S.; Winsor, P.; Cole, R. H.; Matsuo, K.; Stockmayer, W. H. *Macromolecules* **1986**, *19*, 682.

(9) Adachi, K. *Macromolecules* **1990**, *23*, 1816.

(10) Yoshizaki, T.; Yamakawa, H. *J. Chem. Phys.* **1993**, *99*, 9145.

(11) Takaeda, Y.; Yoshizaki, T.; Yamakawa, H. *Macromolecules* **1994**, *27*, 4248.

(12) Sasaki, T.; Yamamoto, M. *Macromolecules* **1989**, *22*, 4009.

(13) Ono, K.; Okada, Y.; Yokotsuka, S.; Ito, S.; Yamamoto, M. *Macromolecules* **1994**, *27*, 6482.

(14) Ono, K.; Sasaki, T.; Yamamoto, M.; Yamasaki, Y.; Ute, K.; Hatada, K. *Macromolecules* **1995**, *28*, 5012.

(15) Ono, K.; Ueda, K.; Sasaki, T.; Murase, S.; Yamamoto, M. *Macromolecules* **1996**, *29*, 1584.

(16) Ono, K.; Ueda, K.; Yamamoto, M. *Polym. J.* **1994**, *26*, 1345.

(17) Horinaka, J.; Ono, K.; Yamamoto, M. *Polym. J.* **1995**, *27*, 429.

(18) Waldow, D. A.; Johnson, B. S.; Hyde, P. D.; Ediger, M. D.; Kitano, T.; Ito, K. *Macromolecules* **1989**, *22*, 1345.

(19) *Poly(Ethylene Glycol) Chemistry*; Harris, J. M., Ed.; Plenum: New York, 1992.

(20) Bailey, F. E., Jr.; Callard, R. W. *J. Appl. Polym. Sci.* **1959**, *1*, 373.

(21) Bailey, F. E., Jr.; Koleske, J. V. *Polyethylene Oxide*; Academic Press: New York, 1976.

(22) Nakayama, H. *Bull. Chem. Soc. Jpn.* **1970**, *43*, 1683.

(23) Saeki, S.; Kuwahara, N.; Nakata, M.; Kaneko, M. *Polymer* **1976**, *17*, 685.

(24) Tasaki, K.; Abe, A. *Polym. J.* **1985**, *17*, 641.

(25) Tasaki, K. *J. Am. Chem. Soc.* **1996**, *118*, 8459.

(26) Matsuura, H.; Fukuhara, K. *J. Mol. Struct.* **1985**, *126*, 251.

(27) Matsuura, H.; Fukuhara, K. *Bull. Chem. Soc. Jpn.* **1986**, *59*, 763.

(28) Koenig, J. L.; Angood, A. C. *J. Polym. Sci.* **1970**, *8*, 1787.

(29) Maxfield, J.; Shepherd, I. W. *Polymer* **1975**, *16*, 505.

(30) Tasaki, K. *Macromolecules* **1996**, *29*, 8922.

(31) *Advances in Chemistry Series No. 29 Physical Properties of Chemical Compounds III*, Am. Chem. Soc. 1961.

(32) Bahar, I.; Erman, B.; Monnerie, L. *Macromolecules* **1990**, *23*, 1174.

(33) Bahar, I.; Erman, B.; Monnerie, L. *Adv. Polym. Sci.* **1994**, *116*, 147.

(34) Gény, F.; Monnerie, L. *J. Polym. Sci., Polym. Phys. Ed.* **1979**, *17*, 131; 147.

(35) Viovy, J. L.; Monnerie, L.; Brochon, J. C. *Macromolecules* **1983**, *16*, 1845.

(36) Flory, P. J. *Statistical Mechanics of Chain Molecules*; John Wiley and Sons: New York, 1969.

(37) Adolf, D. B.; Ediger, M. D.; Kitano, T.; Ito, K. *Macromolecules* **1992**, *25*, 867.

(38) Glowinkowski, S.; Gisser, D. J.; Ediger, M. D. *Macromolecules* **1990**, *23*, 3520.

(39) Ono, K.; Okada, Y.; Yokotsuka, S.; Ito, S.; Yamamoto, M. *Polym. J.* **1994**, *26*, 199.

(40) Velsko, S. P.; Fleming, G. R. *J. Chem. Phys.* **1982**, *76*, 3553.

(41) Velsko, S. P.; Waldeck, D. H.; Fleming, G. R. *J. Chem. Phys.* **1983**, *78*, 249.

(42) Grote, R. F.; Hynes, J. T. *J. Chem. Phys.* **1980**, *73*, 2715.

(43) Bagchi, B.; Oxtoby, D. W. *J. Chem. Phys.* **1983**, *78*, 2735.

Chapter 3

Molecular Weight Effect on Local Motion of Polystyrene Studied by the Fluorescence Depolarization Method

3-1. Introduction

The flexible polymer chain in dilute solutions has various motional scales with regard to time and space resulting from its high degree of intramolecular freedom. Because this chain dynamics governs a variety of properties of polymers, extensive experimental and theoretical efforts have been made to understand the polymer chain dynamics.[1-21] For the local motion, which is fairly a fundamental process in chain dynamics, many experimental methods have been utilized, e.g., NMR,[5-7] ESR,[8] dielectric relaxation,[9-11] dynamic light scattering,[12,13] neutron scattering,[14] and fluorescence depolarization.[15-21] The fluorescence depolarization method provides direct information about the local motion of polymer chains through a fluorescent probe that is covalently bonded to the polymer main chain. By using this method, the influence of molecular structure,[16,19] stereoregularity,[17] and quality of solvent[16,18] on the chain dynamics of a variety of polymers have been examined.

The local chain dynamics in dilute solutions is influenced by the molecular weight of the polymer in addition to those factors mentioned above. Concerning the fluorescence depolarization study, Waldow et al. have examined the molecular weight effect on polyisoprene (PI) chain dynamics and concluded that the chain dynamics is governed by the segment density in the vicinity of the fluorescent probe labeled in the middle of the main chain.[21] Previously, the molecular weight effect for poly(methyl methacrylate) samples was reported and the behavior of the local chain dynamics was

explained by the segment density as well.[19] The local chain dynamics of poly(oxyethylene) (POE) in good solvents was also reported and the molecular weight effect was discussed (Chapter 2).[20]

The static and dynamic properties of polystyrene (PS), a common polymer, have been widely studied.[2,6-9,16,17] The effects of the solvent quality on the local dynamics of PS[17] has been reported and the difference of the chain mobility for styrene derivative polymers was discussed.[16] From the standpoint of the molecular structure, it is interesting to compare the molecular weight effect of PS with that of POE, which is dynamically more flexible than PS.[20]

Monnerie et al. studied the molecular weight effect of PS on the local motion by NMR,[6] and concluded that the effect of the overall rotational diffusion is negligible on the spin-spin relaxation time of the local motion in a high molecular weight region and that the correlation time remains constant in $MW > 10^4$. Prior to Monnerie's work, similar findings have been reported by Allerhand and Hailstone,[7] Stockmayer and Matsuo,[9] and Bullock et al.[8] They all concluded that at high molecular weights the relaxation time of local motion is independent of chain length, while as the molecular weight decreases the end-over-end rotation contributes to the relaxation process.

In this chapter, the local motion of four PS samples in dilute solutions was examined by the fluorescence depolarization method. PS samples were labeled in the middle of the main chain with the anthryl group. The molecular weight effect on the chain dynamics of PS was examined in two solvents, and the molecular weight effect for PS was also compared with that for POE.

3-2. Experimental Section

3-2-1. Sample Preparation

Anthryl group-labeled PS samples used in this study were synthesized by the living anionic polymerization in vacuo initiated by butyllithium, in which the living ends were coupled with 9,10-bis(bromomethyl)anthracene. The polymerization was

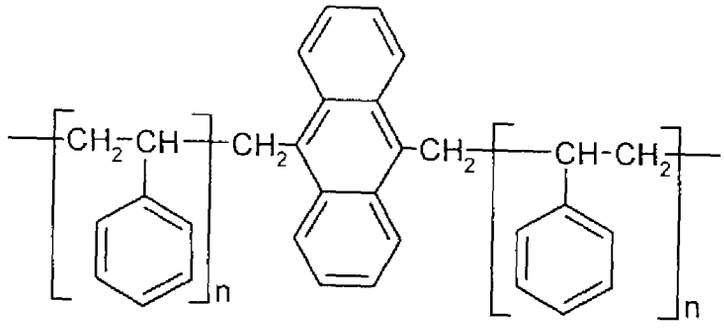

Figure 3-1. Molecular structure of the PS sample labeled with anthryl group in the middle of the main chain.

carried out at 40 °C (except aPS92) in benzene, which was dried over sodium. Styrene monomer (Nacalai Tesque) was dried over fresh calcium hydride after distillation. The coupling reaction was carried out at ca. 5 °C. The coupler, 9,10-bis(bromomethyl)anthracene, was dissolved in dried tetrahydrofuran before use. Further details of procedure appear elsewhere.[22] The product polymer was purified by reprecipitation from benzene in methanol. The incompletely coupled fraction was removed from the original sample by GPC. The weight-average molecular weight M_w and the number-averaged molecular weight M_n of fractionated PS were determined by GPC. Figure 3-1 and Table 3-1 show the molecular structure and the characterization of PS samples, respectively. aPS92 was the same sample used in previous studies.[16,17] The molecular weight distribution of all the samples was sufficiently narrow.

Table 3-1. Characterization of Polystyrene Samples Used in This Study

sample	$M_w \times 10^{-4}$	$M_n \times 10^{-4}$	M_w/M_n
aPS92	9.7	9.2	1.05
aPS69	7.2	6.9	1.04
aPS13	1.39	1.31	1.06
aPS6	0.72	0.64	1.13

Solvents used in measurements were benzene (Dojin, spectrosol) and ethyl acetate (Nacalai Tesque, spectrophotometric grade). Both were used without further purification. The quality of these solvents for PS was obtained by the intrinsic viscosity measurement.[17] Benzene ($\overline{\alpha_\eta}^3 = 1.66$) was a better solvent than ethyl acetate ($\overline{\alpha_\eta}^3 = 1.12$). In preparing the sample solutions, each polymer concentration was kept less than 10^{-5} M. Each solution was put into a quartz cell and degassed.

3-2-2. Data Analysis

The fluorescence anisotropy ratio, $r(t)$, is defined as

$$r(t) = (I_{VV}(t) - GI_{VH}(t))/(I_{VV}(t) + 2GI_{VH}(t)) \quad (3\text{-}1)$$

where G is the compensating factor and was estimated to be unity in this study. For discussion about the chain mobility, the integrated relaxation time, T_m, which is defined as eq 3-2 was used. T_m represents the average value of the relaxation times.

$$T_m = r_0^{-1} \int_0^\infty r(t)dt \quad (3\text{-}2)$$

where r_0 is the initial anisotropy ratio.

3-3. Results and Discussion

3-3-1. Relaxation Time

Figure 3-2 shows the molecular weight dependence of the reduced relaxation time T_m/η for PS in benzene and in ethyl acetate at 20 °C. Benzene was used as a good solvent and ethyl acetate was used as a poor solvent in this study. Note that the relaxation time T_m was reduced by the solvent viscosity η according to the theory of Kramers' diffusion limit. The solvent viscosity was estimated from the values reported in the literature:[25] 0.65 cP for benzene and 0.45 cP for ethyl acetate at 20 °C. The solvent viscosity dependence of the relaxation time was discussed repeatedly in the

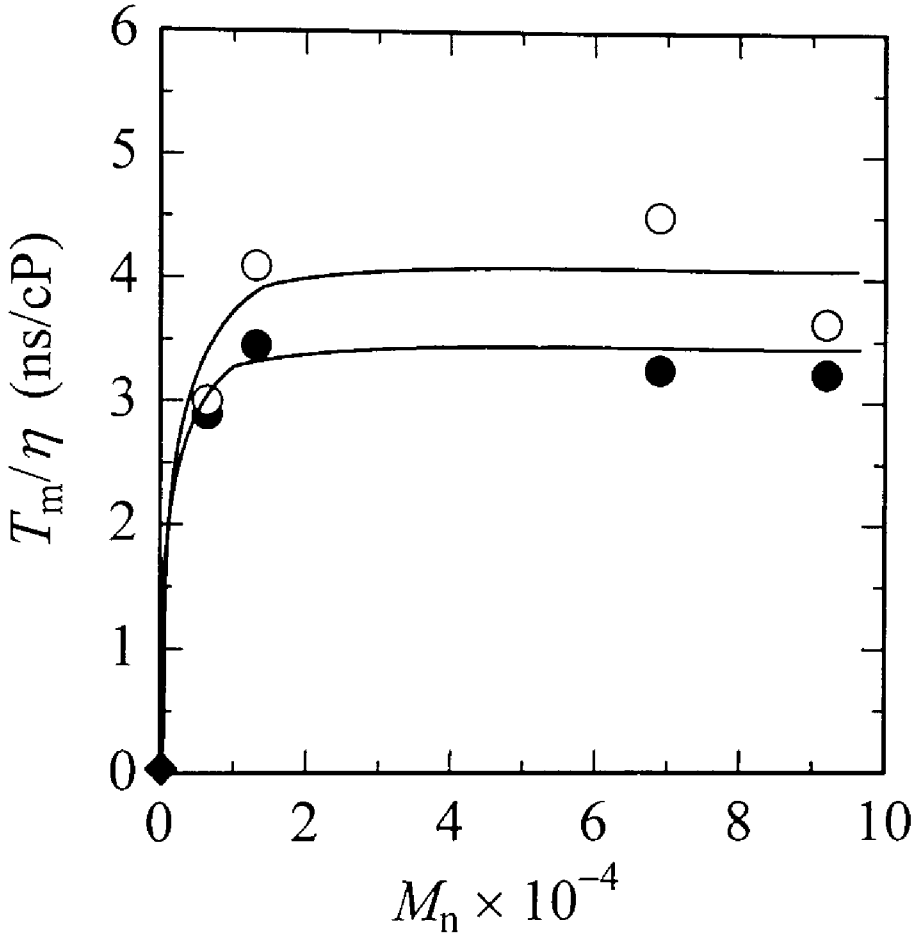

Figure 3-2. Molecular weight dependence of the reduced relaxation time T_m/η for PS at 20 °C: (●) in benzene; (○) in ethyl acetate. Filled diamond (◆) represents the rotational relaxation time of DMA, the probe molecule.

previous studies.[20,26-32] Consequently, the relaxation time for the local motion of PS labeled in the middle of the main chain in a low viscosity solvent below 1 cP is inversely proportional to the solvent viscosity, i.e., the Kramers' theory holds. The formulation of Kramers' theory is given in the following subsection. The filled diamond in Figure 3-2 indicates the reduced rotational relaxation time of the model compound, 9,10-dimethylanthracene (DMA), in benzene at 20 °C estimated by the steady-state measurement. The rotational relaxation time for DMA can be regard as the limiting value of low molecular weight PS. Figure 3-2 shows that T_m/η in each solvent increases with molecular weight and reaches an asymptotic value at about MW of 10^4. This indicates that the local motion, which contributes to the fluorescence depolarization, occurs within the scale of MW = 10^4. In other words, the local motion for PS of a higher molecular weight is independent of the entire rotational motion.

Waldow et al. showed that the relaxation time for the local motion of the chain center of PI does not change with molecular weight in a good solvent, whereas the relaxation time increases with molecular weight in a Θ solvent.[21] They explained these observations by the local segment concentration about the labeled segment. That is, the molecular weight independence of the relaxation time in a good solvent is due to the excluded-volume effect, which tends to keep segments which are far apart along the chain contour far separated in space. In a Θ solvent, where the excluded-volume effect is almost canceled, the local concentration increases with molecular weight. In the case of POE, the result that the relaxation time in a good solvent was kept constant against molecular weight in a high molecular weight region was similarly explained by the excluded-volume effect.[20] However in this study, the relaxation time in ethyl acetate (poor solvent) was almost constant against molecular weight as in benzene (good solvent) in a wide range of high molecular weight, i.e., the values of T_m/η near MW = 10^5 are almost equal to that for aPS13. Ethyl acetate is a poor solvent, and the coil expansion due to excluded-volume effect for high molecular weight PS is considered to be rather weak. Then the segment density of each molecular weight sample would be different, but this is not the case.

Abe et al. have studied the excluded-volume effects on the mean-square radius of gyration $\langle S^2 \rangle$ and on the intrinsic viscosity $[\eta]$ of oligo- and polystyrenes in dilute

solutions.[2,23,24] The values of $\langle S^2 \rangle$ and $[\eta]$ for *atactic*-PS (a-PS) in toluene at 15 °C were compared with those in cyclohexane at 34.5 °C (Θ) in the range of M_w from 5.78×10^2 to 3.84×10^6. They used the oligomer samples to realize an unperturbed state without intramolecular excluded-volume interaction even in a good solvent. In practice, they chose the solvent (toluene) and temperature (15 °C) so that the unperturbed dimension of the PS chain in a good solvent may coincide with that in the Θ condition taken as a reference standard. It was shown that, for the weight-average degree of polymerization $x_w < 20$, the data of both $\langle S^2 \rangle$ and $[\eta]$ in toluene at 15 °C are in good agreement with those in cyclohexane at Θ temperature. This agreement implies that the dimensions and conformations of the a-PS chain in the unperturbed state is considered the same under the two solvent conditions. For large x_w, the data points for the toluene solutions deviate progressively from those for the cyclohexane solutions with increasing x_w, clearly due to the excluded-volume effect. Their data show that the intramolecular interaction at $M_w = 10^5$ is sufficiently larger than that at $M_w = 10^4$, which leads to the difference in the segment density in the case of no or weak excluded-volume effect. Consequently, the segment density cannot explain the behavior of T_m/η in this study, because the relaxation time is almost constant in the high molecular weight region even in a poor solvent. Then, another reason will be proposed. The local motion consists of the conformational transition over the potential barrier and the librational motion within the potential well.[34] Therefore, there is a possibility that the local potential energy for the conformational transition of the main chain bond is affected by the solvent condition as well as by the molecular structure of each segment. The potential energy is a local factor compared with the segment density, so that it has no relation with the excluded-volume effect between the segments far apart.

Now the difference in the asymptotic T_m/η and in the critical molecular weight between two solvents, good and poor solvents, will be discussed. Figure 3-2 shows that the value of T_m/η for ethyl acetate solution is larger than that for benzene solution at each molecular weight. Figure 3-2 also shows that the critical molecular weight, M_c, at which T_m/η reaches its asymptotic value, is slightly larger in ethyl acetate. As mentioned above, it is considered that the difference between two solvents comes

from the difference in the potential energy for the local conformational transition due to the degree of chain expansion with the solvent quality. It is noteworthy that the difference in T_m/η is observed even for low molecular weight PS samples, aPS13 and aPS7. Abe et al. showed that the difference between the values of $<S^2>$ or $[\eta]$ in the two solvents is almost negligible below x_w of 10^2 ($M_w = 10^4$). So PS of MW $\cong 10^4$ can be considered nearly an unperturbed chain that is little influenced by the excluded-volume effect. The fact that the difference in T_m/η between solvents was observed even for nearly an unperturbed chain supports the proposition that the potential energy is the main governing factor of the local motion. The local potential energy is considered to affect the local motion even in the low molecular weight region. Although the relation between local potential energy and solvent condition is unclear, it is assumed that the poorer the solvent condition the higher the potential energy. The studies on the local motion of oligo- and polystyrene chain ends which supports this explanation more definitely will be reported in Chapter 6.[33]

The objection may be raised that above scheme supposing the difference in the potential energy between two solvents, in benzene and in ethyl acetate, is inconsistent with Abe's findings that the dimensions and conformations may be the same under the two solvent conditions in $x_w < 20$. This can be explained by the fact that the unperturbed chain dimension is not independent of solvent and temperature. That is, in our case, it is possible that the chain dimension is slightly different between the two solvents. Therefore, the difference in the value of the relaxation time and in its molecular weight dependence may be due to the difference in the local potential energy for the conformational transition of the main chain bond. In addition, the dynamic properties are influenced by both the value of energy potential minimum and the energy barrier height, while the static properties are influenced by the former.

Here, some comments are given on previous works. The suggestion in this study does not intend to deny the concept of the segment density proposed by Waldow et al.[21] In a previous study, it was shown that PI is dynamically more flexible than PS.[17] Therefore, the excluded-volume effect for PI may be more effective than that for PS and the local motion is mainly determined by the segment density in the high molecular weight region.

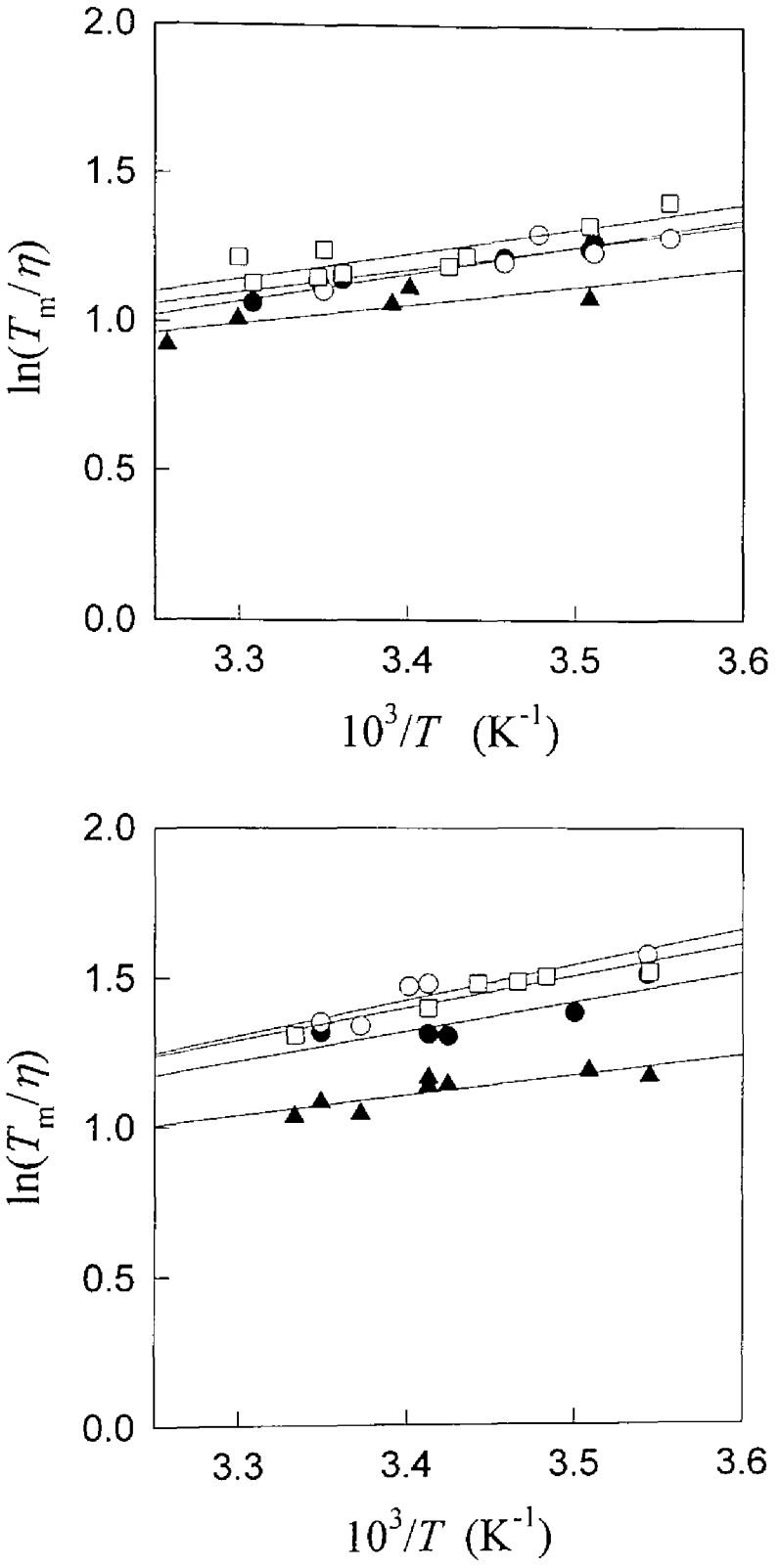

Figure 3-3. $\ln(T_m/\eta)$ vs. $1/T$ plot according to the theory of Kramers' diffusion limit. T_m was measured (a) in benzene, and (b) in ethyl acetate: (●) aPS92; (○) aPS69; (□) aPS13; (▲) aPS6.

3-3-2. Activation Energy

Next, the activation energy of the local motion was estimated according to the theory of Kramers' diffusion limit as follows.[1] Here the formulation of Kramers' theory is given. The velocity coefficient, k, of a particle with a frictional coefficient, ζ, passing over an energy barrier of the height E is represented as

$$k \propto \zeta^{-1} \exp(-E/RT), \tag{3-3}$$

where R is the gas constant and T is absolute temperature. The fact that T_m is proportional to the reciprocal of k and the solvent viscosity, η, is proportional to ζ, according to Stokes' law, leads to

$$T_m/\eta = A\exp(E^*/RT). \tag{3-4}$$

Figure 3-3 shows a temperature dependence of T_m for PS, (a) in benzene, and (b) in ethyl acetate solvents. The relaxation time T_m/η, which was reduced by the solvent viscosity, η, was plotted according to the theory of Kramers' diffusion limit so that the activation energies could be estimated from the slope of the plot in Figure 3-3.

Figure 3-4 shows the relationship between the molecular weight and the estimated activation energy in benzene. The activation energy as well as the relaxation time tends to increase with molecular weight and to become constant at MW $\cong 10^4$. The fact that the activation energy is constant in the high molecular weight region indicates that the mode of local motion is the same in the region. Figure 3-4 also shows that the activation energy in ethyl acetate is larger than that in benzene. This is due to the difference in the energy potential for the conformational transition.

3-3-3. Chain Length of Cooperative Motion

Finally, the molecular weight effect on the local motion of PS was compared with that of POE[20] and discuss the critical number of bonds, N_c, at which the relaxation time becomes constant. It is considered that the cooperative local motion of polymer chain operates up to this critical number of bonds and this value may indicate a kind of dynamic chain stiffness. Figure 3-5 shows the plots of T_m/η vs. number of bonds for both PS at 20 °C and POE at 13 °C in each good solvent. It shows that the value of reduced relaxation time for PS is larger than that for POE. For PS, this is due to the

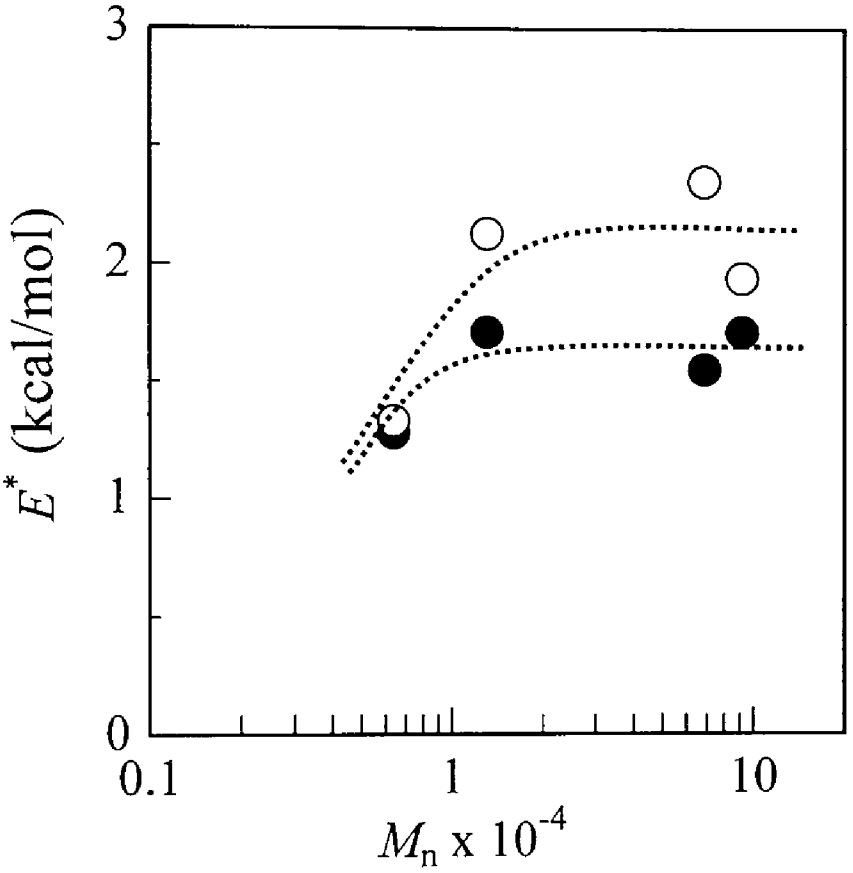

Figure 3-4. Molecular weight dependence of the activation energy E^* for PS estimated from the slope of the Arrhenius plot in Figure 3-3 (a) and (b): (●) in benzene; (○) in ethyl acetate.

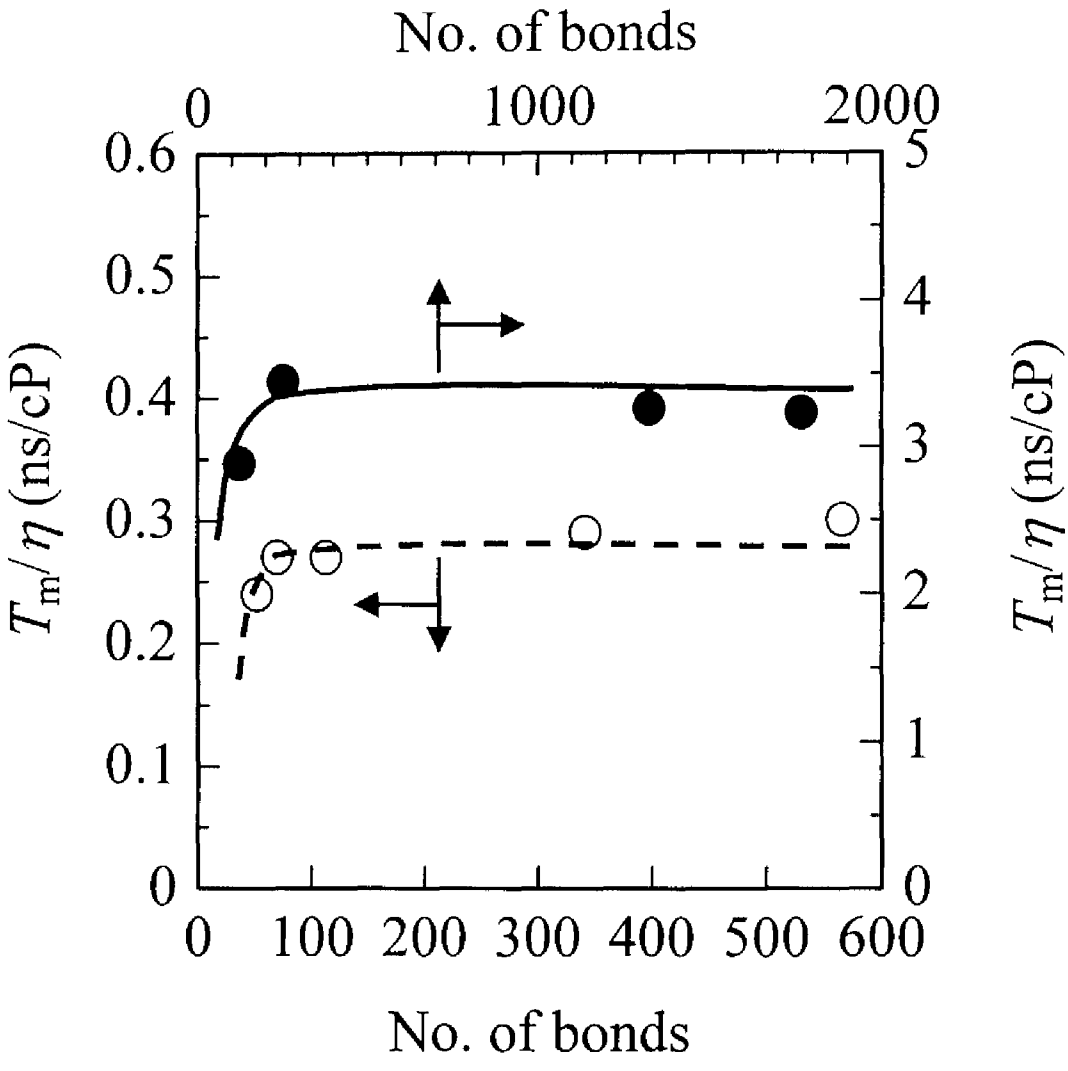

Figure 3-5. Relationship between the reduced relaxation time T_m/η and the number of bonds for PS in benzene (●) at 20 °C and POE in DMF (▲) at 13 °C.

large substituent attached to the main chain, the benzene ring.[20] Here, N_c of PS was compared with that of POE. N_c for POE was estimated to be ca. 70, while for PS, N_c is 200. That is, PS is dynamically stiffer than POE. The chain length of cooperative motion reflects the molecular structure of the monomer unit and closely correlates with the absolute value of the relaxation time above N_c.

3-4. Conclusion

The molecular weight effect on the local motion of PS labeled in the middle of the main chain in dilute solutions was studied by the fluorescence depolarization method. Four samples in the molecular weight from *ca.* 6.4×10^3 to 9.2×10^4, were synthesized by living anionic polymerization. Benzene was used as a good solvent, while ethyl acetate was used as a poor solvent. The relaxation time as well as the activation energy increased with molecular weight up to MW of 10^4 and reached an asymptotic value in both solvents. The critical molecular weight, M_c, corresponds to the largest size unit in the local motion measured by the fluorescence depolarization method. The difference in the relaxation time and molecular weight dependence between two solutions may result from the local potential for the conformational transition of main chain bond, rather than the segment density. The critical chain length of the local motion, which indicates a kind of the dynamic chain stiffness, of PS is larger than that of POE.

References

(1) Helfand, E. *J. Chem. Phys.* **1971**, *54*, 4651.

(2) Yamakawa, H. *Helical Wormlike Chains in Polymer Solutions*, Springer-Verlag: Berlin, 1997.

(3) Ferry, J. D. *Viscoelastic Properties of Polymers 3rd Ed.*, John Wiley and Sons: New York, 1980.

(4) Doi, M.; Edwards, S. F. *The Theory of Polymer Dynamics*, Clarendon Press: Oxford, 1986.

(5) Glowinkowski, S.; Gisser, D. J.; Ediger, M. D. *Macromolecules* **1990**, *23*, 3520.

(6) Lauprêtre, F.; Noël, C.; Monnerie, L. *J. Polym. Sci., Polym. Phys. Ed.* **1977**, *15*, 2127.

(7) Allerhand, A.; Hailstone, R. K. *J. Chem. Phys.* **1972**, *77*, 1635.

(8) Bullock, A. T.; Cameron, G. G.; Smith, P. M. *J. Phys. Chem.* **1973**, *77*, 1635.

(9) Stockmayer, W. H.; Matsuo, K. *Macromolecules* **1972**, *5*, 766.

(10) Mashimo, S.; Winsor, P.; Cole, R. H.; Matsuo, K.; Stockmayer, W. H. *Macromolecules* **1986**, *19*, 682.

(11) Adachi, K. *Macromolecules* **1990**, *23*, 1816.

(12) Yoshizaki, T.; Yamakawa, H. *J. Chem. Phys.* **1993**, *99*, 9145.

(13) Takaeda, Y.; Yoshizaki, T.; Yamakawa, H. *Macromolecules* **1994**, *27*, 4248.

(14) Kanaya, T.; Kaji, K.; Inoue, K. *Macromolecules* **1991**, *24*, 1826.

(15) Sasaki, T.; Yamamoto, M. *Macromolecules* **1989**, *22*, 4009.

(16) Ono, K.; Okada, Y.; Yokotsuka, S.; Sasaki, T.; Ito, S.; Yamamoto, M. *Macromolecules* **1994**, *27*, 6482.

(17) Ono, K.; Ueda, K.; Sasaki, T.; Murase, S.; Yamamoto, M. *Macromolecules* **1996**, *29*, 1584.

(18) Ono, K.; Sasaki, T.; Yamamoto, M.; Yamasaki, Y.; Ute, K.; Hatada, K. *Macromolecules* **1995**, *28*, 5012.

(19) Horinaka, J.; Ono, K.; Yamamoto, M. *Polym. J.* **1995**, *27*, 429.

(20) Horinaka, J.; Amano, S.; Funada, H.; Ito, S.; Yamamoto, M. *Macromolecules* **1998**, *31*, 1197.

(21) Waldow, D. A.; Johnson, B. S.; Hyde, P. D.; Ediger, M. D.; Kitano, T.; Ito, K. *Macromolecules* **1989**, *22*, 1345.

(22) Sasaki, T.; Yamamoto, M.; Nishijima, Y. *Makromol. Chem., Rapid Commun.* **1986**, *7*, 345.

(23) Abe, F.; Einaga, Y.; Yoshizaki, T.; Yamakawa, H. *Macromolecules* **1993**, *26*, 1884.

(24) Abe, F.; Einaga, Y.; Yamakawa, H. *Macromolecules* **1993**, *26*, 1891.

(25) Riddick, J. A.; Bunger, W. B. *Techniques of Chemistry II, Organic* Solvents, 3rd ed: Wiley-Interscience: New York, 1970.

(26) Adolf, D. B.; Ediger, M. D.; Kitano, T.; Ito, K. *Macromolecules* **1992**, *25*, 867.

(27) Glowinkowski, S.; Gisser, D. J.; Ediger, M. D. *Macromolecules* **1990**, *23*, 3520.

(28) Ono, K.; Okada, Y.; Yokotsuka, S.; Ito, S.; Yamamoto, M. *Polym. J.* **1994**, *26*, 199.

(29) Velsko, S. P.; Fleming, G. R. *J. Chem. Phys.* **1982**, *76*, 3553.

(30) Velsko, S. P.; Waldeck, D. H., Fleming, G. R. *J. Chem. Phys.* **1983**, *78*, 249.

(31) Grote, R. F.; Hynes, J. T. *J. Chem. Phys.* **1980**, *73*, 2715.

(32) Bagchi, B.; Oxtoby, D. W. *J. Chem. Phys.* **1983**, *78*, 2735.

(33) Horinaka, J.; Maruta, M.; Ito, S.; Yamamoto, M. *Macromolecules* submitted.

(34) Moro, G. J. *J. Chem. Phys.* **1992**, *97*, 5749.

Chapter 4

Local Motion of Oligo- and Polystyrene Chain End Studied by the Fluorescence Depolarization Method

4-1. Introduction

Every linear polymer has two main chain ends. The chain end has a large effect on the physical and chemical properties of polymers. From the standpoint of polymer physics, it becomes more and more widely recognized that the chain end has important roles in both static and dynamic properties. Yamakawa has considered the possible effects of the chain end on the second and third virial coefficient, and has shown semiquantitative agreement between theory and experiment.[1-3] There have been several ESR studies on polymer chain end mobility,[4,5,29-33] and obtained correlation times and activation energies for the chain end were compared with those for the chain center and the side chain.[29-32] Friedrich et al.[32] compared the mobility of polystyrene chain end estimated by ESR with the results obtained by other techniques. Recently, Sakaguchi et al. have observed the molecular motion of polyethylene chain ends tethered to a surface of poly(tetrafluoroethylene) by the ESR method and assigned molecular motion modes based on spectral simulations.[4,5] More generally, the dynamic properties of bulk polymer also depend sufficiently on the molecular weight due to the effect of the chain end.[6,7] For example, the glass transition temperature of a bulk polymer decreases as the molecular weight decreases due to larger free volume around a chain end compared with the middle segment. On the other hand, from the view of chemical reaction, the chain end is often the start point of the succeeding reactions, e.g., polymerization with another monomer, coupling with a functional group, and tethering

to a surface. In this case, information about the dynamics of the chain end is also important to control the molecular construction.

Although a study on the static or the dynamic properties with regard to the polymer chain end is no doubt important as mentioned above, it is difficult to pick up experimentally the information focused on the chain end effect. Nowadays experimental methods using spin or fluorescent probe techniques are powerful for such a purpose,[4,5,8-14] supposing that the sample labeled with a probe at a designated position can be obtained. The local chain dynamics of various polymers in dilute solutions have been examined by the fluorescence depolarization method.[9-14] So far, in our labolatory, attentions have been concentrated on the center of the main chain. The local chain mobility have been compared between polymers, which differ in molecular structure[9,10,12] or stereoregularity.[14] Since the dynamic properties of polymer chains depend on the position of polymer chains, the information on the polymer chain end is indispensable. It is interesting to compare the chain mobility between the chain center and the chain end on the same linear polymer.

Waldow et al. have studied the molecular weight effect on the local motion of polyisoprene (PI) by the fluorescence depolarization method.[8] They explained the molecular weight independence of the relaxation times in a good solvent and the molecular weight dependence in a poor solvent by the segment density around the fluorescent probe. That is, the segment density in a good solvent is kept constant in the high molecular weight region due to the excluded-volume effect, while in a poor solvent the density increases with the molecular weight. Recently, the molecular weight effect on the local motion of the chain center of poly(oxyethylene) (POE)[12] and polystyrene was examined.[13] For POE in a good solvent, the result was explained by the segment density according to Waldow et al. However, for polystyrene in both solvents, the relaxation time as well as the activation energy of the local motion increased with molecular weight below a MW of 10^4 and reached an asymptotic value. It was proposed that the relaxation time of local motion may be governed by the potential for the conformational transition of the main chain bond, rather than the segment density around the target of observation. It was also concluded that the critical molecular weight, at which the molecular weight dependence saturates,

corresponds to the largest size of the local motion measured by the fluorescence depolarization method as discussed previously.[28]

In this chapter, the local dynamics of the oligo- and polystyrene chain end in dilute solutions was examined by the fluorescence depolarization method. Solvents are the same as in Chapter 3,[13] benzene as a good solvent and ethyl acetate as a poor solvent. The molecular weight effect on the local motion of the chain end of oligo- and polystyrene (PS) was examined. Moreover, the relaxation times of the local motion for the chain center was compared with that for chain end. The size of the local motion which contributes to the fluorescence depolarization was estimated and compared with that of the chain center. Finally, the molecular weight dependence of the local motion of the styrene chain end was compared with that of the PS chain center.

4-2. Experimental Section

4-2-1. Sample Preparation

Oligo- and polystyrene samples labeled with the anthryl group at the chain end were synthesized by the living anionic polymerization in vacuo initiated by butyllithium and by termination of the living ends with 9-bromomethyl-10-methylanthracene. The polymerization was carried out in benzene that was dried over sodium in vacuo. The styrene monomer (Nacalai Tesque) was dried over fresh calcium hydride after distillation. For the polymerization of oligostyrenes, the benzene solution of butyllithium was first frozen. The styrene monomer was added to the frozen solution and the temperature of the mixture was gradually raised to slightly above the freezing point of the solution, ca. 7 °C, with occasional stirring. The retardation of the initiation reaction leads to broadening of the molecular weight distribution. In the case of polystyrene, styrene monomer was added to the benzene solution of butyllithium at ca. 7 °C with constant stirring. Then the termination reaction was carried out at ca. 5 °C. Detailed procedures were the same as described elsewhere.[15] The product polymer was purified by reprecipitation from benzene in methanol. Then the polymer was fractionated into several parts so that each part had a narrow molecular weight

distribution. The weight-average molecular weight M_w and the number-averaged molecular weight M_n of fractionated PS were determined by GPC. The molecular structure and the characterization of PS samples used in this study are shown in Table 4-1

Table 4-1. Characterization of End-Labeled Oligo- and Polystyrene Samples Used in This Study

Sample	$M_n \times 10^3$	M_w/M_n
DMA	0.206	-
eOS5	0.51	1.03
eOS6	0.60	1.01
eOS12	1.18	1.11
eOS24	2.4	1.27
eOS38	3.8	1.16
eOS66	6.6	1.06
ePS25	25.2	1.13

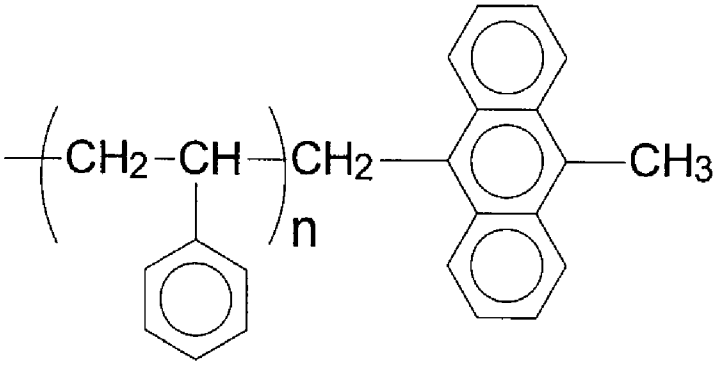

Figure 4-1. Molecular structure of oligo- and polystyrene labeled with anthryl group at the chain end.

and Figure 4-1, respectively. The molecular weight varies from ca. 5.1×10^2 to 2.5×10^4.

Solvents used in measurement were benzene (Dojin, spectrosol) and ethyl acetate (Nacalai Tesque, spectrophotometric grade). Both of them were used without further purification. The quality of these solvents for polystyrene was obtained by the intrinsic viscosity measurement in an earlier study.[9] Benzene ($\overline{\alpha_\eta}^3 = 1.66$) is better than ethyl acetate ($\overline{\alpha_\eta}^3 = 1.12$). In preparing the sample solution, each polymer concentration was kept less than 10^{-5} M. Each solution was put into a quartz cell and degassed.

4-2-2. Data Analysis

The fluorescence anisotropy ratio, $r(t)$, is defined as

$$r(t) = (I_{VV}(t) - GI_{VH}(t))/(I_{VV}(t) + 2GI_{VH}(t)) \quad (4\text{-}1)$$

where G is the compensating factor and was estimated to be unity in this study. For discussion about the chain mobility, the mean relaxation time, T_m, which is defined as eq 4-2, was used.

$$T_m = r_0^{-1} \int_0^\infty r(t)dt \quad (4\text{-}2)$$

where r_0 is the initial anisotropy ratio.

4-3. Results and Discussion

4-3-1. Relaxation Time

Figure 4-2 shows the temperature dependence of the relaxation time for oligo- and polystyrene in benzene. The logarithm of the relaxation time reduced by the solvent viscosity, $\ln(T_m/\eta)$, was plotted against $1/T$ according to the theory of Kramers' diffusion limit. Figure 4-2 shows that the values of $\ln(T_m/\eta)$ for eOS5 and eOS6 are sufficiently lower than those for the other samples. It is also clearly observed that the value and its temperature dependence for the higher molecular weight samples are the

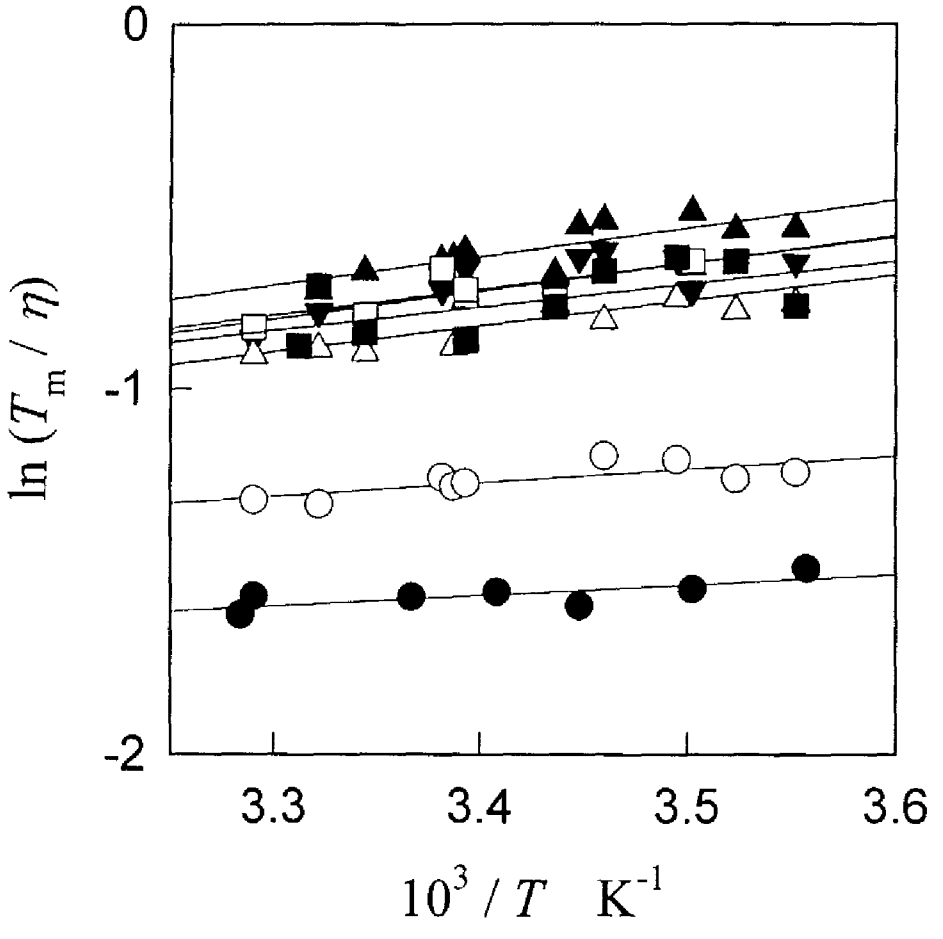

Figure 4-2. Arrhenius plot of T_m/η according to the theory of Kramers' diffusion limit. T_m was measured in benzene: (●) eOS5; (○) eOS6; (■) eOS12; (□) eOS24; (▲) eOS38; (△) eOS66; (▼) ePS25. Solvent viscosity at each temperature was estimated from the reported value in the literature.

same within the experimental error. These facts indicate that the relaxation time increases with molecular weight and reaches an asymptotic value in the oligomer region.

Figure 4-3 shows the relationship between T_m/η and MW at 20 °C. T_m/η at 20 °C was evaluated from the least-squares fitting for the plot in Figure 4-2. Figure 4-3 also shows the relaxation times in ethyl acetate; they were evaluated in the same way as those for benzene solution. The filled diamond in Figure 4-3 indicates the reduced rotational relaxation time of the model compound, 9,10-dimethylanthracene (DMA), in benzene at 20 °C estimated by the steady-state. The relaxation time of DMA can be treated as the limiting value of low molecular weight oligostyrene. The solvent viscosities at 20 °C are 0.65 cP for benzene and 0.45 cP for ethyl acetate.[18] The influence of the solvent viscosity on the local motion is discussed in the following subsection of the activation energy. T_m/η in benzene increases with molecular weight and reaches an asymptotic value at about MW = 2×10^3, with the asymptotic value of $T_m \cong 0.3$ ns. The local motion of oligo- and polystyrene chain end in benzene had the relaxation time in the order of subnanoseconds that saturates in the oligomer region. This indicates that the local motion of oligostyrene chain end in benzene measured by the fluorescence depolarization method reflects the entire end-to-end rotational motion to some extent in MW < 2×10^3, while the local motion is independent of the overall motion in MW > 2×10^3. In other words, the local motion of oligostyrene chain end in benzene consists of 20 monomers or less. The relaxation time for ethyl acetate solution similarly increases with molecular weight and reaches an asymptotic value at MW $\cong 4 \times 10^3$. The asymptotic T_m/η in ethyl acetate is larger than that in benzene. Figure 4-3 also shows that the critical molecular weight, M_c, at which the relaxation time reaches its asymptotic value, is somewhat larger in ethyl acetate than in benzene.

As mentioned in the introduction, concerning the local motion of PI and POE, the molecular weight dependence was explained by the concept of segment density.[8,12] That is, the relaxation time in a good solvent with a molecular weight in the high molecular weight region was constant because the segment density is kept constant in the high molecular weight region due to the excluded-volume effect. To the contrary, for the polystyrene chain center, the relaxation time became constant irrespective of the

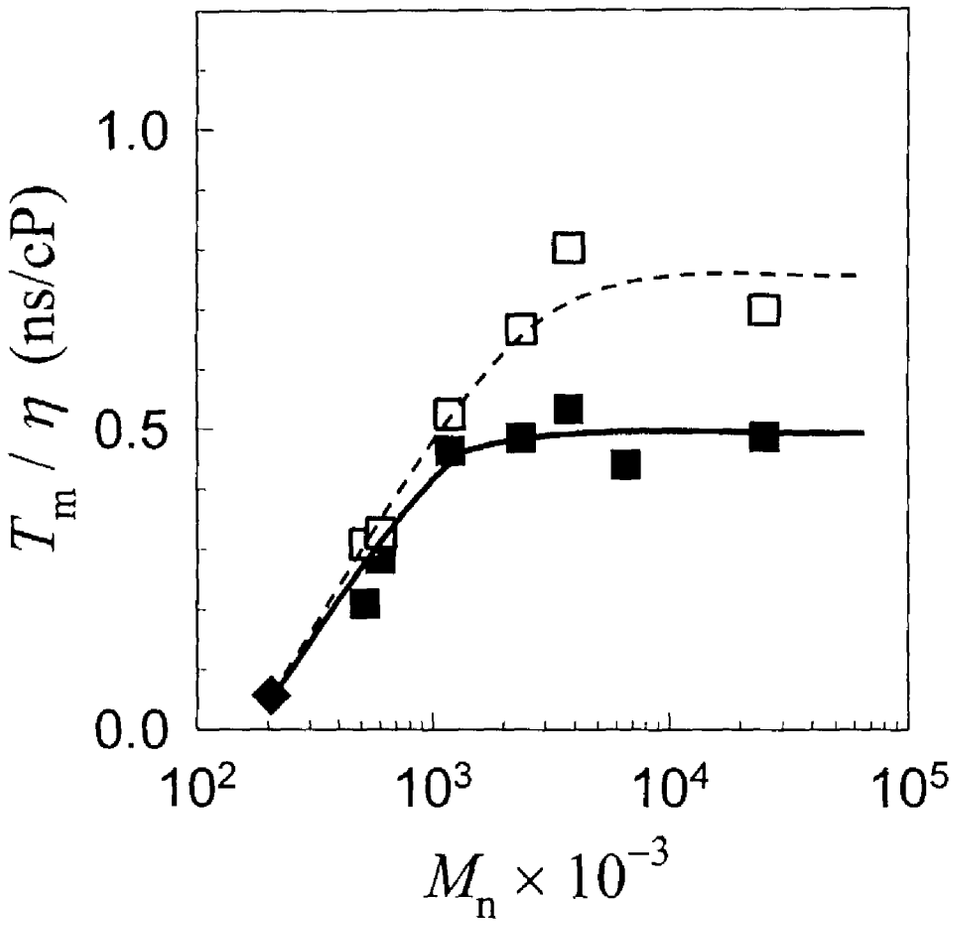

Figure 4-3. Molecular weight dependence of the relaxation time T_m/η at 20 °C in benzene (■) and in ethyl acetate (□). (◆) represents the rotational relaxation time for DMA, the probe molecule. The relaxation time was reduced by the solvent viscosity.

change of molecular weight even in a poor solvent.[13] Thus, the local potential for the conformational transition of the main chain bond was proposed as the cause instead of the concept of the segment.

Abe et al. have studied the excluded-volume effects on the mean-square radius of gyration $\langle S^2 \rangle$ and on the intrinsic viscosity $[\eta]$ for oligo- and polystyrenes in dilute solutions.[1,16,17] They showed that the data of both $\langle S^2 \rangle$ and $[\eta]$ in toluene, a good solvent, at 15 °C are in good agreement with those in cyclohexane at Θ for the weight-average degree of polymerization $x_w < 20$. This agreement implies that the dimensions and conformations of the polystyrene chain may be considered the same under the two solvent conditions and may be in the unperturbed state. In this way, oligostyrene in MW $< 2 \times 10^3$ is free from the intramolecular excluded-volume effect, and so the concept of segment density is not applicable. Figure 4-3 shows that the relaxation time for the oligostyrene chain end in each solvent reaches its asymptotic value in such a low molecular weight region. Moreover, the value of T_m/η for ethyl acetate solution is larger than that for the benzene solution over the whole measured molecular weight range. These facts obviously indicate that the local motion of the oligo- and polystyrene chain end is independent of the segment density, but that there is something local that causes the difference between the two solvents. According to the case of the PS chain center, it was proposed that the local potential energy for conformational transition of the main chain bond affects the local motion of the PS chain end. Although above scheme seems to be inconsistent with Abe's results that the dimensions and conformations are the same under the two solvent conditions in $x_w < 20$, the effect of the potential energy on the dynamic properties is different from that on the static one. That is, the dynamic property is influenced by both the value of energy potential minimum and the energy barrier height, while the static property is influenced by the former. Moreover, the unperturbed chain dimension is not independent of solvent and temperature. In this case, it is possible that the chain dimension is slightly different between the two solvents. At the present stage, the relationship between the local potential energy and solvent effect for C-C bond rotation so far has not been understood, and this is a future problem to be solved.

4-3-2. Activation Energy

The activation energy of the local motion of oligo- and polystyrene chain end in benzene was evaluated from the slope of the plot in Figure 4-2 according to the theory of Kramers' diffusion limit as follows. The velocity coefficient, k, of a particle with a frictional coefficient, ζ, passing over an energy barrier of the height E is represented as

$$k \propto \zeta^{-1} \exp(-E/RT), \tag{4-3}$$

where R is the gas constant and T is the absolute temperature. The fact that T_m is proportional to the reciprocal of k and the solvent viscosity, η, is proportional to ζ, according to Stokes' law, leads to

$$T_m/\eta = A\exp(E^*/RT). \tag{4-4}$$

Thus, the activation energies were estimated from the slope of the plot in Figure 4-2. The solvent viscosity was estimated from the value reported in the literature.[18]

Figure 4-4 shows the relationship between the molecular weight and the estimated activation energy in benzene solution. The activation energy as well as the relaxation time tends to increase with molecular weight and to become constant near MW = 2×10^3 with E^* = ca. 1.5 kcal/mol. The fact that the activation energy is constant in MW > 2×10^3 implies that the mode of the measured local motion is the same, i.e., independent of the molecular weight in this region. That is, the local motion of the oligo- and polystyrene chain end consists of 20 monomers or less as stated in the discussion for relaxation time.

The solvent viscosity dependence of the relaxation time previously have been discussed, i.e., whether the Kramers' theory can be applied to the measured local motion or not. In Kramers' theory the correlation time of the motion of the solvent particles is thought to be much shorter than that of the solute (polymer chain) so that the assumption of white noise holds and the local chain dynamics linearly depends on the zero frequency shear viscosity of the solvent. When the frequency of the solute at the barrier is quite high, effective friction is smaller than the zero frequency shear viscosity of the solvent. That is, in such a case the effect of solvent viscosity is overestimated by Kramers' theory and the activation energy is underestimated. Through some theoretical and experimental studies several groups have proposed a power law

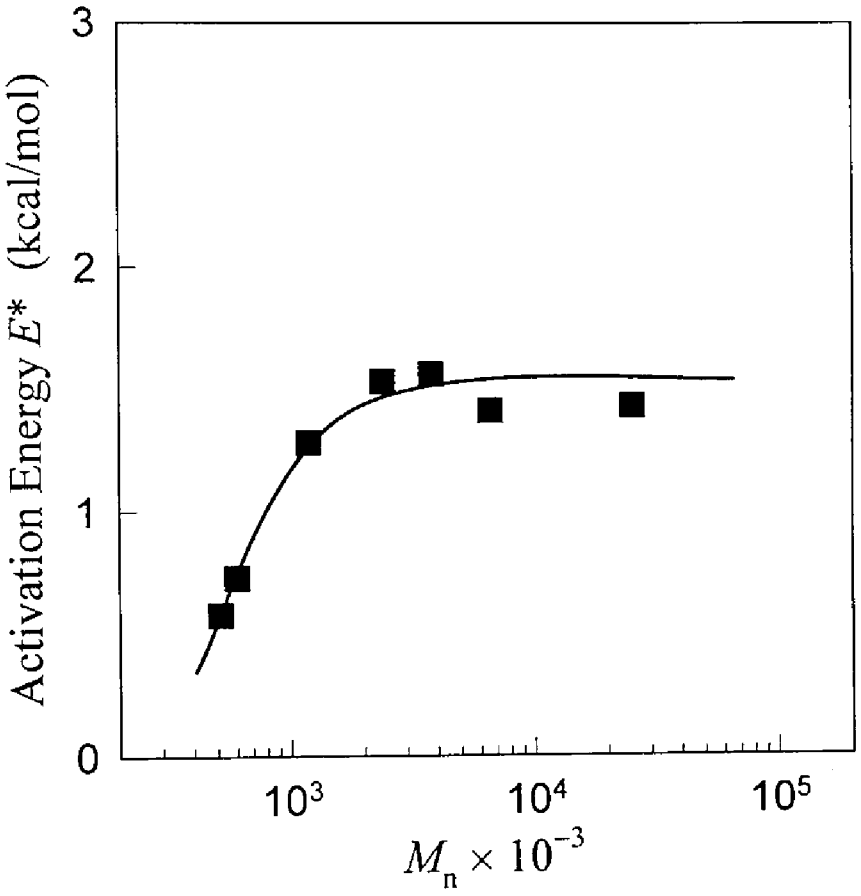

Figure 4-4. Molecular weight dependence of the activation energy for benzene solution evaluated from the temperature dependence of the relaxation time according to the theory of Kramers' diffusion limit.

dependence on the solvent viscosity with a power, α, of less than unity,[19-24] namely

$$T_{1} \propto \eta^{\alpha} \exp(E^{*} / RT) . \quad (7)$$

The power law dependence of the local dynamics on solvent viscosity results from the breakdown of the white noise assumption, so that α becomes small as the chain mobility and/or the solvent viscosity becomes high. However, the fact that the value of α should change with the chain mobility and solvent viscosity makes the estimation of α quite complicated. So far, it was concluded that as long as the local motion of polymer chain center, like polystyrene,[9,10,13] poly(methyl methacrylate),[11,14] and POE,[12] is examined in low viscosity solvents below 1 cP, the evaluation of activation energy with Kramers' theory is appropriate. In the case of POE,[12] the activation energy was estimated from the temperature dependence of the relaxation time of around 0.3 ns in a solvent with a viscosity of ca. 1 cP. In this study, the relaxation time for oligo- and polystyrene is ca. 0.3 ns and the solvent viscosity of benzene is 0.45 cP. That is, it is reasonable to assume that the local motion of oligo- and polystyrene chain end in benzene meets the requirement of Kramers' theory that the correlation time of the motion of the solvent particles is much shorter than that of the solute (polymer chain).

4-3-3. Comparison with Chain Center

Next, the local motion of oligo- and polystyrene chain end in benzene will be compared with that of the polystyrene chain center. Figure 4-5 shows the relationship between the relaxation time as well as the activation energy and the molecular weight both for the chain end and for the chain center. The values for polystyrene chain center in benzene were quoted from Chapter 3.[13] From Figure 4-5, it is clear that the asymptotic relaxation time for the chain end is markedly shorter than that for the chain center. That is, the chain mobility of the chain end is much larger than that of the chain center. It is believed that this result simply reflects the difference of the position along the main chain. At the chain end, the main chain extends in one direction from the fluorescent probe, anthryl-group, as shown in Figure 4-1, whereas at the chain center, the main chain extends in both directions of the probe. For the main chain motion, the neighboring bonds need to delocalize the distortion caused by a

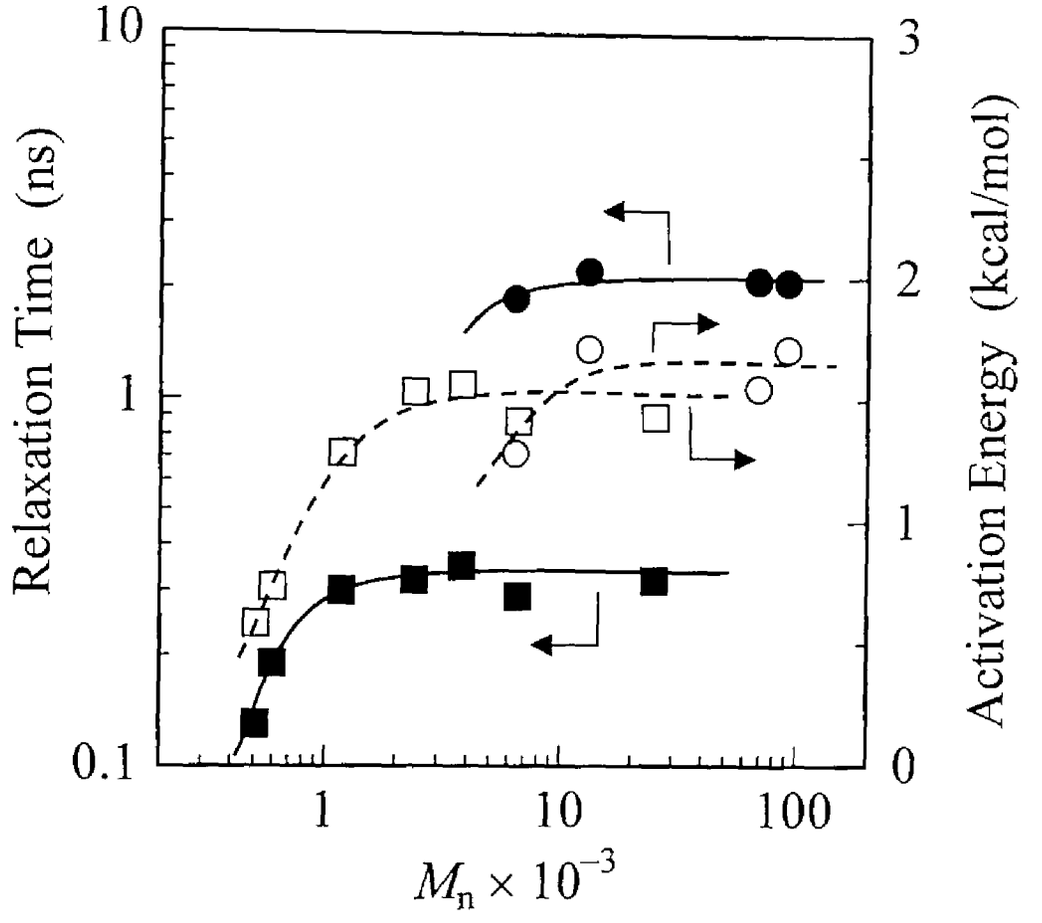

Figure 4-5. Comparison of the molecular weight dependence of the relaxation time and of the activation energy between oligo- and polystyrene chain end and chain center in benzene. Filled symbols represent the relaxation time and unfilled symbols represent the activation energy. (■) and (□) are for the chain end, while (●) and (○) are for the chain center.

certain conformational transition.[25,26] Therefore, for the chain center, the rotational relaxation of a fluorescent probe will be more efficiently suppressed.

The difference in the chain mobility between the chain end and the chain center also appears at the critical molecular weight, at which the relaxation time or the activation energy reaches its asymptotic value. Figure 4-5 shows that the critical molecular weight for the chain end (MW $\cong 2 \times 10^3$) is much smaller than that for the chain center (MW $\cong 10^4$). At the chain end, the rotational relaxation of the fluorescent probe can be realized by the small-scale local motion of an attached main chain due to the high chain mobility. In other words, the chain end is sufficiently flexible and the contribution of the entire rotation that corresponds to the critical molecular weight becomes negligible for the rotational relaxation of the probe.

Here, the activation energy will be discussed. Figure 4-5 shows that the asymptotic value of the activation energy for the chain end ($E^* \cong 1.5$ kcal/mol) is smaller than that for the chain center ($E^* \cong 1.7$ kcal/mol). The low activation energy for the chain end results in the high chain mobility to some extent. However, the difference in the activation energy between the chain end and the chain center is not so marked as compared to the difference in the relaxation time and in the critical molecular weight. Indeed the asymptotic relaxation time and the critical molecular weight nearly differ by one order between the chain end and the chain center. It was assumed that the activation energy is mainly determined by the size of the side group attached to the main chain.

The trend that polystyrene chain end has higher mobility than other chain positions was also observed by ESR.[29,31,32] For example, at room temperature, the correlation time (relaxation time) for the end-labeled polystyrene was about 2.2×10^{-10} s, whereas the correlation time for the ring-labeled one was 5.5×10^{-10} s.[31] They also differ in activation energies, that is, 2.9 and 4.5 kcal/mol for end-labeled and ring-labeled polystyrene, respectively.

4-4. Conclusion

The local motion of the oligo- and polystyrene chain end in dilute solutions was examined by the fluorescence depolarization method. Solvents used were benzene as a good solvent and ethyl acetate as a poor solvent. In each solvent, the relaxation time increases with molecular weight and reaches its asymptotic value in the oligomer region. The critical molecular weight and the asymptotic relaxation time for benzene solution were smaller than those for the ethyl acetate solution. It was suggested that these differences come from the energy potential for conformational transition or libration about the main chain bond, rather than the segment density, because the segment density has nothing to do with the chain mobility in the oligomer region. The local motion of the oligo- and polystyrene chain end was compared with that of the polystyrene chain center. The chain mobility for the chain end is much higher than that for the chain center, so that the relaxation time for the chain end is shorter by about one order. This indicates that the mobility of a linear polymer chain end is much different from that of its chain center.

References

(1) Yamakawa, H. *Helical Wormlike Chains in Polymer Solutions*, Springer-Verlag: Berlin, 1997.

(2) Yamakawa, H. *Macromolecules* **1992**, *25*, 1912.

(3) Yamakawa, H.; Abe, F.; Einaga, Y. *Macromolecules* **1994**, *27*, 3272.

(4) Sakaguchi, M.; Shimada, S.; Yamamoto, K.; Sakai, M. *Macromolecules* **1997**, *30*, 3620.

(5) Sakaguchi, M.; Shimada, S.; Yamamoto, K.; Sakai, M. *Macromolecules* **1997**, *30*, 8521.

(6) Fox, T. G.; Flory, P. J. *J. Appl. Phys.* **1950**, *21*, 581.

(7) Ferry, J. D. *Viscoelastic Properties of Polymers 3rd Ed.*, John Wiley and Sons: New York, 1980.

(8) Waldow, D. A.; Johnson, B. S.; Hyde, P. D.; Ediger, M. D.; Kitano, T.; Ito, K. *Macromolecules* **1989**, *22*, 1345.

(9) Ono, K.; Okada, Y.; Yokotsuka, S.; Sasaki, T.; Ito, S.; Yamamoto, M. *Macromolecules* **1994**, *27*, 6482.

(10) Ono, K.; Ueda, K.; Sasaki, T.; Murase, S.; Yamamoto, M. *Macromolecules* **1996**, *29*, 1584.

(11) Horinaka, J.; Ono, K.; Yamamoto, M. *Polym. J.* **1995**, *27*, 429.

(12) Horinaka, J.; Amano. S.; Funada, H.; Ito, S.; Yamamoto, M. *Macromolecules* **1998**, *31*, 1197.

(13) Horinaka, J.; Aoki, H.; Ito, S.; Yamamoto, M. *Polym. J.* in press.

(14) Ono, K.; Sasaki, T.; Yamamoto, M.; Yamasaki, Y.; Ute, K.; Hatada, K. *Macromolecules* **1995**, *28*, 5012.

(15) Sasaki, T.; Yamamoto, M.; Nishijima, Y. *Makromol. Chem., Rapid Commun.* **1986**, *7*, 345.

(16) Abe, F.; Einaga, Y.; Yoshizaki, T.; Yamakawa, H. *Macromolecules* **1993**, *26*, 1884.

(17) Abe, F.; Einaga, Y.; Yamakawa, H. *Macromolecules* **1993**, *26*, 1891.

(18) Riddick, J. A.; Bunger, W. B. *Techniques of Chemistry II, Organic* Solvents, 3rd

ed: Wiley-Interscience: New York, 1970.

(19) Grote, R. F.; Hynes, J. T. *J. Chem. Phys.* **1980**, *73*, 2715.

(20) Velsko, S. P.; Fleming, G. R. *J. Chem. Phys.* **1982**, *76*, 3553.

(21) Velsko, S. P.; Waldeck, D. H.; Fleming, G. R. *J. Chem. Phys.* **1983**, *78*, 249.

(22) Bagchi, B.; Oxtoby, D. W.; *J. Chem. Phys.* **1983**, *78*, 2735.

(23) Adolf, D. B.; Ediger, M. D.; Kitano, T.; Ito, K. *Macromolecules* **1992**, *25*, 867.

(24) Glowinkowski, S.; Gisser, D. J.; Ediger, M. D. *Macromolecules* **1990**, *23*, 3520.

(25) Fuson, M. M.; Ediger, M. D. *Macromolecules* **1997**, *30*, 5704.

(26) Fuson, M. M.; Hanser, K. H.; Ediger, M. D. *Macromolecules* **1997**, *30*, 5714.

(27) Helfand, E. *J. Chem. Phys.* **1971**, *54*, 4651.

(28) Lauprêtre, F.; Noël, C.; Monnerie, L. *J. Polym. Sci., Polym. Phys. Ed.* **1977**, *15*, 2127.

(29) Bullock, A. T.; Cameron, G. G.; Reddy, N. K. *J. Chem. Soc., Faraday Trans. 2* **1978**, *74*, 727.

(30) Yang, H. W. H.; Chien, J. C. W. *J. Polym. Sci., Polym. Symp.* **1978**, *63*, 263.

(31) Yang, H. W. H.; Chien, J. C. W. *Macromolecules* **1978**, *11*, 759.

(32) Friedrich, C.; Lauprêtre, F.; Noël, C.; Monnerie, L. *Macromolecules* **1981**, *14*, 1119.

(33) Shimada, S.; Suzuki, A.; Sakaguchi, M.; Hori, Y. *Macromolecules* **1996**, *29*, 973.

Chapter 5

Molecular Dynamics Simulation of Local Motion of Polystyrene Chain End; Comparison with the Fluorescence Depolarization Study

5-1. Introduction

Approaches to the polymer chain dynamics[1-12] are generally classified into three fields, that is, experiment, theory, and computational simulation. Since each approach has both advantages and disadvantages, it is meaningful to use more than one approach to elucidate the polymer chain dynamics.

The local motion of polymer chains in dilute solutions has already been studied by the fluorescence depolarization method.[4-8] It is a powerful technique for examining the local motion in the range of nano- to subnanoseconds. The chain mobility can be estimated through the rotational relaxation of the fluorescent probe used as a label in the main chain. In the time-resolved measurement, the decay of the fluorescence anisotropy ratio, which directly represents the orientational autocorrelation function of a unit vector pointing in the direction of the transition moment of the fluorescent probe, was observe. The behavior of decay includes the information of all the motional modes which contribute to the rotational relaxation of the probe, but is too complicated to separate into individual modes at the present stage.[8] Therefore, another technique is desirable for the further understanding of the results obtained by the fluorescence depolarization method. So far, many theoretical models which represent the local motion have been proposed,[4] but none of them are conclusive.

Molecular dynamics (MD) simulation has become a reliable approach for studying the polymer chain dynamics.[9-12] It provides the coordinates and velocities of every atom at each time step, so that various dynamic properties can be calculated at the atomic level. MD simulation generally requires a vast amount of calculation, so the system to be calculated is limited to a small size and a time scale of less than several nanoseconds. Moreover, the force fields used in MD simulation still need to be improved.[14,17-19] Therefore, it is important to compare the results obtained by the simulation with the corresponding experimental results. The C-H bond reorientation of polyisoprene[9] and the C-C and C-O bond torsions of poly(ethylene oxide)[11] obtained in the order of picoseconds by the MD simulation showed good agreement with those obtained by NMR measurements. Recently, the higher capacity of computers has enabled MD simulation of the local chain motion in solution. In other words, the MD simulation supports the results obtained by the fluorescence depolarization method. With the MD simulation, the effect of the fluorescent probe on the local motion studied by the fluorescence depolarization method was also estimated. This subject has been discussed in Chapter 4.[13]

In Chapter 4, the local motion at the PS chain end was studied by the fluorescence depolarization method.[8] The relaxation time of local motion, T_m, in benzene solution increased with the molecular weight and reached an asymptotic value at MW = 2×10^3 with $T_m \cong 0.3$ ns. It was proposed that the molecular weight dependence of the relaxation time results from the change of the local potential for the conformational transition of the main chain bond, rather than the segment density. Moreover, the mobility at the linear polymer chain end was found to be sufficiently different from that at its chain center.

In this chapter, MD simulations of the local motion at PS chain end in benzene was carried out and the results were compared with those obtained by the fluorescence depolarization study in Chapter 4. The molecular weight effects both on the local motion and on the end-to-end rotation were estimated and the contribution of the entire rotation to the local motion was discussed. Next artificial restraints were put on dihedrals and bond angles to estimate the contribution of a specific motional mode on the rotational relaxation of the probe at the chain end. Finally, the MD simulation of

PS chain which is free of the fluorescent probe was performed in vacuo and the difference of the mobility along the main chain was estimated.

5-2. Simulation Methodology

All the MD simulations were carried out with an MD software, Discover 3 (Biosym Technologies),[10,11] on a CRAY Origin 2000 supercomputer. All atoms of both the polymer and the solvent were explicitly represented. The force field used in this study was the class II force field, Biosym CFF91,[17] which took into account bond stretching, bond angle, dihedral, improper, and their seven cross-terms. The dielectric interaction was disregarded and a Lennard-Jones type 6-9 potential was used for nonbonded interactions.[17] The neglect of the dielectric interaction may be reasonable as a first simplification. By disregarding the long-distance interaction, the cutoff distance for nonbonded interactions was reduced to 6 Å. One femtosecond time steps were used in the calculation.

PS chains which had anthryl groups at their chain ends were initially generated using Insight II (Biosym Technologies). The molecular structure and the atom number are shown in Figure 5-1 (DP = 10). The A_9-A_{10} vector corresponds to the transition moment of anthracene, L_a,[20] and the rotational relaxation of this vector is observed by the fluorescence depolarization method. After 300 steps of minimization, dynamics calculations in vacuo were carried out to generate several different starting conformations for the subsequent dynamics simulation in benzene solution.

Then, the PS chain was soaked in benzene molecules with periodic boundary conditions. The molecular weight of PS and the number of benzene molecules were varied as shown in Table 5-1. The solvent molecules overlapping on the chain atoms were removed. After 300 steps of energy minimization, the molecular dynamics calculation was executed at the fixed temperature of 300 K. The total duration time of the dynamics run varied from 300 to 1000 ps according to the size of the system and the atomic coordinates used for analysis were saved every 100 to 1000 fs after at

Table 5-1. Characterization of the Solute, Number of Benzene Molecules, Total Duration Time, and Data Interval

DP	MW	No. of benzene	duration time / ps	data interval* / ps
0**	206	58	300	0.1
3	518	49	1000	1
5	726	105	1000	1
10	1246	95	1100	0.1
20	2286	165	1000	1

* Data of atom coordinates were acquired every "data interval".

** DP = 0 means 9,10-dimethylanthracene.

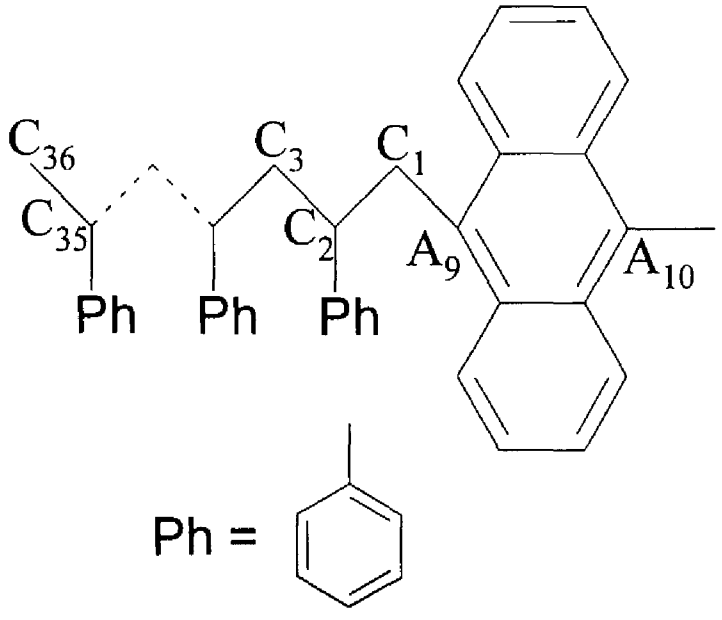

Figure 5-1. The molecular structure and atom number of polystyrene (DP = 10) with anthryl group at the chain end.

least 100 ps of discarded dynamics run for the randomization of the system. It was priorly confirmed that the 100 ps of initial dynamics run is long enough to randomize the system. More than three runs with different starting chain conformations were calculated for each system and the reproducibility was confirmed. The values designated for each system are summarized in Table 5-1. From the data of atom coordinates, the second-order orientational autocorrelation function, $C_2(t)$, for required vectors were calculated according to eq 5-1.

$$C_2(t) = \frac{<3(\mathbf{u}_{mn}(0)\cdot\mathbf{u}_{mn}(t))^2 - 1>}{2}$$

$$\mathbf{u}_{mn}(t) = \frac{\mathbf{r}_{mn}(t)}{r_{mn}(t)} \qquad (5\text{-}1)$$

$\mathbf{r}_{mn}(t)$ is a vector pointing in the direction from the A_9 to A_{10} atom or from the C_m to C_n atom.

Table 5-2. List of Atom Numbers Having Restraints on Dihedrals and Angles, and Resulting Relaxation Times

		dihedral(torsion)	angle(bending)	T_m / ps
polystyrene	run 1	none	none	49
	run 2	(A_9-C_3)	(A_9-C_2)	49
	run 3	(A_9-C_{12})	(A_9-C_{11})	106
	run 4	(C_9-C_{21})	(C_{10}-C_{21})	60
polyethylene	run 5	none	none	10
	run 6	(A_9-C_3)	(A_9-C_2)	23

Next, to examine the contribution of specific bond rotation and bond bending to the rotational relaxation of the probe, a restraint was applied using dihedrals of 180 ° and angles of 108 ° for the PS (DP = 10, see Figure 5-1) chain in benzene. The details of restraints are shown in Table 5-2. In Table 5-2, (A_9-C_3) of run 2 means that the dihedral between the A_9-C_1-C_2 plane and C_1-C_2-C_3 plane was set at 180 °, that is, the rotation at the C_1-C_2 bond was restrained. The symbol (A_9-C_{12}) of run 3 means that the

rotations at the all the bonds between C_1 and C_{11} (closed half of main chain) were restrained. Similarly, (A_9-C_2) of run 1 was a restraint for the angle between the A_9-C_1 bond and C_1-C_2 bond, so that the bending motion of these bonds was restrained. In Discover 3, the setting of the restraint means the addition of a new potential energy and in this study a quadratic potential was applied with a force constant K = 1000. By this restraint, dihedral and angle were restricted around the set value and fluctuated mostly within one degree. The dynamics was run for 500 ps at 300 K. With the data of atom coordinates saved after every 1 ps, $C_2(t)$ for the A_9-A_{10} vector was calculated. As a reference, the MD simulation of polyethylene chain labeled with an anthryl group at the chain end in benzene molecules was performed both with and without the restraints (Table 5-2).

Finally, the difference of the mobility with the position along the main chain was simulated. The molecular dynamics of a 22mer of PS which has no anthryl group was calculated in vacuo at 300 K for 3100 ps and the autocorrelation function of several vectors pointing in the direction connecting the second nearest atoms along the main chain were calculated. That is, the C_{22}-C_{24} vector in Figure 5-2 is at the chain center and the vector from the chain center vector to both the C_2-C_4 and the C_{42}-C_{44} vectors were treated as 10 monomer units.

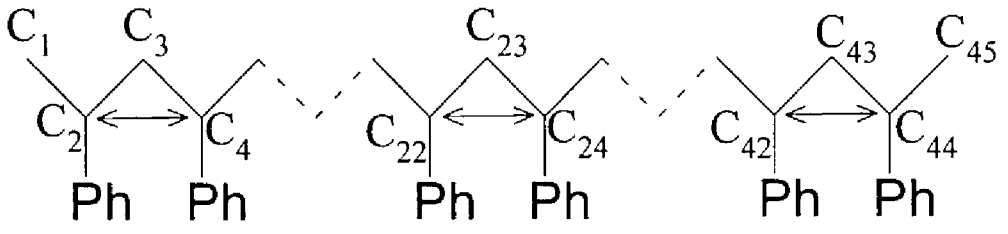

Figure 5-2. Molecular structure and atom number of polystyrene without anthryl group. The arrow between C_{22} and C_{24} indicates the vector whose $C_2(t)$ was calculated and analyzed.

5-3. Results and Discussion

5-3-1. Molecular Weight Effect on the Local Motion of PS Chain End

Figure 5-3 shows the time decays of the autocorrelation function $C_2(t)$ for PS chain ends with different molecular weights. For discussion about the chain mobility, the mean relaxation time, T_m, which is calculated by eq 5-2, was used.

$$T_m = \int_0^\infty C_2(t)\mathrm{d}t \tag{5-2}$$

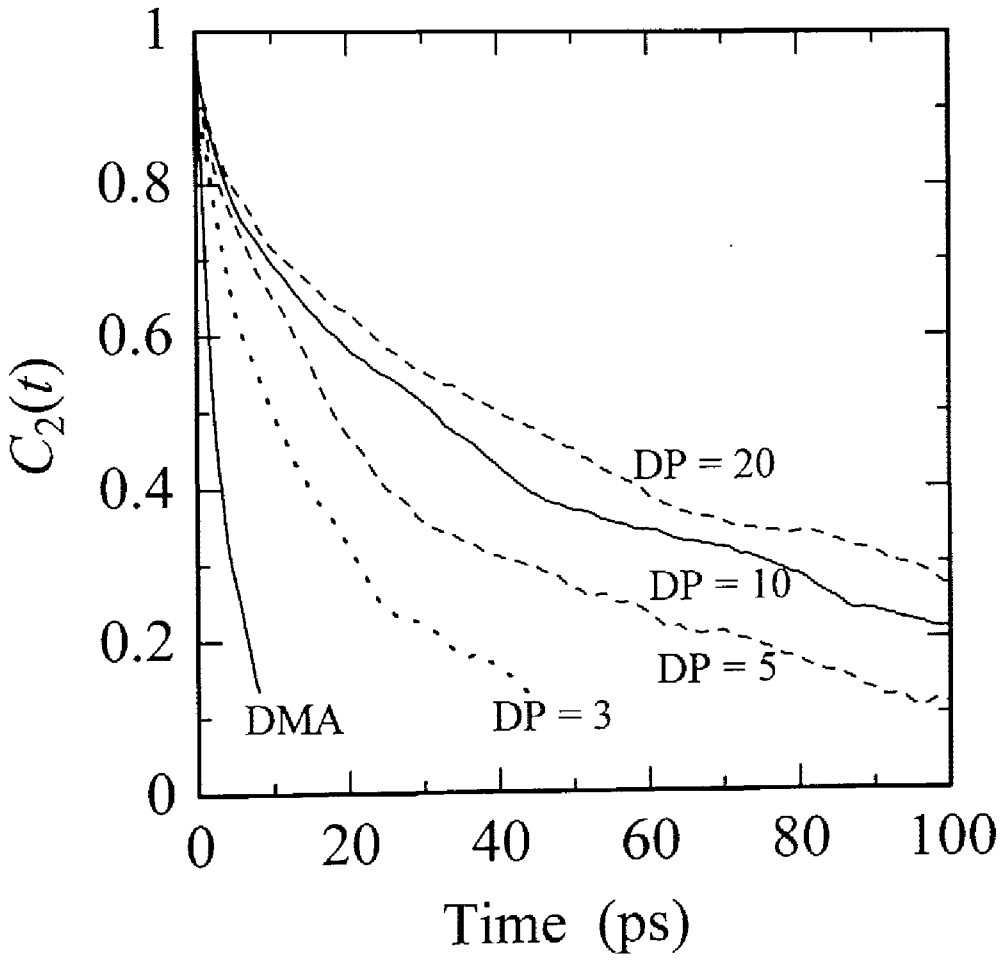

Figure 5-3. Decay of $C_2(t)$ of the A_9-A_{10} vector for PS in benzene.

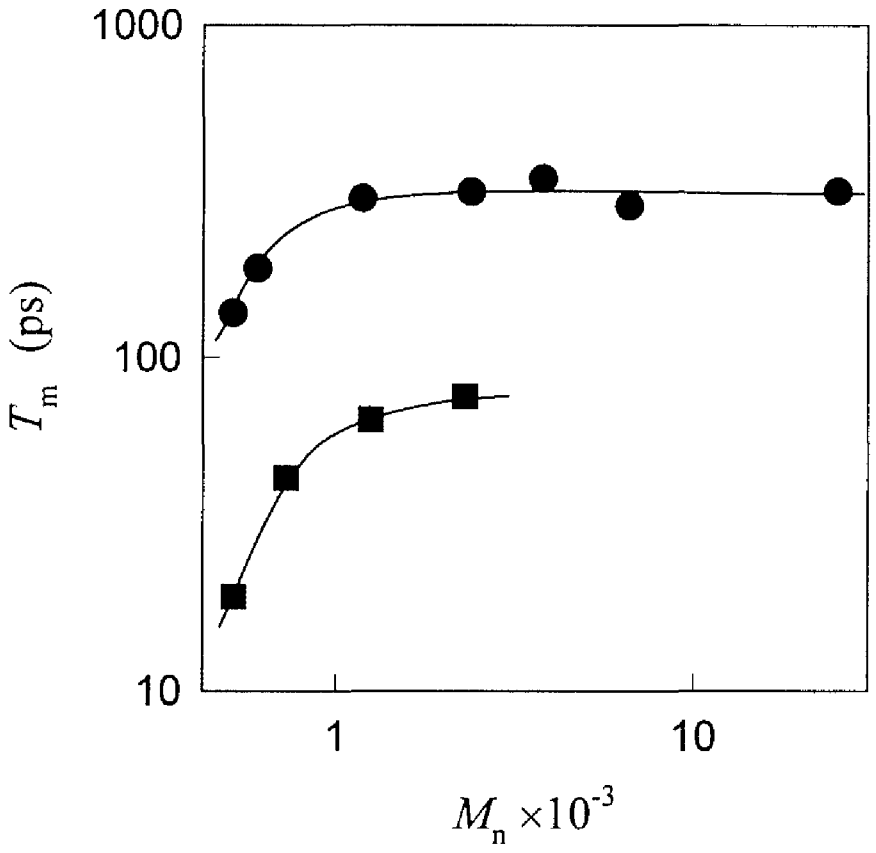

Figure 5-4. Molecular weight dependence of T_m by the fluorescence depolarization study (●) and by the MD simulation (■). M_n means the number-averaged molecular weight of the sample used in the fluorescence depolarization study.

Figure 5-4 shows the molecular weight dependence of the relaxation time T_m for the A_9-A_{10} vector. The relaxation time increased with the molecular weight and appeared to become constant at a certain critical molecular weight, M_c, above 2000. Figure 5-4 also shows the result of the fluorescent depolarization study.[8] Although the relaxation time obtained by the MD simulation is smaller in the absolute magnitude by a factor of about 3, the molecular weight dependence by the MD simulation is qualitatively in agreement with that obtained by the fluorescence depolarization. As stated in Chapter 4, this trend indicates that the local motion which contributes to the rotational relaxation of the fluorescent probe consists of segments less than M_c and that the contribution of the entire rotation above M_c is negligible. Then the molecular weight dependence of the relaxation time for the A_9-A_{10} vector was compared with that for the end-to-end vector and the contribution of the entire rotation was estimated.

Figure 5-5 shows that the relaxation time for the end-to-end vector monotonically increases with the degree of polymerization (DP). The filled triangle indicates the relaxation time for the model compound 9,10-dimethylanthracene (DMA). The relaxation time for the A_9-A_{10} vector was similar to that for the end-to-end vector below DP = 3 and reached a constant value as DP increased. With the increase of DP, the internal degree of freedom increased and the internal motional modes became sufficient to carry out the rotational relaxation of the probe. That is, the contribution of the entire rotation to the relaxation of the A_9-A_{10} vector decreased as DP increased.[8,15]

In the previous fluorescence depolarization studies, the relaxation times of the local motion for the main chain center of polymers were in the order of nanoseconds,[5,6] and, the molecular weight of each polymer was mostly more than 10^4. If the molecular weight of the solute increases, the number of solvent atoms will exponentially increase, and it is impossible at present to calculate the molecular dynamics of such a huge system in the order of nanoseconds. Therefore, some reasonable simplification and/or the advance in the capacity of the computer are needed.

In this study, the relaxation time obtained by the MD simulation and the fluorescence depolarization study was different by a factor of about 6. This deviation probably results from the incomplete force field adopted in the dynamics calculation. Then, the effect of the dielectric interaction, which was disregarded in all

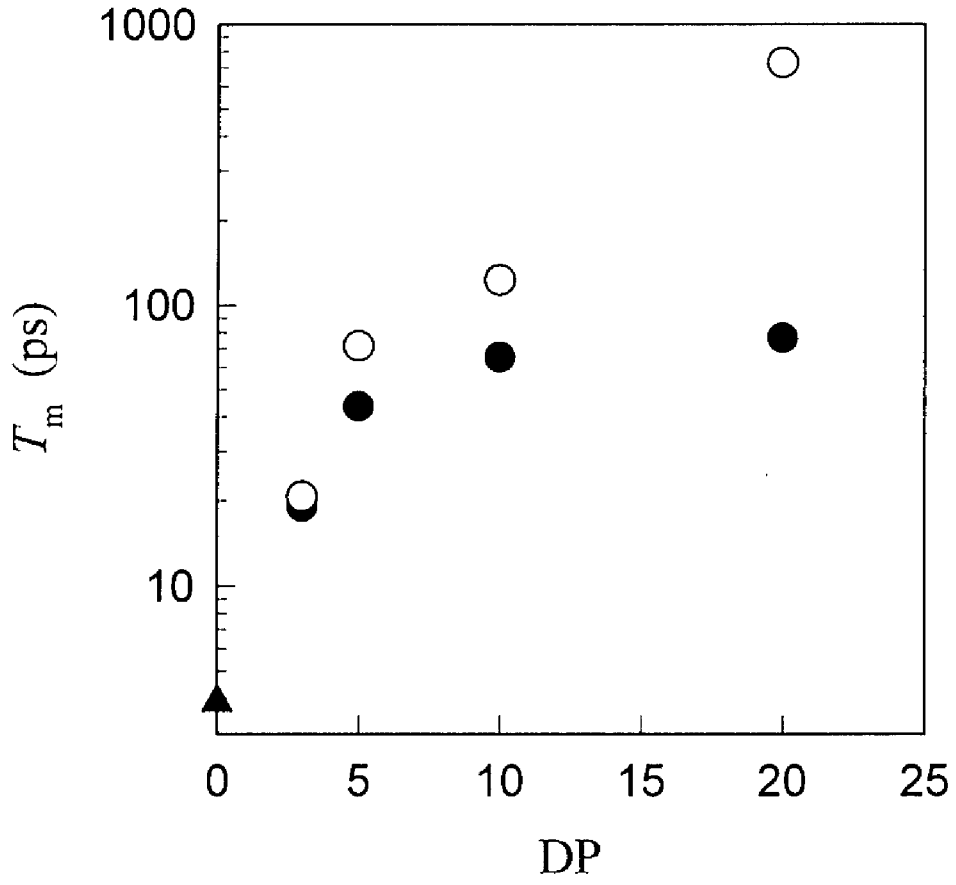

Figure 5-5. Comparison of the DP dependence of T_m between the A_9-A_{10} vector (●) and the end-to-end vector (○). Filled triangle indicates T_m of DMA.

the simulations and may be responsible for the difference, was briefly estimated. The dynamics calculation for PS (DP = 10) in benzene molecules was carried out with the cutoff distance of 9.5 Å for 1000 ps. The dielectric constant, ε, was set to be 2.28 and 7.0. The reported value for benzene at 25 °C is $\varepsilon = 2.28$. For $\varepsilon = 2.28$, the relaxation of the A_9-A_{10} vector was too slow to estimate the relaxation time within the present duration time and for $\varepsilon = 7.0$, the relaxation time was estimated as ca. 100 ps, which is slightly shorter than the experimental value. In this way, the relaxation time was seriously influenced by ε, but the proper choice of ε for the solvent remains to be established.

5-3-2. Effect of Restraints on the Chain Mobility

The values of T_m for the rotational relaxation of the A_9-A_{10} vector for various restraints are shown in Table 5-2. For PS, the restraints on the adjacent bond to the A_9-A_{10} bond (run 2) had no effect and T_m was similar to that for the run 1 (no restraint). On the other hand, for polyethylene chain the same restraint (run 5) had a large effect on the rotational relaxation of the probe and T_m becomes longer by a factor of 2. These results reflect the cooperativity of the local motion of PS chain. Previously, it was found that the larger the size of the side group of a polymer chain the lower is the chain mobility.[5-7] PS has large substituents and the rotational relaxation of the anthryl probe is realized by accumulation of a small amount of rotation at each bond.[11,16] That is, the contribution of the neighboring bond to the rotational relaxation of the probe is small and the restraint on one bond has little effect on T_m. In the case of flexible polyethylene, the contribution of the neighboring bond to the relaxation of the probe at the chain end is so large that the restraint changes T_m considerably. However, the restraints on the closed half of the main chain bond (run 3) for PS chain lead T_m to be larger, although the restraints on one bond had no effect. It is noteworthy that the restraint on the remote half of the main chain bond (run 4) does not change T_m as much as the near half restraint. This indicates that the rotational relaxation of the probe is mostly realized by the internal motional modes within the closed half of the main chain.

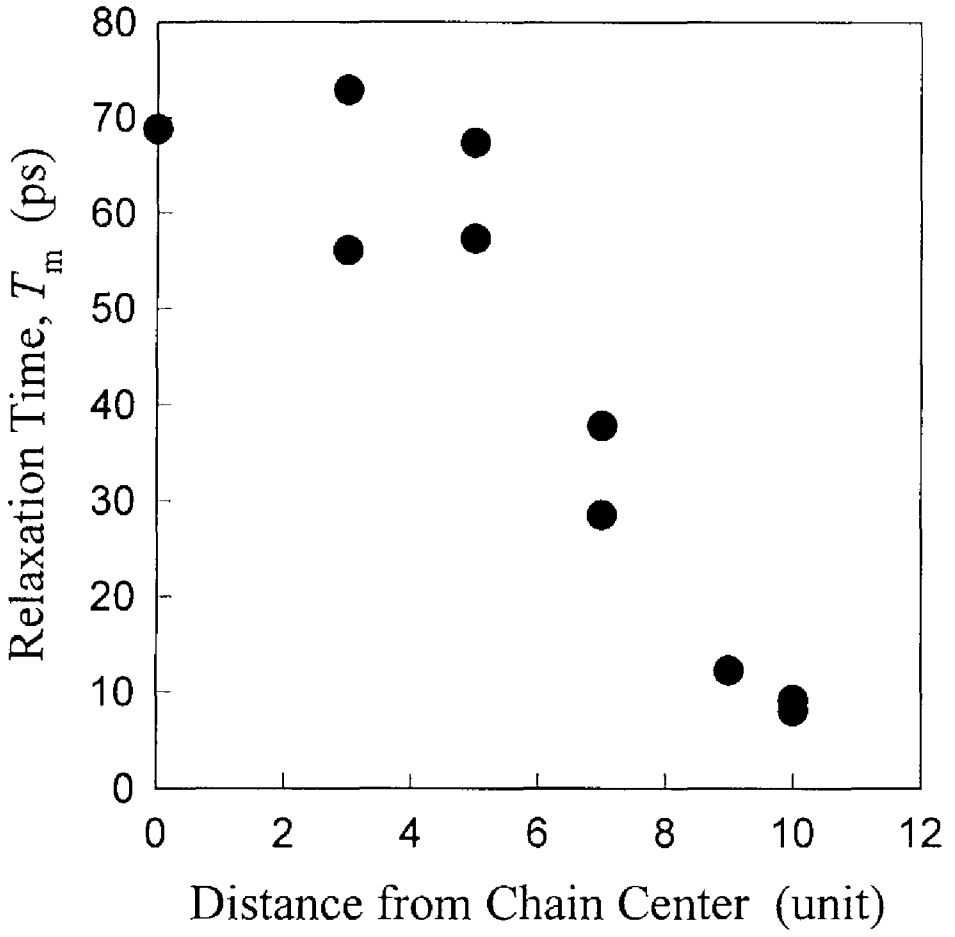

Figure 5-6. The mean relaxation time T_m at the each position along the main chain. The abscissa indicates the distance from the chain center (see text).

5-3-3. Chain Mobility at the Different Positions along the Main Chain

Figure 5-6 shows the change of the relaxation time with the position along the main chain bond. The abscissa indicates the number of monomer units from the chain center. The relaxation time T_m was almost constant in the middle part of the chain more than 5 monomer units apart from the chain end, while T_m markedly decreased near the chain end. T_m at the chain end was smaller than that of the chain center by a factor of 6 or 7. This result comes from the higher flexibility of the chain end in comparison with the chain center. Although the result estimated by the MD simulation in vacuo cannot be quantitatively compared with that obtained by the fluorescence depolarization study in solution,[8] the difference in T_m at the different positions along the main chain was estimated in detail by using the MD simulation.

5-4. Conclusion

MD simulations for the PS chain labeled with an anthryl group used as a fluorescent probe at the chain end surrounded by benzene molecules was carried out. The MD simulation data was compared with the results of the fluorescence depolarization study on the local motion of PS chain end in benzene. The molecular weight effect on the local motion by the MD simulation qualitatively reproduced the trend obtained by the fluorescence depolarization method.

The orientational autocorrelation function of the end-to-end vector was calculated and its molecular weight dependence was compared with that of the A_9-A_{10} vector, which is the transition moment of the probe. Below DP $\leq$ 3, the T_m for end-to-end vector was similar to that for the A_9-A_{10} vector, but with the increase of DP, the T_m for the A_9-A_{10} vector appeared to reach an asymptotic value unlike that for the end-to-end vector, which monotonically increased with DP. This indicates that the local motion becomes less dependent on molecular weight as molecular weight increases.

The MD simulations with artificial restraints revealed the property of the local motion of PS chain end. The restraints on the bond adjacent to the probe had no effect on the T_m at the PS chain end, while for the polyethylene chain, they increased the T_m.

This indicates that for PS, which is dynamically stiff, the probe is rotationally relaxed at the chain end by the cooperative rotation of the main chain bonds. The restraints on the remote half of the main chain had little effect on T_m, indicating that the rotational relaxation of the probe at the PS chain end is mostly carried out by the internal motional modes within 5 monomers. Finally, the change of T_m with different positions along the PS main chain was examined. The flexibility of the chain end influences up to 5 monomer units.

References

(1) Yamakawa, H. *Helical Wormlike Chains in Polymer Solutions* Springer-Verlag: Berlin, 1997.

(2) Ferry, J. D. *Viscoelastic Properties of Polymers 3rd Ed.* John Wiley and Sons: New York, 1980.

(3) Doi, M.; Edwards, S. F. *The Theory of Polymer Dynamics.* Clarendon Press: Oxford, 1986.

(4) Sasaki, T.; Yamamoto, M. *Macromolecules* **1989**, *22*, 4009.

(5) Ono, K.; Okada, Y.; Yokotsuka, S.; Sasaki, T.; Ito, S.; Yamamoto, M. *Macromolecules*, **1994**, *27*, 6482.

(6) Ono, K.; Ueda, K.; Sasaki, T.; Murase, S.; Yamamoto, M. *Macromolecules* **1996**, *29*, 1584.

(7) Horinaka, J.; Amano, S.; Funada, H.; Ito, S.; Yamamoto, M. *Macromolecules*, **1998**, *31*, 1197.

(8) Horinaka, J.; Maruta, M.; Ito, S.; Yamamoto, M. *Macromolecules* submitted.

(9) Moe, N. E.; Ediger, M. D. *Macromolecules*, **1995**, *28*, 2329.

(10) Fuson, M. M.; Ediger, M. D. *Macromolecules* **1997**, *30*, 5704.

(11) Fuson, M. M.; Hanser, K. H.; Ediger, M. D. *Macromolecules* **1997**, *30*, 5714.

(12) Abe, A.; Furuya, H.; Mitra, M. K.; Hiejima, T. *Comp. Theor. Polym. Sci.* **1998**, *8*, 253.

(13) Horinaka, J.; Ito, S.; Yamamoto, M.; Tsujii, Y.; Matsuda, T. *Macromolecules* submitted.

(14) Leontidis, E.; Suter, U. W.; Schutz, M.; Luthi, H. P.; Renn, A.; Wild, U. P. *J. Am. Chem. Soc.*, **1995**, *117*, 7493.

(15) Lauprêtre, F.; Noël, C.; Monnerie, L. *J. Polym. Sci., Polym. Phys. Ed.* **1977**, *15*, 2127.

(16) Moe, N. E.; Ediger, M. D. *Macromolecules* **1996**, *29*, 5484.

(17) Maple, J. R.; Hwang, M. J.; Stockfisch, T. P.; Dinur, U.; Waldman, M.; Ewig, C. S.; Hagler, A. T. *J. Comput. Chem.* **1994**, *15*, 162.

(18) Jaffe, R. L.; Smith, G. D.; Yoon, D. Y. *J. Phys. Chem.* **1993**, *97*, 12745.

(19) Smith, G. D.; Jaffe, R. L.; Yoon, D. Y. *J. Phys. Chem.* **1993**, *97*, 12752.

(20) Michl, J.; Thulstrup, E. W. *Spectroscopy with Polarized Light* VCH: New York, 1986.

Chapter 6

Influence of a Fluorescent Probe on the Local Relaxation Times for a Polystyrene Chain in the Fluorescence Depolarization Method

6-1. Introduction

The fluorescence method has been widely used for studies of the structure and dynamic properties of polymer systems.[1-4] The method has several advantages such as high microscopic sensitivity and high resolution in space and time. Therefore, one can obtain irreplaceable information using the fluorescent probe labeled at a designated position in the system. In particular, the fluorescence depolarization method provides information on the rotational relaxation of the transition moment of the fluorescent probe. The relaxation time of the probe was estimated through the measurements of the decay of the fluorescence anisotropy ratio. The local motion of polymer chain has been extensively studied for polymers with the fluorescent probe labeled in the main chain.[5-19] In our laboratory, the local motion of polymer chains labeled with anthracene as the fluorescent probe in dilute solutions was examined and the effects of several molecular factors such as solvent condition,[13,15] molecular structure of polymer,[13-16] molecular weight,[15-18] and the position along a chain on the local chain mobility[18] were discussed. However, there still remain some questions to be solved.

First, a fluorescent probe must be used in the fluorescence method and therefore the observed results always include the influence of the probe to some extent. Then estimation of the perturbation by the probe is necessary for analysis, but few

works have been reported.[12,16,20] Pant et al. proposed the complex damped orientational diffusion model of local polymer chain motion including the effects of attached probes on the dynamics.[20] Moreover, in the fluorescence method, the molecular structure in the vicinity of the fluorescent probe is also expected to influence the observed result. The molecular structure in the vicinity of the fluorescent probe is usually controlled by the synthetic scheme. Sample polymers have been synthesized by the living anionic polymerization and subsequent coupling with 9,10-bis(bromomethyl)anthracene. The polymers were highly controlled in molecular structure and molecular weight. By this synthetic procedure, the 9,10-dimethylanthryl group was introduced into the middle of the main chain. Recently, well-defined anthracene-labeled polystyrene (PS) was synthesized by the atom transfer radical polymerization. The obtained PS has a different molecular structure in the vicinity of anthryl group from that of the former polymer. This synthetic success enabled us to examine the effect of the molecular structure in the vicinity of the probe on the chain mobility.

Recently, molecular dynamics (MD) simulation has been utilized for the local chain dynamics study.[21-26] MD simulation gives coordinates of all atoms, so that several requested properties can be estimated at the atomic level. With higher capacity of computers and with the improvement of the available force field, the experimental results can be well simulated. In MD simulation, the molecular structure of a polymer can be modified as necessary. Therefore, the local chain dynamics of the PS chain differently labeled with anthryl groups and even that of a probe-free PS chain can be evaluated and the influence of the probe on the fluorescence depolarization study estimated. In addition, the effect of the direction of the transition moment to the main chain can be estimated.

In this chapter, the local motion of two series of PS in dilute benzene solutions was first examined by the fluorescence depolarization method. Two series of PS chains are differently labeled with anthryl group. The relaxation times of the local motion and their molecular weight dependence were compared for these polymers. Then, the MD simulation for both 20mer labeled PS and 22mer probe-free PS in vacuo were carried out and the mobility at the chain center was compared between these model compounds. The rotational relaxation times of different vectors pointing in

directions other than parallel to the main chain were also calculated.

(a)

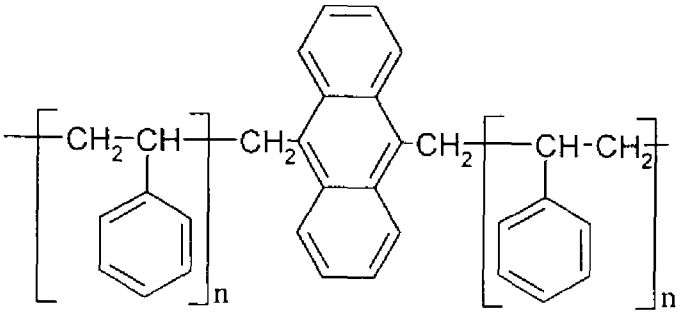

(b)

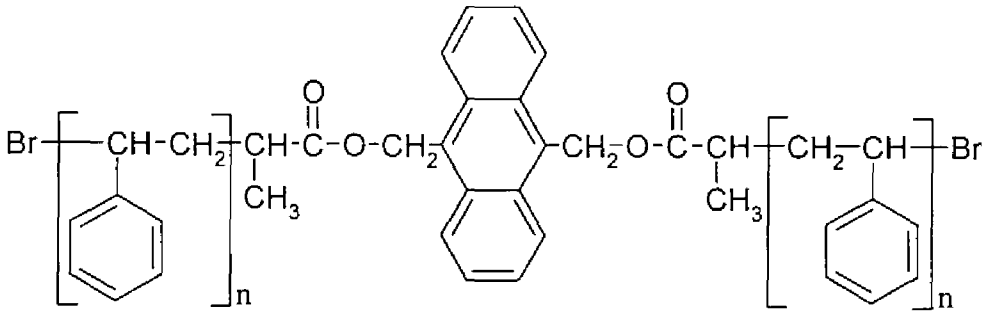

Figure 6-1. Molecular structures of PS labeled with anthryl group in the middle of the main chain used in the fluorescence depolarization study; (a) a-PS and (b) r-PS.

6-2. Experimental Section

6-2-1. Fluorescence Depolarization Study

6-2-1-1. Sample Preparation. One series of the anthryl group-labeled PS samples used in this study was synthesized by the living anionic polymerization in vacuo initiated by butyllithium, in which the living ends were coupled with 9,10-bis(bromomethyl)anthracene. Details of the synthetic procedure have been reported in Chapter 3.[17,27] The incompletely coupled fraction was removed from the original sample by GPC. Figure 6-1 (a) shows the molecular structure of this series of PS (a-PS) and Table 6-1 shows the weight-average molecular weight M_w and the number-average molecular weight M_n of a-PS.

Table 6-1. Characterization of PS Samples Used in the Fluorescence Depolarization Study

	M_n	M_w/M_n
a-PS1	6.4	1.13
a-PS2	13.1	1.06
a-PS3	69	1.04
a-PS4	92	1.05
r-PS1	2.7	1.10
r-PS2	4.1	1.09
r-PS3	6.5	1.08
r-PS4	10.0	1.10
r-PS5	12.5	1.10
r-PS6	15.8	1.12
r-PS7	20	1.12
r-PS8	149	1.21

The other series of the anthryl group-labeled PS samples was synthesized by the atom transfer radical polymerization with 9,10-bis(1-bromoethylcarbalkoxymethyl)anthracene as a bifunctional initiator. The synthetic procedure of this series of PS (r-PS) has been described elsewhere.[28] The molecular

structure of r-PS is shown in Figure 6-1 (b) and the characterization in Table 6-1.

Benzene (Dojin, spectrosol) (a good solvent) was used as a solvent for measurements without further purification. The concentration of each polymer in the sample solutions was kept below 10^{-5} M. Each solution was put into a quartz cell and degassed.

6-2-1-2. Data Analysis. The fluorescence anisotropy ratio, $r(t)$, is defined as

$$r(t) = (I_{VV}(t) - GI_{VH}(t))/(I_{VV}(t) + 2GI_{VH}(t)) \quad (6\text{-}1)$$

where G is the compensating factor and was estimated to be unity in this study. For discussion about the chain mobility, the mean relaxation time, T_m was used. T_m is the time integral of the reorientational autocorrelation function defined as eq 6-2.

$$T_m = r_0^{-1} \int_0^\infty r(t)dt \quad (6\text{-}2)$$

where r_0 is the initial anisotropy ratio.

6-2-2. MD Simulation Methodology

MD simulations were carried out with an MD software, Discover 3 (Biosym Technologies)[24,25], on a CRAY Origin 2000 supercomputer in the same way as the previous MD simulation study.[26] The force field used in this study was Biosym CFF91, [29,30] which took into account bond stretching, bond angle, dihedral, improper, and their seven cross-terms. The dielectric interaction was disregarded and a Lennard-Jones type 6-9 potential was used for nonbonded interactions with a cutoff distance of 6 Å. One femtosecond time steps were used in the calculation.

PS chains labeled with anthryl groups in the middle of the main chain were initially generated using Insight II (Biosym Technologies). The molecular structure of PS sample in the vicinity of the probe was changed by inserting methylene chains between the anthryl group and styrene unit. 22mer probe-free PS was also generated. The molecular structures and the atom numbers for PS-*n* used in the MD simulation are shown in Figure 6-2. The molecular weight for probe-free PS is almost the same as that for PS-0 (2304 and 2286, respectively). The C_9-C_{10} vector in the anthryl group corresponds to the transition moment, L_a, of anthryl group.[31]

(a)

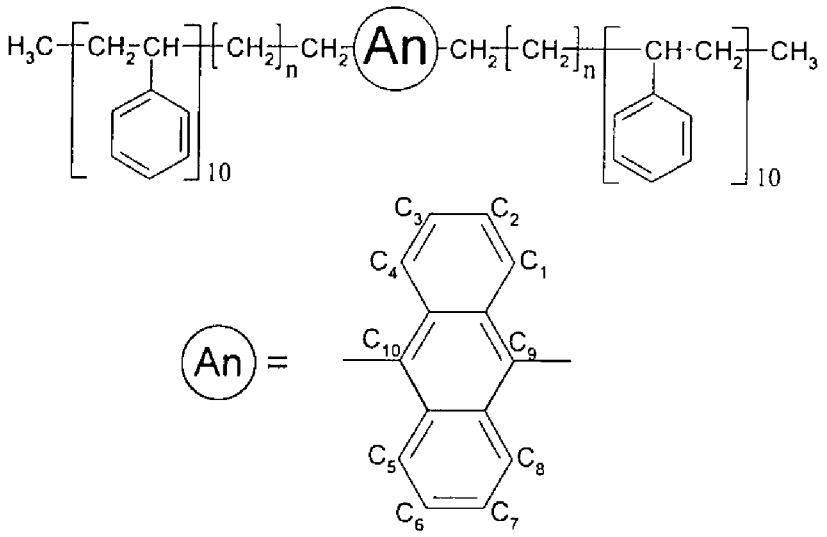

(b)

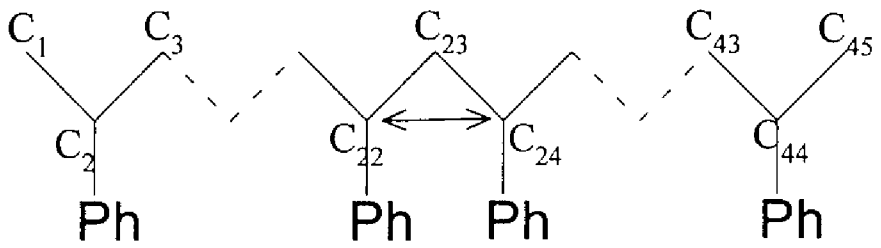

Figure 6-2. Molecular structures and atom numbers for PS model compound used in the MD simulation. (a) Anthryl group-labeled PS model with *n* methylene groups, PS-*n*. (b) Probe-free PS model. The arrow indicates the vector whose $C_2(t)$ was analyzed.

After 300 steps of minimization, the molecular dynamics was calculated in vacuo under a constant temperature of 300 K. The total duration time of the dynamics run was 2100 ps and the atom coordinates used for analysis were saved every 1 ps after 100 ps of discarded dynamics run. From the data of atom coordinates, the second-order orientational autocorrelation functions, $C_2(t)$, were calculated for the C_9-C_{10} vector of anthryl group and the C_{22}-C_{24} vector for probe-free PS according to eq 6-3.

$$C_2(t) = \frac{<3(\mathbf{u}_{mn}(0)\cdot\mathbf{u}_{mn}(t))^2 - 1>}{2}$$

$$\mathbf{u}_{mn}(t) = \frac{\mathbf{r}_{mn}(t)}{r_{mn}(t)} \qquad (6\text{-}3)$$

$\mathbf{r}_{mn}(t)$ is a vector pointing in the direction from C_m to C_n atom. Then, the relaxation time was estimated with eq 6-2 in the same way as the fluorescence depolarization study.

In order to estimate the effect of the direction of the transition moment of the fluorescent probe, $C_2(t)$ was also calculated for the C_2-C_6 vector of PS-0, which is nearly perpendicular to the C_9-C_{10} vector.

6-3. Results and Discussion

6-3-1. Fluorescence Depolarization Study

6-3-1-1. Relaxation Time. Figure 6-3 shows the molecular weight effect on the relaxation time T_m at 20 °C for both a-PS and r-PS. The relaxation time for a-PS increases with molecular weight and reaches an asymptotic value of $T_m \cong 2$ ns at $M_n \cong 10^4$, while for r-PS, the asymptotic relaxation time in $M_n > 8 \times 10^3$ is ca. 1 ns. The trend that the relaxation time becomes constant above a certain molecular weight indicates that the local motion of PS in benzene measured by the fluorescence depolarization method is independent of the overall motion in higher molecular weight region. The molecular weight dependence of the relaxation time has been discussed previously.[17] Although this trend is similar for both a-PS and r-PS, the

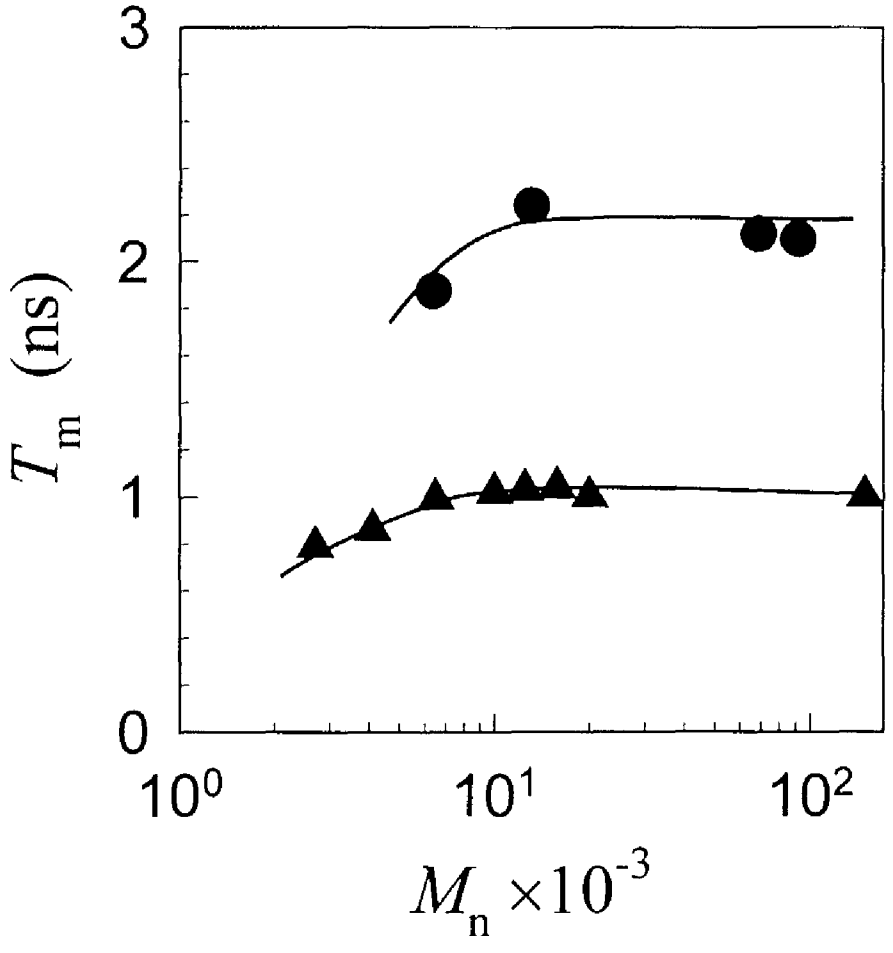

Figure 6-3. Molecular weight dependence of T_m for a-PS (●) and r-PS (▲) in benzene at 20 °C.

absolute magnitude of T_m for a-PS is larger than that for r-PS by a factor of 2. The critical molecular weight, M_c at which the relaxation time becomes constant, for a-PS is also slightly larger than that for r-PS. These differences certainly result from the molecular structure in the vicinity of the fluorescent probe. By taking into account the difference in the molecular structures shown in Figure 6-1 (a) and (b), the cause of the difference of the relaxation times may be due to the steric effect of styrene unit around the anthryl group. It is reasonable to consider that the steric hindrance between these two bulky units influences the relaxation time of the anthryl group. That is, the anthryl group for r-PS has longer spacers to the nearest styrene unit than that for a-PS, so that the probe of r-PS rotates more freely than that of a-PS. The result indicates that the observed relaxation time reflects the molecular structure in the vicinity of the fluorescent probe. In other words, attention has to be paid to how and where a fluorescent probe is attached to the polymer chains.

6-3-1-2. Activation Energy. Next, the activation energy of the local motion, E^*, was estimated according to the theory of Kramers' diffusion limit, namely,

$$T_m / \eta = A\exp(E^* / RT). \qquad (6\text{-}4)$$

where R is the gas constant, T is absolute temperature, η is the solvent viscosity. The solvent viscosity for benzene was estimated from the value reported in the literature,[32] e.g., 0.65 cP at 20 °C. Figure 6-4 shows the temperature dependence of T_m for both a-PS and r-PS in benzene. The reduced relaxation time T_m/η, which was reduced by the solvent viscosity, η, was obtained by eq 6-4, then the activation energies could be estimated from the slope of the plot in Figure 6-4.

Figure 6-5 shows the relationship between the molecular weight and the estimated activation energy in benzene. The activation energy as well as the relaxation time tends to increase with molecular weight and to become constant at $M_n \cong 10^4$. The absolute magnitude of E^* ($\cong$ 1.7 kcal mol^{-1}) for r-PS in the saturated region is almost the same as that for a-PS, although the relaxation time is markedly different. The obtained activation energy tends to reflect the higher barrier height. That is, it is assumed that the activation energy reflects the inherent higher energy barrier in the styrene sequence for both a-PS and r-PS.

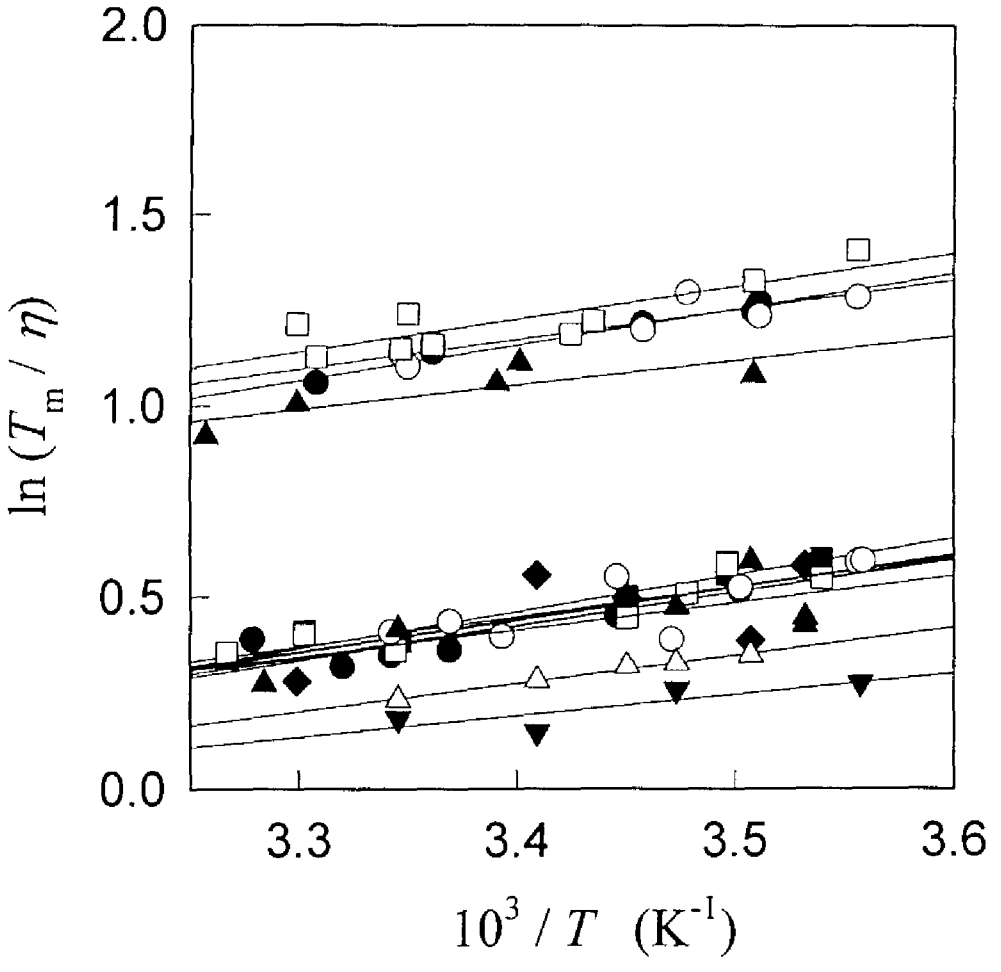

Figure 6-4. Arrhenius plot of T_m /η according to Kramers' theory. η is the viscosity of benzene, which is estimated from the value reported in the literature. The upper four lines are for the a-PS series; (▲) a-PS1, (□) a-PS2, (○) a-PS3, (●) a-PS4. The lower lines are for the r-PS series; (▼) r-PS1, (△) r-PS2, (▲) r-PS3, (○) r-PS4, (□) r-PS5, (■) r-PS6, (●) r-PS7, (◆) r-PS8.

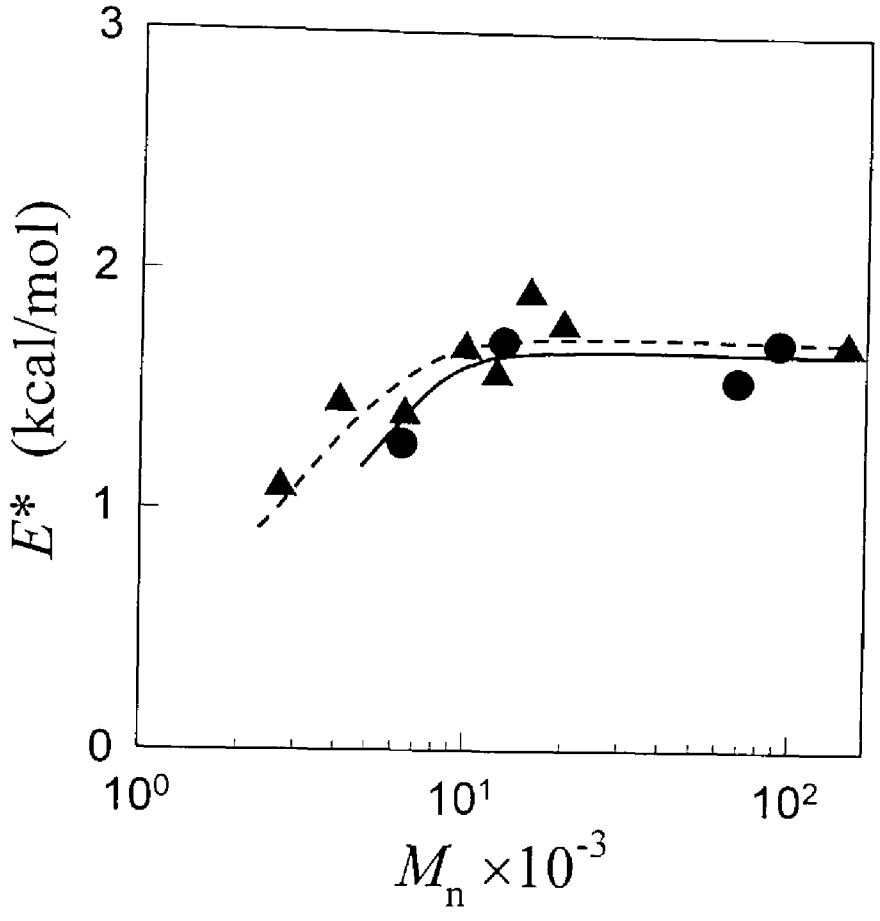

Figure 6-5. Molecular weight dependence of E^* for a-PS (●) and r-PS (▲).

6-3-2. MD Simulation

Figure 6-6 shows the decay of the autocorrelation function $C_2(t)$ for PS labeled with anthryl groups having various numbers of methylene groups as a spacer. The more methylene groups the PS chain has the shorter is the relaxation time. Figure 6-7 shows the relationship between the number of methylene groups and the relaxation time of the anthryl group. With the increase in the number of methylene groups up to 4, T_m sufficiently decreased by a factor of ca. 2.5. The number of bonds between the anthryl group and styrene unit for r-PS corresponds to that for PS-4 and the difference in the

relaxation time of PS-4 from that of PS-0 is in agreement with the difference in the relaxation time of r-PS from that of a-PS.

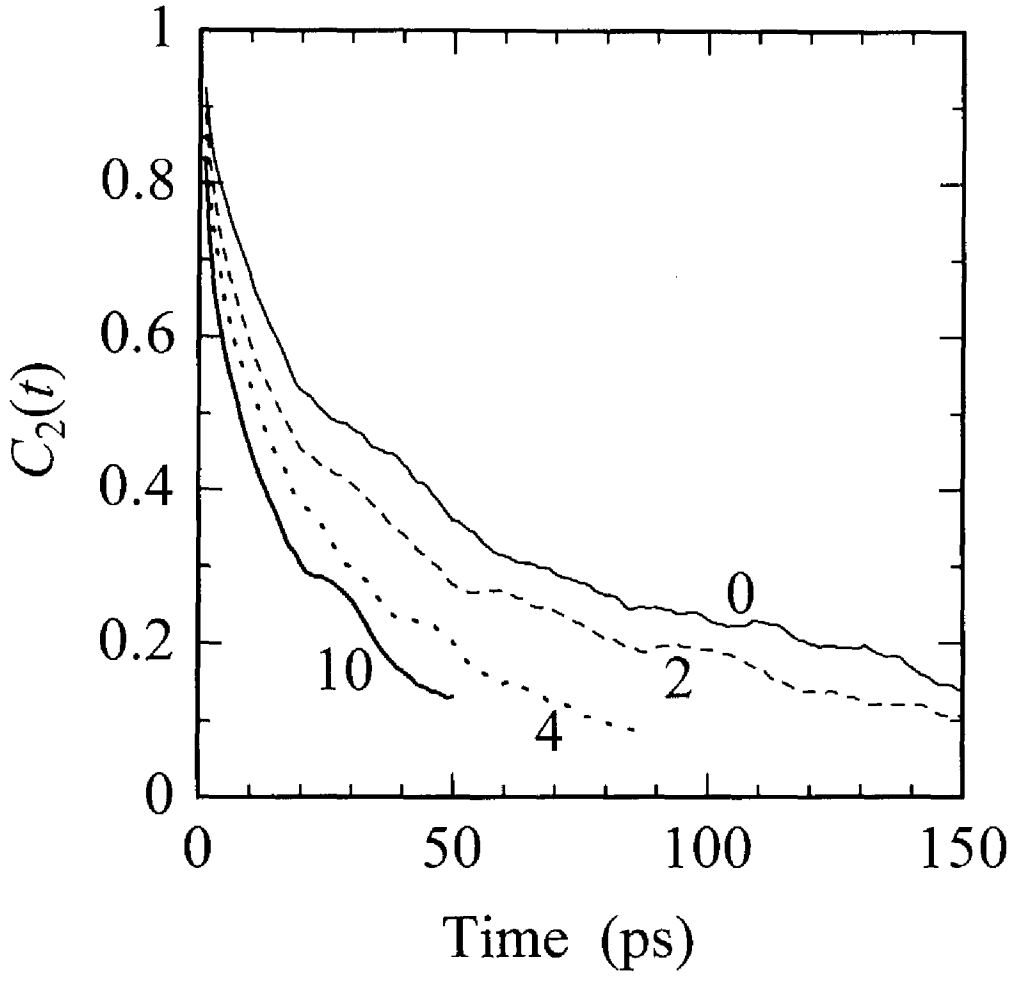

Figure 6-6. Decay of $C_2(t)$ for PS-n by the MD simulation. The numbers shown in the figure indicate the number of methylene groups, n.

Figure 6-7 also shows the relaxation time of the probe-free PS chain (unfilled circle). The T_m of the probe-free PS chain is slightly smaller than that of the PS-0 chain. The result shows that the chain mobility may not be influenced so much by the introduction of anthryl group as the fluorescent probe to the chain center of PS. The molecular weight of the anthryl group (= 176) is larger than that of the styrene monomer unit (= 104), but one of the rings of the anthryl group stands with the interval of three main chain carbon atoms from a neighboring phenyl group of styrene unit like the normal styrene sequence. Therefore, the steric hindrance between the anthryl group and styrene unit is considered to be similar to that between adjacent styrene units and the relaxation times are not much different. If this is the case, the local motion of polyethylene (PE), which is considered to be more flexible than PS, is expected to be more influenced by the introduction of an anthryl group. The T_m was 4.3 ps for the probe-free PE chain, but decreased to 2.4 ps for the anthryl group-labeled PE chain as expected.

Table 6-2. Comparison of the Relaxation Times for Vectors Pointing Different Directions

	C_2-C_6	C_9-C_{10}
T_m / ps	41	73

Table 6-2 shows the influence of the direction of the transition moment of the anthryl group, which was used as the fluorescent probe, on the observed relaxation time. The relaxation time T_m of the C_2-C_6 vector in anthryl group is smaller than that of the C_9-C_{10} vector. This is due to the relaxation by the rotation around the main chain and this rotational mode has no effect on the relaxation of the C_9-C_{10} vector. Consequently, the direction of the transition moment of the fluorescent probe is also important in the fluorescence depolarization study. The relaxation time of the C_9-C_{10} vector is longer than that of the C_2-C_6 vector and the C_9-C_{10} vector represents the mobility of the vector along the main chain bond well.

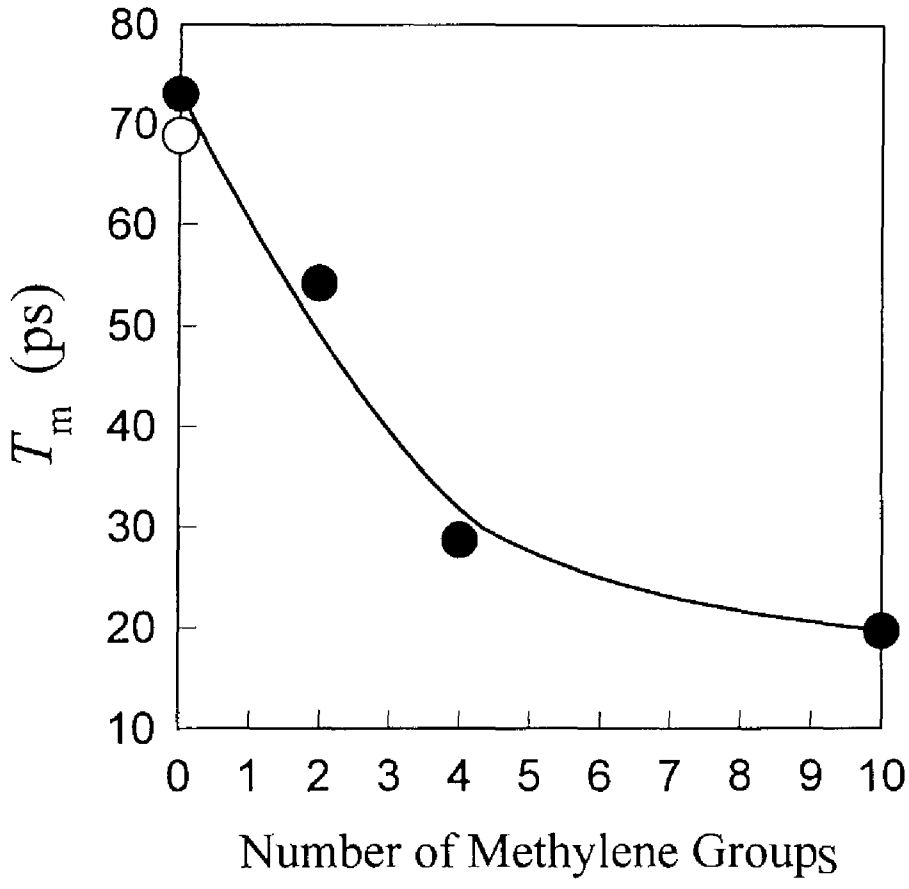

Figure 6-7. Influence of the number of methylene groups on T_m. Unfilled circle (○) indicates T_m for the probe-free PS chain.

6-4. Conclusion

The effect of the fluorescent probe and the structure around the probe in the fluorescence depolarization analysis was examined by using MD simulation. The absolute magnitude of T_m for r-PS, which has a longer flexible spacer between the anthryl group and PS unit, is smaller by a factor of 2 than that for a-PS. This shows that the relaxation time is sufficiently influenced by the structure around the probe.

Next, the MD simulation was carried out for various distance between the anthryl group and styrene unit separated by flexible methylene groups. As the number of methylene groups increased up to 4, T_m sufficiently decreased by a factor of 2.5 in agreement with the fluorescence depolarization study. The local motion of the probe-free PS chain was also simulated and the relaxation time at the chain center was compared with that of anthryl group-labeled PS. The chain mobility of PS slightly changed with the introduction of an anthryl group. The relaxation time of the vector that is nearly perpendicular to the direction of the transition moment of anthryl group is considerably shorter than that of the vector corresponding to the transition moment, L_a, which represents the chain mobility of the vector along the main chain bond.

References

(1) Nishijima, Y. In *Progress in Polymer Science, Japan*; Onogi, S., Uno, K.. Eds.; Kodansha: Tokyo, John Wiley and Sons: New York, 1973; p. 199.

(2) Monnerie, L. In *Photophysical and Photochemical Tools in Polymer Science*; Winnik, M. A. Ed.; D. Reidel: Dordrecht, Netherlands, 1985; pp. 193, 371, 449, 589.

(3) Morawetz, H. *J. Lumin.* **1989**, *43*, 59.

(4) Ediger, M. D. *Ann. Rev. Phys. Chem.* **1991**, *42*, 225.

(5) Valeuer, B.; Monnerie, L. *J. Polym. Sci., Polym. Phys. Ed.* **1976**, *14*, 11.

(6) Viovy, J. -L.; Curtis, W. F.; Monnerie, L.; Brochon, J. C. *Macromolecules* **1983**, *16*, 1845.

(7) Viovy, J. -L.; Curtis, W. F.; Monnerie, L. *Macromolecules* **1985**, *18*, 2606.

(8) Valeuer, B.; Viovy, J. L.; Monnerie, L. *Polymer* **1989**, *30*, 1262.

(9) Waldow, D. A.; Johnson, B. S.; Hyde, P. D.; Ediger, M. D.; Kitano, T.; Ito, K. *Macromolecules* **1989**, *22*, 1345.

(10) Waldow, D. A.; Ediger, M. D.; Yamaguchi, Y.; Matsushita, Y.; Noda, I. *Macromolecules* **1991**, *24*, 3147.

(11) Adolf, D. B.; Ediger, M. D.; Kitano, T.; Ito, K. *Macromolecules* **1992**, *25*, 867.

(12) Sasaki, T.; Yamamoto, M. *Macromolecules* **1989**, *22*, 4009.

(13) Ono, K.; Okada, Y.; Yokotsuka, S.; Sasaki, T.; Ito, S.; Yamamoto, M. *Macromolecules* **1994**, *27*, 6482.

(14) Ono, K.; Ueda, K.; Sasaki, T.; Murase, S.; Yamamoto, M. *Macromolecules* **1996** *29*, 1584.

(15) Horinaka, J.; Ono, K.; Yamamoto, M. *Polym. J.* **1995**, *27*, 429.

(16) Horinaka, J.; Amano, S.; Funada, H.; Ito, S.; Yamamoto, M. *Macromolecules* **1998**, *31*, 1197.

(17) Horinaka, J.; Aoki, H.; Ito, S.; Yamamoto, M. *Polym. J.* in press.

(18) Horinaka, J.; Maruta, M.; Ito, S.; Yamamoto, M. *Macromolecules* submitted.

(19) Soutar, I.; Swanson, L.; Christensen, R. L.; Drake, R. C.; Phillips, D. *Macromolecules* **1996**, *29*, 4931.

(20) Pant, B. B.; Skolnick, J.; Yaris, R. *Macromolecules* **1985**, *18*, 253.

(21) Zuniga, I.; Bahar, I.; Dodge, R.; Mattice, W. L. *J. Chem. Phys.* **1991**, *95*, 5348.

(22) Bahar, I.; Neuburger, N.; Mattice, W. L. *Macromolecules* **1992**, *25*, 2447; 4619.

(23) Moe, N. E.; Ediger, M. D. *Macromolecules* **1995**, *28*, 2329.

(24) Fuson, M. M.; Ediger, M. D. *Macromolecules* **1997**, *30*, 5704.

(25) Fuson, M. M.; Hanser, K. H.; Ediger, M. D. *Macromolecules* **1997**, *30*, 5714.

(26) Horinaka, J.; Ito, S.; Yamamoto, M.; Matsuda, T.; *Comp. Theor. Polym. Sci.* submitted.

(27) Sasaki, T.; Yamamoto, M.; Nishijima, Y. *Makromol. Chem., Rapid Commun.* **1986**, *7*, 345.

(28) Ohno, K.; Fujimoto, K.; Tsujii, Y.; Fukuda, T. *Polymer* **1999**, *40*, 759.

(29) Leontidis, E.; Suter, U. W.; Schutz, M.; Luthi, H. P.; Renn, A.; Wild, U. P. *J. Am. Chem. Soc.* **1995**, *117*, 7493.

(30) Maple, J. R.; Hwang, M. J.; Stockfisch, T. P.; Dinur, U.; Waldman, M.; Ewig, C. S.; Hagler, A. T. *J. Comput. Chem.* **1994**, *15*, 162.

(31) Michl, J.; Thulstrup, E. W. *Spectroscopy with Polarized Light* VCH: New York, N. Y., 1986.

(32) Riddick, J. A.; Bunger, W. B. *Techniques of Chemistry II, Organic Solvents 3rd ed* Wiley-Interscience: New York, N. Y., 1970.

Chapter 7

Microscopic Observation of Thermally-Induced Phase Separation of Poly(ethoxyethyl Vinyl Ether) by Fluorescence Methods

7-1. Introduction

The discontinuous changes in physical properties of polymers at a certain condition have attracted a great deal of attention from both theoretical and experimental viewpoints.[1-12,22-25] For example, methylcellulose,[2] poly(vinyl ether),[1] and poly(acrylamide) derivatives[2-8] are well known as thermally-induced phase separation polymers, the solubility of which in water suddenly changes with a temperature. Although in general, polymers become more soluble with the increase in temperature, these polymer/solvent systems cause so-called LCST-type phase separation at a certain temperature and the polymers become insoluble above it. The dynamics of the phase separation has been studied extensively,[1,3,5,8,25] but molecular-level details of the phase separation behavior remain to be solved. Because the phase separation behavior is influenced by the molecular structure such as stereoregularity, molecular weight and its distribution, it is experimentally needed to use polymers having highly controlled molecular structure.

Structure-controlled poly(vinyl ether) derivatives have been synthesized by living cationic polymerization and the phase separation behavior of aqueous solutions was examined.[9,10] By using the structure-controlled polymers, it was revealed that the phase separation temperature, T_{sp}, depends greatly on the oxyethylene chain length of

the side group and/or the structure of the end of the side chain. Even in the case of polymers of the same molecular structure, T_{sp} depends on the molecular weight and the concentration of aqueous solution.

Experimental techniques using fluorescent probe are powerful for examining microscopic structure and dynamics. F. Winnik has examined the thermoreversible phase separation of aqueous solution of poly(*N*-isopropylacrylamide) (PNIPAM) by the energy transfer technique.[8] Meewes et al. used the fluorescence depolarization technique as well as the light scattering technique for the phase separation of high molecular weight PNIPAM aqueous solution.[6,7] They observed two-step phase separation, i.e., intra- and intermolecular aggregation of polymer chains. Hu et al. studied the volume phase transition in poly(acrylamide) gels using the fluorescent technique[3,31,32] and discussed the interaction between the polymer network and solvent molecules as well as the dynamic fluctuation at the discontinuous transition.

The fluorescence depolarization method has been utilized for the local polymer chain dynamics in dilute solutions.[14-21] By this method, microscopic chain mobility can be estimated through the motion of the fluorescence probe labeled in the middle of a main chain. Application of this technique to the study of phase separation will give us valuable microscopic information in the vicinity of the phase separation temperature. For the fluorescence depolarization measurement, it is necessary for a polymer sample to be labeled with a fluorescent probe in the polymer chain. Then, at the termination reaction of living cationic polymerization of poly(ethoxyethyl vinyl ether) (PEVE), a unique terminator was used, and PEVE with anthryl-group labeled in the middle of the main chain was obtained.

In this chapter, fluorescence intensity, fluorescence lifetime, and fluorescence depolarization were measured during the course of phase separation of PEVE aqueous solution. Then, the microscopic behavior of PEVE in an aqueous solution around the phase separation temperature was discussed including the preceding stage. Furthermore, fluorescence behavior of other systems, where the phase separation does not occur, was examined.

7-2. Experimental Section

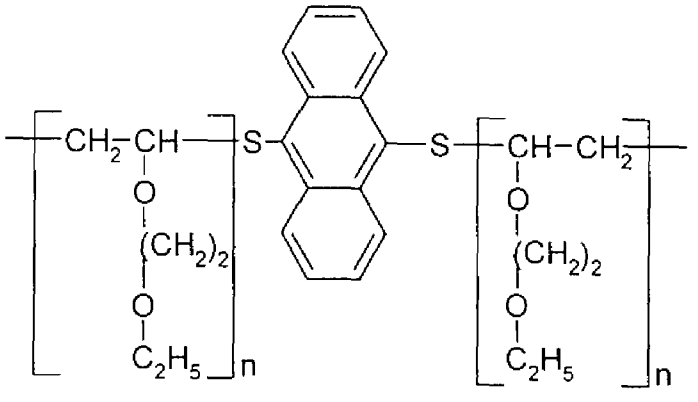

Figure 7-1. Molecular structure of poly(ethoxyethyl vinyl ether) (PEVE) labeled with anthryl-group in the middle of the main chain.

7-2-1. Sample Preparation

Poly(ethoxyethyl vinyl ether) (PEVE) sample was synthesized by the living cationic polymerization. The reaction was initiated by addition of $Et_{1.5}AlCl_{1.5}$ into a mixture of ethoxyethyl vinyl ether as a monomer, ethyl acetate as an added base, and 1-(isobutoxy)ethyl acetate as a cationogen in toluene at 0 °C. More details of the material preparation and polymerization were described elsewhere.[10] At the termination reaction, the living ends were coupled with 9,10-anthracenedithiol[13] so that an anthryl-group was attached in the middle of the PEVE main chain as a fluorescent probe. Figure 7-1 shows the molecular structure of the labeled PEVE sample. The obtained polymer had a M_w of ca. 1.1×10^4 and M_w/M_n of 1.13. For measurements, the high molecular weight part of the obtained PEVE, which was fractionated by GPC, was used to eliminate the incompletely coupled products. PEVE used for measurements had a M_w of ca. 2×10^4 by GPC reduced as polystyrene. Water (Dojin,

nonfluorescence) was used as a solvent without further purification. T_{sp} of PEVE aqueous solution was reported to be about 20 °C by transmittance measurement;[10] the PEVE aqueous solution suddenly becomes turbid at this temperature. PEVE aqueous solution was prepared to be ca. 0.02 wt%. Such a low concentration was selected to minimize the influence of turbidity at the phase separation. Moreover, sodium dodecyl sulfate (SDS) (Nacalai Tesque) was used as a surfactant for PEVE aqueous solution. Hexane solution of PEVE, which does not induce the phase separation, was prepared and the absorbance of the solution at 411 nm was ca. 0.1. PEVE bulk, which melts at room temperature, was applied to a quartz substrate. Each sample was put into a quartz cell and was degassed.

7-2-2. Fluorescence Measurements

The temperature dependence of fluorescence intensity for a PEVE aqueous solution was measured under continuous illumination using a fluorescence spectrophotometer (Hitachi 850). The excitation wavelength was set at 396 nm and the fluorescence intensity was measured at 457 nm.

Next, the time-resolved fluorescence measurement was carried out and the fluorescence lifetime and anisotropy ratio for anthracene-labeled PEVE in aqueous solutions were estimated. The time-resolved fluorescence intensity was measured by the single-photon counting system.[20] A diode laser (Hamamatsu Photonics PLP-01, wavelength: 411 nm, FWHM: ca. 50 ps) was used as a light source. The repetition rate of the diode laser was 1 MHz. The FWHM of the total instrumental function was ca. 300 ps. The other instruments for the single-photon counting system and the procedure of the data analysis were the same as described in Chapter 1. The fluorescence lifetime measurements were also carried out for hexane solution, PEVE bulk, and the SDS-added aqueous solution.

7-2-3. Light Scattering Measurement

Static light scattering was measured to determine the phase separation temperature of a PEVE aqueous solution. Light intensity scattered at an angle of 30

degree was recorded as a function of temperature by using a light scattering apparatus (Otsuka Electronics DLS-7000). PEVE sample having no fluorescent probe was synthesized especially for the light scattering measurement, M_w and M_w/M_n of which were 2.3×10^4 and 1.17, respectively. The sample aqueous solution was prepared to be the same concentration 0.02 wt% as the solution for the fluorescence measurements. The sample solution was filtered through 0.5 μm and 0.2 μm pores before measurement. First the solution was heated gradually up to the phase separation region and then was cooled down to 17 °C, and again was heated up to the phase separation region. The heating or cooling rate was kept less than 0.1 °C /min.

7-3. Results and Discussion

7-3-1. Scattering Intensity

Figure 7-2 shows the relationship between temperature and the scattering light intensity. On both the first and the second heating, the intensity increased sharply above 20 °C. This indicates that the polymer chains start to aggregate at 20 °C and form large aggregates. On the other hand, on cooling, the scattering intensity started to decrease at a temperature lower than 18 °C. It was assumed that two notable temperatures, that is, ca. 18 °C and 20 °C, correspond to the binodal and the spinodal temperatures at the composition of our system, respectively, although this may merely come from the fact that the phase separation and/or the dissolution of the aggregate could not follow the continuous temperature variation of 0.1 °C /min.

7-3-2. Fluorescence Intensity and Lifetime

Figure 7-3 shows the plot of fluorescence intensity against temperature. A marked decrease can be seen between ca. 16 °C and 20 °C, i.e., an effective quenching occurs in this region.

Halary et al. showed that poly(vinyl methyl ether) (PVME) quenches the fluorescence of anthryl-group labeled in the middle of polystyrene main chain in the

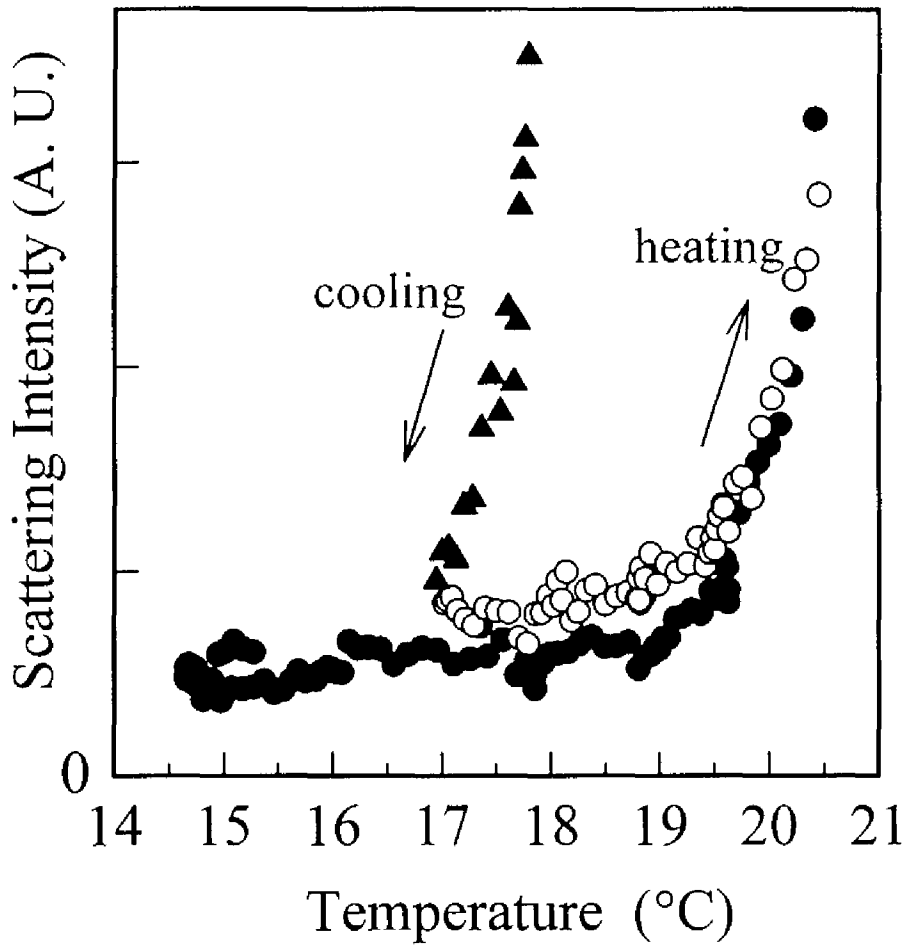

Figure 7-2. Plots of scattering light intensity from a PEVE aqueous solution against temperature. Symbols are for the first heating (●), cooling (▲), and the second heating (○), respectively.

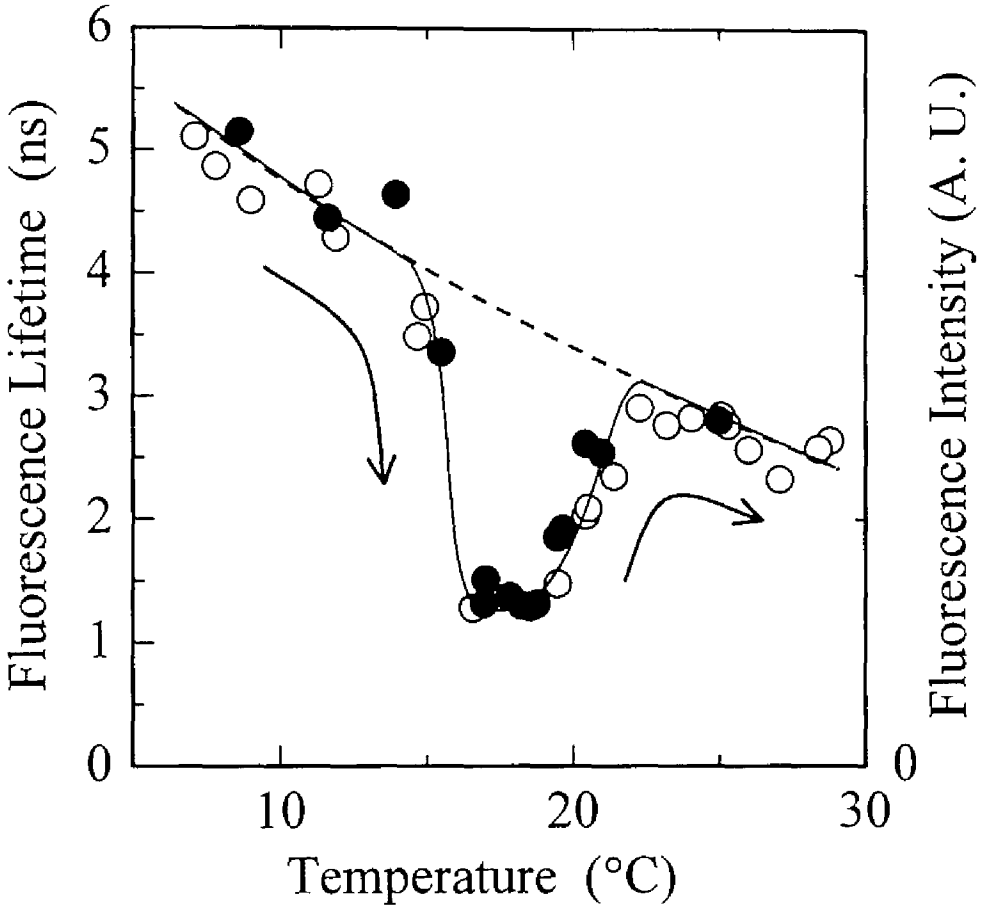

Figure 7-3. Plots of fluorescence intensity and fluorescence lifetime $<\tau>$ against temperature in a PEVE aqueous solution; fluorescence intensity (●) and fluorescence lifetime (○).

ternary blend film of PVME, polystyrene, and labeled polystyrene.[1] They considered that the mechanism of the fluorescence quenching is static with the lifetime remaining constant. Since the molecular structure of PEVE is similar to that of PVME, it is reasonable that PEVE quenches fluorescence emission of labeled anthracene.

Then, it was examined whether the fluorescence lifetime changes with the fluorescence intensity. Figure 7-3 shows that the fluorescence lifetime changed quantitatively as did fluorescence intensity. Therefore, it is believed that the decrease in the fluorescence intensity is due to the so-called dynamic quenching, in which the fluorescence intensity becomes proportional to the fluorescence lifetime. The difference between static and dynamic quenching may come from the fact that the present system is a solution instead of a film as was the case of Halary et al.

Such a marked temperature dependence of lifetime was not observed in the previous anthracene-labeled polystyrene or poly(methyl methacrylate) system. It is noteworthy that this quenching occurred in a few degrees below the phase separation temperature (20 °C). Consequently, it is obvious that the dynamic quenching in the fluorescence intensity and lifetime takes place at the pre-stage of the phase separation. That is, the microenvironment around the fluorescent probe in the aqueous solution changes even in this temperature range in connection with the phase separation.

7-3-3. Chain Mobility

Figure 7-4 shows the plot of relaxation time T_m for the local motion of the PEVE chain against temperature. Figure 7-4 shows that the relaxation time increases of an order of magnitude in the vicinity of 20 °C. This indicates that the chain mobility decreases at 20 °C or above. Notice that the relaxation time does not change remarkably in the temperature range that the dynamic quenching occurs. The behavior of the relaxation time against temperature is rather similar to that of the scattering light intensity on heating in Figure 7-2. The decrease in the chain mobility results from the intra- and intermolecular aggregation due to the phase separation.

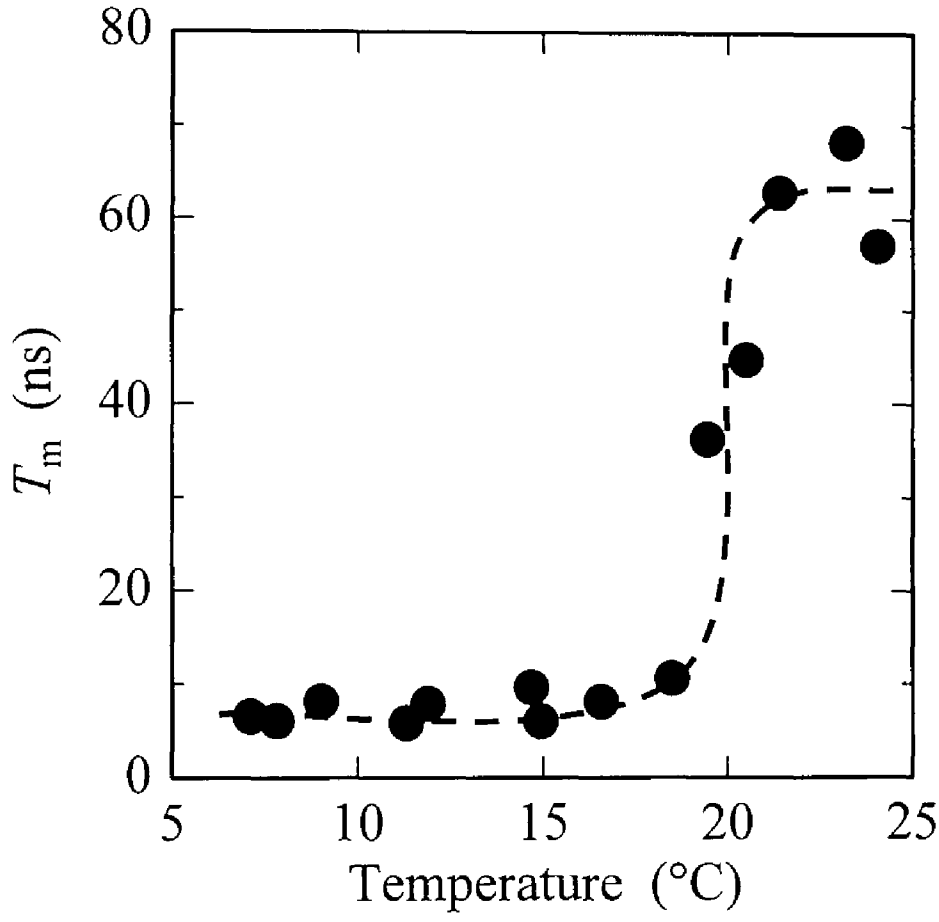

Figure 7-4. Plots of the relaxation time T_m for the local motion of PEVE against temperature.

7-3-4. Dynamic Quenching

In this section, the process of phase separation will be discussed with attention mainly to the dynamic fluorescence quenching preceding the phase separation. That is, two different temperatures, i.e., ca. 16 °C and ca. 20 °C, are focused on. The fluorescence intensity and the lifetime decreased sharply at ca. 16 °C and increased at ca. 20 °C. On the other hand, the relaxation time and the scattering intensity increased at ca. 20 °C and no change was observed around 16 °C.

In the temperature range from 16 °C to 20 °C, where is just below the phase separation temperature, thermal fluctuation of local segment density becomes vigorous preceding the phase separation, and the PEVE chain causes frequently momentary high local density. At a moment of high density, the PEVE segment (quencher) comes in contact with the fluorescent probe, then the dynamic fluorescence quenching occurs effectively. Although the segment density fluctuates widely with time, the time-averaged segment density may not change in this narrow temperature range. That is why the chain mobility does not change in this temperature range.

F. Winnik examined the thermoreversible phase separation of aqueous solutions of poly(*N*-isopropylacrylamide) by the fluorescence experiments. She monitored the phase separation by measuring electronic exitation energy transfer efficiency between donor and acceptor chromophores attached to the same polymer chain.[8] The results were interpreted in terms of a mechanism of phase separation initiated by a gradual shrinking of solvated polymer coils into a collapsed state, followed by aggregation of individual chains into larger particles. The change in the energy transfer efficiency begins to occur below LCST temperature. She concluded that this might result either from a continuous decrease in the size of the polymer coil, or from an enhancement in the density fluctuation. In this study, the decrease in the size of the polymer coil will cause suppression in the chain mobility, i.e., the relaxation time will become long. Therefore it is suggested that at this stage the enhancement in the density fluctuation is the best explanation both for Winnik's work and for this study.

The phase separation at 20 °C means the intermolecular aggregation on a large scale. The aggregation of polymer chains suppresses chain mobility as indicated in the

marked increase of relaxation time at 20 °C. The aggregation results in the restraint on the dynamic collision between quencher segments with the fluorescent probe, and therefore the dynamic fluorescence quenching disappears. The observed increase of fluorescence intensity and lifetime at 20 °C reflects the disappearance of the dynamic quenching due to the intra- and intermolecular aggregation. In other word, if the dynamic quenching were negligible, the fluorescence intensity and lifetime for PEVE aqueous solution would change monotonically and gradually with temperature. In the following section, the dynamic quenching preceding the phase separation will be further examined with the systems where no phase separation occurs.

7-3-5. Systems without Phase Separation

Figure 7-5 shows that in hexane solvent, the fluorescence lifetime of PEVE decreases monotonically and gradually with the increase of temperature. As was expected, no fluorescence quenching was observed when no phase separation took place. This result supports the proposition that the dynamic quenching takes place at the stage preceding the phase separation.

Figure 7-5 also shows that the fluorescence lifetime in the PEVE bulk decreases monotonically and gradually with the increase of temperature without marked quenching. Although the gradual decrease is similar to that in the hexane solution, it is noteworthy that the value of fluorescence lifetime is sufficiently lower than that of hexane solution and near the value of dynamically-quenched lifetime in Figure 7-3. In the bulk, the PEVE segment, which is considered as a quencher, exists at a high concentration (ca. 10 M) and may have mobility to some extent, and so the dynamic quenching takes place at every temperature measured. That is, the frequent collision between the fluorescence probe and PEVE segment results in the quenching of the fluorescence in PEVE bulk like the stage preceding the phase separation.

7-3-6. Effect of Surfactant

Meewes et al. studied surfactant effects on a PNIPAM aqueous solution, which has LCST, by light scattering[7]. They showed that intermolecular aggregation was

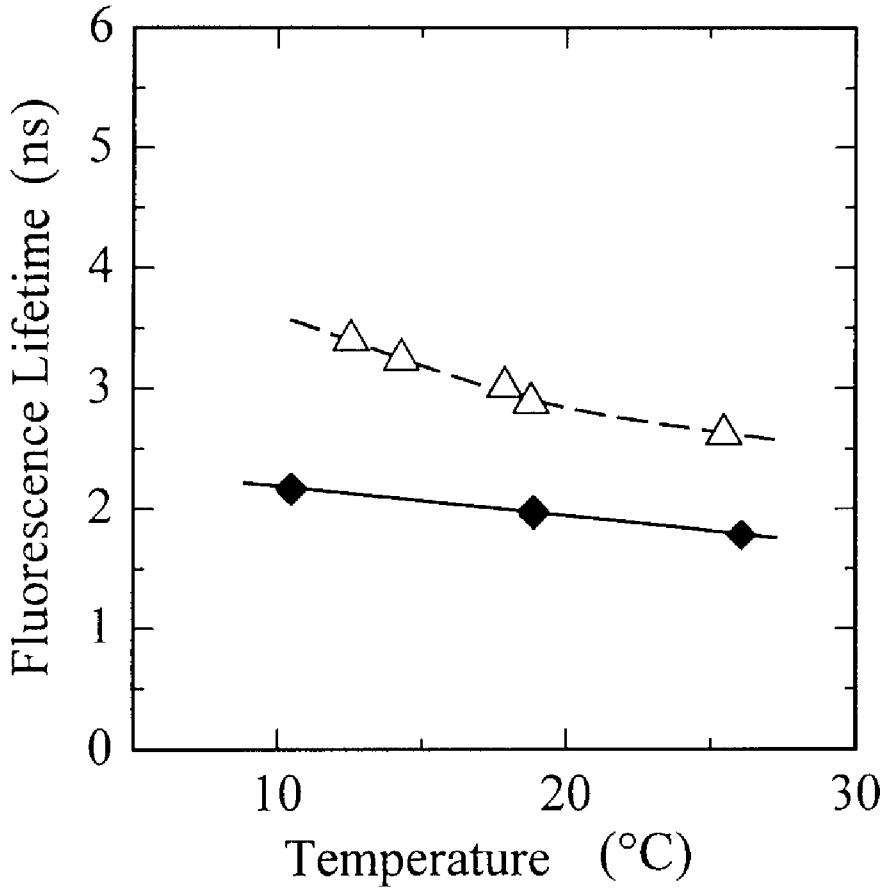

Figure 7-5. Fluorescence lifetime of PEVE in hexane (0.02 wt%) (△) and in PEVE bulk (◆), where no phase separation occurred.

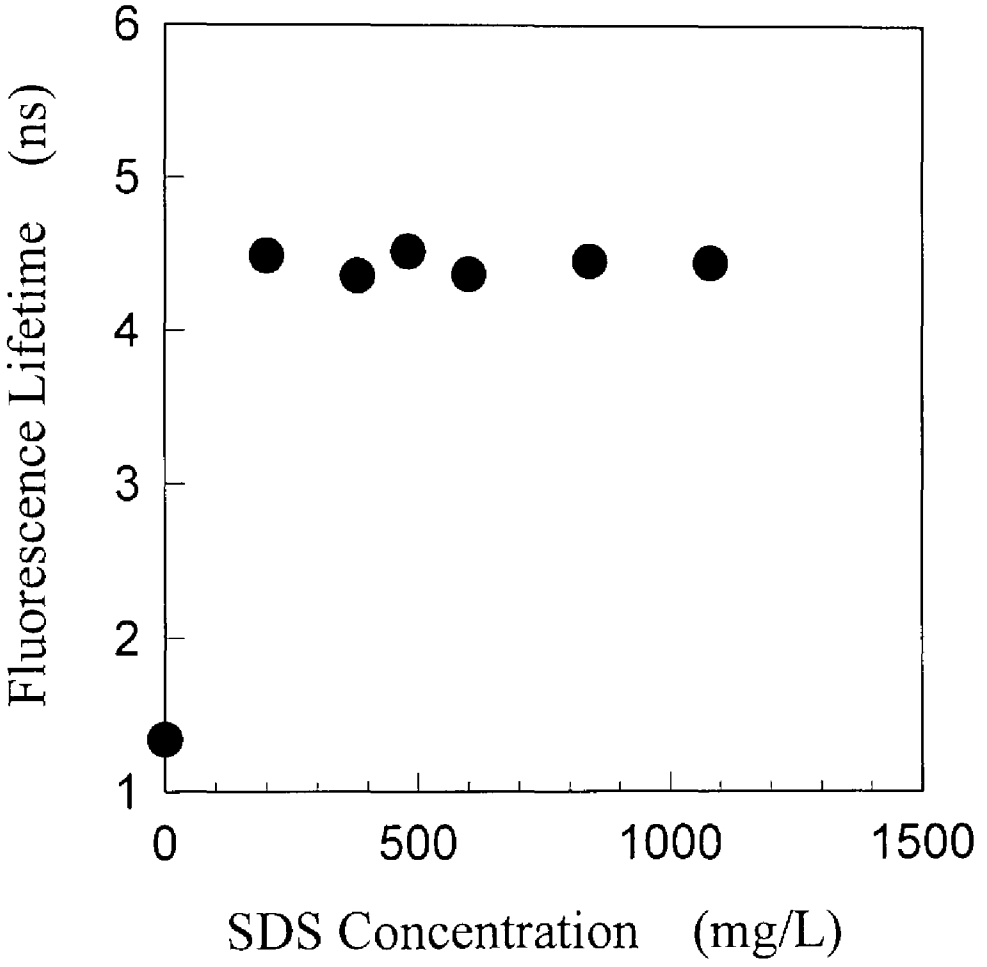

Figure 7-6. Plots of the fluorescence lifetime for PEVE aqueous solution (0.02 wt%) against SDS concentration, C_{SDS}. Measurements were carried out at 18 °C.

completely inhibited by addition of SDS up to 250 mg L^{-1}. Moreover, at an SDS concentration of 300 mg L^{-1}, intramolecular swelling was induced by the surfactant both above and below the LCST. That is, above the LCST, the radius of a particle markedly decreased by addition of SDS up to 250 mg L^{-1} due to the intermolecular dissociation and increased by successive addition of SDS due to the intramolecular swelling. Below the LCST, where an intermolecular dissociation was not involved, only the intramolecular coil swelling was induced by SDS. They considered that the surfactant binds cooperatively to the polymer chain and at the critical concentration of 300 mg L^{-1}, the repulsive interactions between the firmly adsorbed amphiphiles becomes enough to influence the polymer conformation. They proposed that the critical concentration is close to the concentration that the surfactant is adsorbed cooperatively in the form of micelles. Thus, SDS was expected to prevent both the phase separation and the preceding fluctuation of the segment density in PEVE aqueous solution as well. Then, the fluorescence lifetime by addition of the surfactant SDS was measured at a pre-stage temperature of 18 °C. Figure 7-6 shows the plot of the fluorescence lifetime against SDS concentration, C_{SDS}. In C_{SDS} > 200 mg L^{-1}, the fluorescence lifetime suddenly increased up to ca. 4.4 ns and remained constant. This indicates that SDS prevents the dynamic quenching at the pre-stage. That is, the dynamic quenching comes from the thermal fluctuation of segment density precedent to the phase separation. Moreover, Figure 7-3 shows that the fluorescence lifetime of 4.4 ns at 18 °C corresponds nearly to the value along the broken line. In other word, if the dynamic quenching were negligible, the fluorescence intensity and lifetime for PEVE aqueous solution would change monotonically and gradually with temperature similar to that for PEVE in hexane as described by the broken line in Figure 7-3.

7-4. Conclusion

The phase separation behavior of PEVE aqueous solution, which becomes turbid abruptly at 20 °C, was examined. PEVE labeled with anthryl group in the middle of the main chain was synthesized by the living cationic polymerization. The

fluorescence intensity and lifetime measurements showed noticeable temperature range. In the range from 16 to 20 °C, where the thermal fluctuation of segment density is thought to become large preceding the phase separation, the dynamic fluorescence quenching effectively occurs by the collision between the fluorescent probe and the PEVE segments. At 20 °C, intra- and intermolecular aggregation due to the phase separation suppresses the chain mobility and the dynamic quenching disappears. Moreover, in the systems without phase separation of the hexane solution of PEVE and PEVE bulk, the fluorescence lifetime decreased monotonically with the increase of temperature, but the lifetime in the latter system was about two thirds as long as that of the former. That is, in the hexane solution, no dynamic quenching occurred while in bulk, the dynamic quenching occurred at all temperatures measured. SDS was added as a surfactant to a PEVE aqueous solution just below the phase separation temperature. The fluorescence lifetime sufficiently increased up to the estimated value assuming no dynamic quenching. These results supported that the dynamic quenching is induced precedent to the phase separation through the collision between the fluorescent probe and the PEVE segments.

References

(1) Halary, J. L.; Ubrich, J. M.; Nunzi, J. M.; Monnerie, L. *Polymer* **1984**, *25*, 956.

(2) Fujishige, S.; Kubota, K.; Ando, I. *J. Phys. Chem.* **1989**, *93*, 3311.

(3) Hu, Y.; Horie, K.; Ushiki, H.; Tsunomori, F. *Eur. Polym. J.* **1993**, *29*, 1365.

(4) Hirokawa, Y.; Tanaka, T. *J. Chem. Phys.* **1984**, *81*, 6379.

(5) Tanaka, T.; Fillmore, D. J. *J. Chem. Phys.* **1979**, *70*, 1214.

(6) Binkert, Th.; Oberreich, J.; Meewes, M.; Nyffenegger, R.; Ricka, J. *Macromolecules* **1991**, *24*, 5806.

(7) Meewes, M.; Ricka, J.; de Silva, M.; Nyffenegger, R.; Binkert, Th. *Macromolecules* **1991**, *24*, 5811.

(8) Winnik, F. M. *Polymer* **1990**, *31*, 2125.

(9) Aoshima, S.; Higashimura, T. *Macromolecules* **1989**, *22*, 1009.

(10) Aoshima, S.; Oda, H.; Kobayashi, E. *J. Polym. Sci., Polym. Chem. Ed.* **1992**, *30*, 2407.

(11) Kobayashi, E.; Sadahito, A. *Kagaku to Kogyo* **1993**, *46*, 62.

(12) Aoshima, S.; Oda, H.; Kobayashi, E. *Kobunshi Ronbunshu* **1992**, *49*, 937.

(13) Kobayashi, E.; Jiang, J.; Ohta, H.; Furukawa, J. *J. Polym. Sci., Polym. Chem. Ed.* **1990**, *28*, 2641.

(14) Sasaki, T.; Yamamoto, M.; Nishijima, Y. *Macromolecules* **1988**, *21*, 610.

(15) Yokotsuka, S.; Okada, Y.; Tojo, Y.; Sasaki, T.; Yamamoto, M. *Polym. J.* **1991**, *23*, 95.

(16) Sasaki, T.; Arisawa, H.; Yamamoto, M. *Polym. J.* **1991**, *23*, 103.

(17) Ono, K.; Okada, Y.; Yokotsuka, S.; Ito, S.; Yamamoto, M. *Polym. J.* **1994**, *26*, 199.

(18) Ono, K.; Okada, Y.; Yokotsuka, S.; Sasaki, T.; Yamamoto, M. *Macromolecules* **1994**, *27*, 6482.

(19) Ono, K.; Ueda, K.; Yamamoto, M. *Polym. J.* **1994**, *26*, 1345.

(20) Horinaka, J.; Ono, K.; Yamamoto, M. *Polym. J.* **1995**, *27*, 429.

(21) Ono, K.; Sasaki, T.; Yamamoto, M.; Yamasaki, Y.; Ute, K.; Hatada, K. *Macromolecules* **1995**, *28*, 5012.

(22) Flory, P. J.; Orwoll, R. A.; Vrij, A. *J. Am. Chem. Soc.* **1964**, *86*, 3507.

(23) Flory, P. J. *J. Am. Chem. Soc.* **1965**, *87*, 1833.

(24) Eichinger, B. E.; Flory, P. J. *Trans. Faraday Soc.* **1968**, *64*, 2035.

(25) Flory, P. J. *Discuss. Faraday Soc.* **1970**, *49*, 7.

(26) Ptitsyn, O. B.; Kron, A. K.; Eizner, Y. Y. *J. Polym. Sci.: Part C* **1968**, *16*, 3509.

(27) de Gennes, P. G. *J. Phys. Lett.* **1975**, *36*, L-55.

(28) Norisuye, T.; Nakamura, Y. *Polymer* **1993**, *34*, 1440.

(29) Chu, B.; Ying, Q.; Grosberg, A. Y. *Macromolecules* **1995**, *28*, 180.

(30) Riddick, J. A.; Bunger, W. B. *Techniques of Chemistry II, Organic* Solvents, 3rd ed: Wiley-Interscience: New York, 1970.

(31) Hu, Y.; Horie, K.; Ushiki, H.; Tsunomori, F.; Yamashita, T. *Macromolecules* **1992**, *25*, 7324.

(32) Hu, Y.; Horie, K.; Ushiki, H.; Yamashita, T.; Tsunomori, F. *Macromolecules* **1993**, *26*, 1761.

Chapter 8

Local Chain Dynamics of Several Polymers in Θ Solvents Studied by the Fluorescence Depolarization Method

8-1. Introduction

Both the chain conformation and its molecular chain dynamics have been investigated extensively.[1-5] However, the relationship between the structure of polymer chains and the molecular chain dynamics is not clearly understood yet.

In this chapter, polymer samples labeled with anthracene in the middle of the main chain were prepared, and the relaxation time of the local motion of the polymer chains was examined by the fluorescence depolarization technique. The relaxation time of a polymer chain in the dilute solution usually depends on the segment density around the anthracene probe, which is governed by the solvent quality.[6] Therefore, the relaxation time, T_m/η, must be compared among polymers under the Θ condition. Here, the relationship between the structure and dynamics was examined using five kinds of labeled polymers, i.e., *cis*-polyisoprene (*cis*-PI), polystyrene (PS), poly(α-methylstyrene) (PαMS), *syndiotactic*-poly(methyl methacrylate) (*s*-PMMA), and poly(*N*-vinylcarbazole) (PVCz). The mean relaxation time, T_m , and the activation energy, E^*, of the local motion were obtained in each Θ solvent and the local motion was compared in the same unperturbed state at almost the same temperature.

8-2. Experimental Section

Table 8-1. Characteristics of Polymers Used in This Study.

	$M_w \times 10^{-4}$	M_w / M_n	f_r
cis-PI	14.5	1.10	-
PS	9.7	1.05	0.54
PαMS	21.5	1.05	0.67
s-PMMA	15.0	1.18	0.93
PVCz	1.3	1.17	-

Four kinds of anthracene-labeled polymers, *cis*-PI, PS, PαMS, and *s*-PMMA, were prepared by the living anionic polymerization and the living ends were coupled by 9, 10-bis(bromomethyl)anthracene. PVCz was prepared by the living cationic polymerization with HI at -40 °C and the living ends were coupled by 9,10-anthracenedithiol. Table 8-1 shows the characteristics of the five kinds of polymers. The molecular weights were measured by GPC. The racemo fraction f_r was measured by ^{13}C-NMR and ^{1}H-NMR. The microstructure of *cis*-PI was as follows: *cis*-1,4 content is 76%, *trans*-1,4 is 19%, and 1,2-content is 5%. The polymer concentrations of all the sample solutions were kept less than 0.1 wt%, and all the solutions were degassed before the measurements were made.

The Θ solvent and temperature for each polymer are as follows; 1,4-dioxane at 34.0 °C for *cis*-PI, cyclohexane at 34.5 °C for PS and PαMS, butyl chloride at 35.0 °C for *s*-PMMA, and toluene at 37 °C for PVCz.

The fluorescence depolarization measurement and the procedure of estimation of the relaxation time were carried out as described in Chapter 1.

8-3. Results and Discussion

8-3-1. Relaxation Time and Activation Energy

Table 8-2. Reduced Relaxation Times at 35°C and Activation Energies for Polymers in Each Θ Solvent.

polymer/ Θ solvent	T_m/η (ns/cP)	E^* (kcal/mol)
cis-PI/dioxane	1.3	1.5
PS/cyclohexane	5.4	2.6
PαMS/cyclohexane	9.0	3.0
s-PMMA/butyl chloride	12.7	5.0
PVCz/toluene	12.6	4.3

Table 8-2 shows the reduced relaxation time T_m/η at 35 °C and the activation energy E^* for five kinds of polymers. The order of the relaxation time, T_m/η, was; *cis*-PI < PS < PαMS < PVCz < *s*-PMMA. The order of E^* was the same. The results show that the higher the activation energy, the longer the relaxation time.

The values of the relaxation time were compared from the aspect of polymer structure. First, the relaxation time, 1.3 ns/cP and the activation energy E^*, 1.5 kcal/mol for *cis*-PI were the smallest among these polymers. *cis*-PI has the double bond in the main chain, but its single bonds are mostly freely-rotating ones. Furthermore, it does not have a large substituent besides the methyl group. Second, PS and PαMS had a bulky phenyl group differing from *cis*-PI, so that the relaxation time became longer and E^* became higher than those of *cis*-PI. Furthermore, PαMS has a larger relaxation time and higher activation energy than PS, because α-methyl substitution of the PS main chain increases the internal potential and the relaxation time. *s*-PMMA is a di-substituted polymer like PαMS, but the relaxation time of *s*-PMMA was longer than that of PαMS. This may be due to the difference in both stereoregularity and solvation. As for the stereoregularity, the difference in racemo fraction between *s*-PMMA (f_r = 0.93) and PαMS (f_r = 0.67) extends the relaxation time of *s*-PMMA. It was shown experimentally that T_m/η for *s*-PMMA is

about two times larger than that for *i*-PMMA in the Θ solvent.[7] Generally, for the same kind of polymer, the static stiffness of the polymer chain with syndiotactic regularity is larger than that with isotactic regularity.[8] The dynamic chain stiffness has a parallel relationship to the static chain stiffness; the higher racemo fraction of a polymer increases

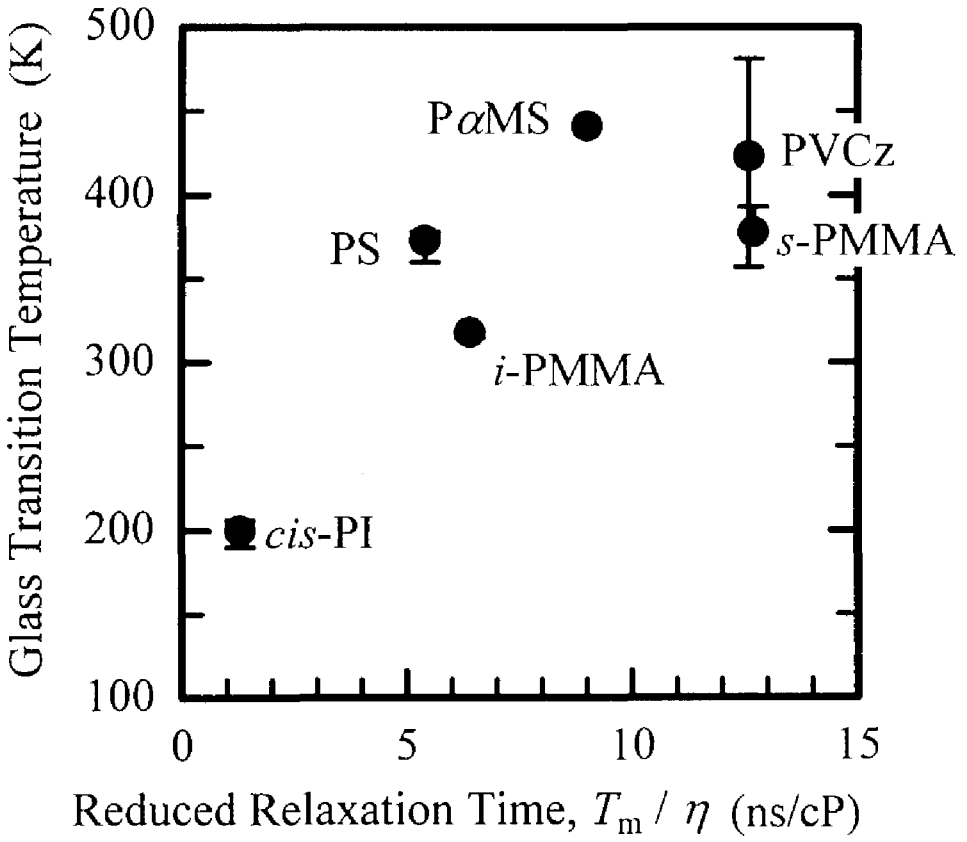

Figure 8-1. Relationship between glass transition temperature and reduced relaxation time.

the relaxation time.[9] As for the solvation, the ester group is polar and more strongly solvated with solvent molecules, *i.e.*, the methoxy carbonyl group makes the hydrodynamic volume larger than that of the phenyl group in PαMS, and this may make the steric hindrance higher for the conformational transition. At the present stage, it is not clear which of these factors, stereoregularity or solvation, is dominant in *s*-PMMA, but both may be operating. PVCz had a longer relaxation time and higher activation energy than PS. The reduced relaxation time was more than two times that for PS. The bulky carbazolyl group makes the relaxation time longer and activation energy higher.

8-3-2. Relation of Glass Transition Temperature to the Reduced Relaxation Time

The glass transition appears as the result from the reduction of chain mobility as the temperature drops. In the solid state the chain mobility is influenced by internal and external friction. The reduced relaxation time indicates a kind of internal friction. Figure 8-1 shows the relationship between the glass transition temperature T_g and the reduced relaxation time T_m/η. There is a positive correlation between T_m/η and T_g. This result means that the internal friction is a predominant factor to T_g at least for these polymers.

8-4. Conclusion

The relaxation times for five kinds of polymers, i.e., *cis*-PI, PS, PαMS, *s*-PMMA, and PVCz were measured in the Θ solvents by the fluorescence depolarization technique. The local chain dynamics was evaluated without the effect of the segment density.

The relaxation time T_m/η was in the order of *cis*-PI < PS < PαMS < PVCz < *s*-PMMA. The activation energies have the same order as the reduced relaxation time. The relaxation time and the height of the energy barrier depend on whether the polymer is either mono-substituted or di-substituted, and also on the bulkiness of the substituents. However, the stereoregularity is the important factor when the relaxation time is compared among various kinds of polymers. It was also found that T_g is closely correlated with the local chain mobility in a dilute solution.

References

(1) Stockmayer, W. H. *Pure Appl. Chem.* **1976**, *15*, 539.

(2) Bailey, R. T.; North, A. M.; Pethrick, R. A. *Molecular Motion in High Polymers* Clarendon: Oxford, 1981.

(3) Helfand, E. *Photophysical and Photochemical Tools in Polymer Science* Winnik, M. A. ed., D. Reidel: Dordrecht, p151, 1986.

(4) Doi, M.; Edwards, S. F. *The Theory of Polymer Dynamics* Clarendon: Oxford, 1986.

(5) Yamakawa, H. *Molecular Conformation and Dynamics of Macromolecules in Condensed Sytems* Nagasawa, M. ed., Elsevier: Berlin, p21, 1988.

(6) Horinaka, J.; Ono, K.; Yamamoto, M. *Polym. J.* **1995**, *27*, 429.

(7) Ono, K.; Sasaki, T.; Yamamoto, M.; Yamasaki, Y.; Ute, K.; Hatada, K. *Macromolecules* **1995**, *28*, 3736.

(8) Fujii, M.; Nagasawa, K.; Shimada, J.; Yamakawa, H. *Macromolecules* **1983**, *16*, 1613.

(9) Yoshizaki, T.; Yamakawa, H. *J. Chem. Phys.* **1984**, *81*, 982.

Summary

In Chapter 1, the backgrounds of the local chain dynamics, the fluorescence depolarization method, and the MD simulation were described as the introduction to this thesis. First, the importance of local chain dynamics study in the field of the polymer science was explained with the brief historical background, and available approaches to the local chain dynamics were introduced. Next, the fluorescence depolarization method, which was the main technique in this thesis, was explained with regard to the concept, apparatus, data analysis. Then, the previous fluorescence depolarization studies were summarized to clarify unsolved problems and the motivation of this thesis. Finally, the advantage as well as the disadvantage of the MD simulation was mentioned. Furthermore, the outline of this thesis was described.

In Chapter 2, the local chain dynamics of poly(oxyethylene) (POE) labeled with anthryl group in the middle of the main chain was examined by the fluorescence depolarization method. The relaxation time of the local motion was evaluated and its molecular weight dependence was shown. POE had a mean relaxation time in the order of sub-nanoseconds. The value of the relaxation time increased with the molecular weight in the range of MW < 1000 and reached an asymptotic value at MW of about 1000. The relaxation time and the activation energy for local motion of POE were compared with those of some styrene and methacrylate polymers and the characteristics of POE chain were discussed. POE had a much higher local chain mobility than other polymers. This high local chain mobility of POE results from the molecular structure of POE chain.

In Chapter 3, the molecular weight effect on the local motion of polystyrene (PS) was examined in dilute solutions by the fluorescence depolarization method. Four PS samples with the fluorescent probe, anthryl group, in the middle of the main chain were synthesized by the living anionic polymerization. The molecular weight of samples varied from ca. 6.4×10^3 to 9.2×10^4. Solvents were benzene, a good solvent

and ethyl acetate, a poor solvent. In both solvents, the relaxation time increased with the molecular weight up to MW = 10^4 at which it reached an asymptotic value. The activation energies were also estimated from the temperature dependence of the relaxation time, and its molecular weight dependence appeared to be similar to that of the relaxation time. It was suggested that the relaxation time of the local motion is determined by the potential for the conformational transition of main chain bonds, rather than by the segment density. Finally, the molecular weight effect on the relaxation time for PS was compared with that for poly(oxyethylene) (POE). The results showed that PS is dynamically stiffer than POE.

In Chapter 4, local motion of the oligo- and polystyrene chain end in dilute solutions was examined by the fluorescence depolarization method. The molecular weight of the sample varied from 5.1×10^2 to 2.5×10^4. The relaxation time of local motion, T_m, in a benzene solution increased with molecular weight and reached an asymptotic value at MW = 2×10^3 with $T_m \cong 0.3$ ns. In ethyl acetate, which is a poorer solvent than benzene, T_m became constant at a higher molecular weight than in benzene and the asymptotic relaxation time was longer than that in benzene. It was proposed that the difference in the relaxation time and in its molecular weight dependence between the two solutions may result from the local potential for the conformational transition of the main chain bond, rather than the segment density. In comparison with the relaxation time for the polystyrene chain center, both the critical molecular weight and the asymptotic relaxation time for the chain end were about one order smaller than those for the chain center. This indicates that the mobility of a linear polymer chain end is sufficiently different from that of its chain center.

In Chapter 5, molecular dynamics (MD) simulation of polystyrene (PS) chain with anthryl group at the chain end surrounded by benzene molecules was performed and the results were compared with the experimental result on the local motion of PS chain end studied by the fluorescence depolarization method. The molecular weight dependence of the relaxation time of the probe obtained by the MD simulation qualitatively reproduced the trend measured by the fluorescence depolarization method. The molecular weight dependence of the relaxation time for the end-to-end vector was also estimated. Below the degree of polymerization (DP) ≤ 3, the mean relaxation

time T_m for the end-to-end vector was almost the same as that for the vector corresponding to the transition moment of the probe. With the increase of DP, T_m for the probe tended to reach an asymptotic value unlike that for the end-to-end vector, which monotonically increased with DP. This result indicates that the entire motion of a polymer coil contributes to the local motion to a lesser extent as the molecular weight increases. The MD simulations with artificial restraints showed that the rotational relaxation of the probe at the chain end for PS chain is realized by the cooperative rotation about main chain bonds. It was also shown that the internal modes which take place below 5 monomer units mainly leads to the rotational relaxation of the probe at the PS chain end. Finally, the change of T_m with the position along the PS main chain was examined.

In Chapter 6, the influence of a fluorescent probe on the fluorescence depolarization study was examined by using MD simulation together with the fluorescence depolarization measurement. The relaxation times of the local motion, T_m, for two series of polystyrene (PS) (r-PS and a-PS), which have different molecular structures in the vicinity of the fluorescent probe, anthryl group, were compared. T_m for r-PS, which has more space between anthryl group and PS unit than a-PS, was smaller by a factor of 2 than that for a-PS, which has one methylene group as the spacer. The steric hindrance of anthryl group with the phenyl ring of PS is considered to make the relaxation time longer. On the other hand, the activation energy may predominantly reflect the inherent chain mobility of PS chain. MD simulation of anthryl group-labeled PS chain was run for the cases of various numbers of methylene group between the probe and styrene unit. The result explains the difference in the relaxation time between a-PS and r-PS. T_m for the local motion of the probe-free PS segment at the chain center showed that the chain mobility of PS is slightly reduced by the introduction of anthryl group The effect of the direction of the transition moment in the fluorescent probe for the relaxation time was also examined.

In Chapter 7, the phase separation behavior of poly(ethoxyethyl vinyl ether) in an aqueous solution was examined both below and above the phase separation temperature. Some fluorescence techniques were utilized, e.g., fluorescence intensity, fluorescence lifetime, and fluorescence depolarization. First, the phase separation

temperature, T_{sp}, was determined to be 20 °C by the light scattering technique. The fluorescence intensity and lifetime changed quantitatively in the same way against temperature and markedly decreased between 16 °C and 20 °C, just below T_{sp}. On the other hand, the relaxation time for the local motion of PEVE estimated from the fluorescence depolarization measurement increased at T_{sp}. The dynamic fluorescence quenching disappeared by addition of a surfactant and the fluorescence lifetime increased up to the estimated value assuming no phase separation. In systems without the phase separation of both the hexane solution of PEVE and the PEVE bulk, the fluorescence lifetime decreased monotonically with the increase of temperature. It was concluded that in the range from 16 to 20 °C, the thermal fluctuation of segment density becomes large preceding the phase separation, so that the dynamic fluorescence quenching effectively occurs by the collision between the fluorescent probe and the PEVE segments. At 20 °C, intra- and intermolecular aggregation due to the phase separation suppressed the chain mobility and the dynamic quenching disappeared.

In Chapter 8, the relaxation times of local motion for five kinds of polymers: *cis*-polyisoprene (*cis*-PI), polystyrene (PS), poly(α-methylstyrene) (PαMS), *syndiotactic*-poly(methyl methacrylate) (*s*-PMMA), and poly(*N*-vinylcarbazole) (PVCz) were measured in the Θ solvents by the fluorescence depolarization technique. The viscosity reduced relaxation time T_m / η was in the following order with the activation energy in the same order: *cis*-PI < PS < PαMS < PVCz < *s*-PMMA. The relaxation time and the activation energy depend on whether the polymer is either mono-substituted or di-substituted, the bulkiness of the substituents, and also the stereoregularity. It was found that T_g is closely correlated with the local chain mobility obtained in dilute solutions.

List of Publications

Chapter 2.

Local Chain Dynamics of Poly(oxyethylene) Studied by the Fluorescence Depolarization Method

Horinaka, J.; Amano, S.; Funada, H.; Ito, S.; Yamamoto, M. *Macromolecules* **1998**, *31*, 1197.

Chapter 3

Molecular Weight Effect of Local Motion of Polystyrene Studied by the Fluorescence Depolarization Method

Horinaka, J.; Aoki, H.; Ito, S.; Yamamoto, M. *Polym. J.* in press.

Chapter 4

Local Motion of Oligo- and Polystyrene Chain End Studied by the Fluorescence Depolarization Method

Horinaka, J.; Maruta, M.; Ito, S.; Yamamoto, M. *Macromolecules* in press.

Chapter 5

Molecular Dynamics Simulation of Local Motion of Polystyrene Chain End; Comparison with the Fluorescence Depolarization Method

Horinaka, J.; Ito, S.; Yamamoto, M.; Matsuda, T. *Comp. Theor. Polym. Sci.* submitted.

Chapter 6

Influence of a Fluorescent Probe on the Local Relaxation Times for a Polystyrene Chain in the Fluorescence Depolarization Method

Horinaka, J.; Ito, S.; Yamamoto, M.; Tsujii, Y.; Matsuda, T. *Macromolecules*

submitted.

Chapter 7

Microscopic Observation of Thermally-Induced Phase Separation of Poly(ethoxyethyl Vinyl Ether) by Fluorescence Methods

Horinaka, J.; Ono, K.; Yamamoto, M.; Aoshima, S.; Kobayashi, E. *"Solvents and Self-Organization of Polymers"* Weber, S. E. Ed., Kluwer Academic Publishers: Dordrecht, 1996, 359.

Dynamic Fluorescence Quenching Precedent to Thermally-Induced Phase Separation of Poly(ethoxyethyl Vinyl Ether) Aqueous Solution

Horinaka, J.; Matsumura, Y.; Yamamoto, M.; Aoshima, S.; Kobayashi, E. *Polym. Bull.* in press.

Chapter8

Local Chain Dynamics of Several Polymers in Θ solvents Studied by the Fluorescence Depolarization Method

Yamamoto, M.; Horinaka, J.; Aoki, H.; Tawa, K.; Ito, S. *J. Soc. Rheol. Jpn.* **1997**, *25*, 203.

Others

Local Chain Dynamics of *Syndiotactic* Poly(methyl methacrylate) Studied by the Fluorescence Depolarization Method

Horinaka, J.; Ono, K.; Yamamoto, M. *Polym. J.* **1995**, *27*, 429.

Local Motion of Crosslinks for Poly(methyl methacrylate) Gels by the Fluorescence Depolarization Method.

Aoki, H.; Horinaka, J.; Ito, S.; Yamamoto, M. *Polym. Bull.* **1997**, *39*, 109.

Acknowledgments

The present thesis is based on the studies carried out at the Department of Polymer Chemistry, Graduate School of Engineering, Kyoto University, from 1993 to 1998, under the guidance of Professor Masahide Yamamoto. I wish to express my sincere gratitude to Professor Masahide Yamamoto for his continuous guidance and affectionate encouragement throughout this work.

I am sincerely indebted to Dr. Shinzaburo Ito for his valuable suggestions, pointed (sometimes critical) comments, and active instructions throughout this work.

Thanks are also due to Dr. Akira Tsuchida, Department of Applied Chemistry, Gifu University for his kind guidance. I am grateful to Mr. Masataka Ohoka for his kind support in various situations.

I would like to thank Professor Takeaki Miyamoto, Dr. Takeshi Fukuda, Dr. Yoshinobu Tsujii and Mr. Kohji Ohno, Institute for Chemical Research, Kyoto University, for the gift of the anthracene-labeled polystyrene (r-PS) samples and for the light scattering measurement.

I wish to express my sincere thanks to Professor Eiichi Kobayashi, Dr. Sadahito Aoshima, Mr. Shin-ichi Takahashi, and Mr. Koji Ueda, Science University of Tokyo, for the gift of PEVE samples.

I am grateful to Dr. Tsunetoshi Matsuda, Unitika Ltd., for his suggestions and instructions in the molecular dynamics simulation.

I wish to thank Dr. Takashi Sasaki, Fukui University, for his valuable suggestions about the living anionic polymerization of anthracene-labeled polystyrene samples. I deeply thank to Dr. Keiko Tawa, Osaka National Research Institute, for her kind guidance and useful discussions throughout, especially at the beginning of, this work. I am indebted to Mr. Tsuyoshi Sasaki for the preparation of the chain end-labeled polystyrene and the guidance on its synthetic technique.

I express my gratitude to the nice members of Yamamoto Laboratory. I

especially thank Dr. Kenji Hisada, Dr. Masaya Mitsuishi, Dr. Hideo Ohkita, Dr. Nobuhiro Sato, and Dr. Michiaki Mabuchi for their valuable suggestions and kind encouragement. I am grateful to Messrs. Kazutoshi Sugiura, Yasuyuki Nomura, and Tsuyoshi Yasuda for their continuous friendship. I also thank Mr. Shinsuke Amano for his untiring efforts. The study presented in Chapter 2 owes much to him. I have nice places of recreation and relaxation including "46-Kai" in the daily life: Thanks are due to anonymous friends for their active collaborations.

Last, but not least, I wish to thank my father Kenjiro Horinaka and my mother Yasue Horinaka for their devoted support in everything. It is impossible to adequately express my gratitude in words.

December, 1998

Jun-ichi Horinaka